Technical Memorandum No. 33-154

THE UTILITY OF LIBRATION POINT SATELLITES

A. Kliore

Jet Propulsion Laboratory
California Institute of Technology
Pasadena, California

August 31, 1963

Copyright © 1963
Jet Propulsion Laboratory
California Institute of Technology

Prepared Under Contract No. NAS 7-100
National Aeronautics & Space Administration

CONTENTS

I. Introduction 1

II. Discussion of Objectives and Alternate Missions 4

A. Communication Relays 4

1. Lunar Orbiters 5

2. Translunar Libration Point Satellites 7

B. Solar Flare Observations 8

1. Circumlunar Trajectories 8

C. Determination of the Mass of the Moon 9

1. Analysis of Planetary-Probe Trajectories (Mariner 2) 10

2. Lunar Satellite Orbit Determination 11

D. Optical and Radio Astronomy 11

E. Bistatic Radar Astronomy 12

F. Investigation of "Dust-Cloud" Observations 14

G. Navigation Beacon 15

III. Conclusion 17

Appendices

A. Satellite Motion in the Vicinity of the Stable Earth-Moon Libration Points 20

B. Characteristics of Lunar Satellite Orbits 45

C. Injection and Station-Keeping Near the Translunar Libration Point 95

D. Conic Approximations Used in Circumlunar Trajectories 112

E. The Evaluation of Certain Physical Constants from the Radio Tracking of Mariner 2 118

References 141

TABLES

1. Satellite communication systems 7

2. Comparison of libration point satellites and alternate missions 18

FIGURES

A-1. Libration points in the restricted three-body problem 24

A-2. Three-dimensional illustration of the coordinate systems and spacecraft location geometry 24

A-3. Spacecraft motion about L_4 in the restricted three-body problem resulting from an initial displacement error 29

A-4. Unstable spacecraft motion about L_4 in the restricted three-body problem resulting from a large initial displacement error 29

A-5. Spacecraft motion about L_4 in the restricted three-body problem resulting from an initial velocity error 31

A-6. Spacecraft motion about L_4 in the very restricted four-body problem resulting from zero initial displacement and velocity errors (250 days) 31

A-7. Long term spacecraft motion about L_4 in the very restricted four-body problem resulting from zero initial displacement and velocity errors (443 days) 32

A-8. Long term spacecraft motion about L_4 in the very restricted four-body problem resulting from zero initial displacement and velocity errors (700 days) 32

A-9. Spacecraft motion in the z-direction about L_4 in the very restricted four-body problem resulting from zero initial displacement and velocity errors 34

A-10. Spacecraft motion about L_5 in the very restricted four-body problem resulting from zero initial displacement and velocity errors 34

A-11. Spacecraft motion about L_4 in the restricted four-body problem considering several spacecraft area to mass ratios . . . 36

A-12. The dependent equilibrium point location in the L_4 region 36

A-13. Spacecraft motion about L_4 in the very restricted four-body problem with the initial displacement corresponding to a time dependent equilibrium point 38

A-14. Spacecraft motion about L_4 in the very restricted four-body problem with zero initial displacement and an initial time 38

A-15. Spacecraft motion about L_4 in the very restricted four-body problem with an initial velocity of 10 ft/sec at 60 deg 39

FIGURES (Cont'd)

A-16. Spacecraft motion about L_4 in the very restricted four-body problem with an initial velocity of 10 ft/sec at 150 deg 39

A-17. Spacecraft motion about L_4 in the very restricted four-body problem with an initial velocity of 10 ft/sec at 240 deg 41

A-18. Spacecraft motion about L_4 in the very restricted four-body problem with an initial velocity of 10 ft/sec at 330 deg 41

A-19. Component of unit force in the x-direction as a function of time--spacecraft is constrained at L_4 41

A-20. Component of unit force in the y-direction as a function of time--spacecraft is constrained at L_4 42

A-21. Component of unit force in the z-direction as a function of time--spacecraft is constrained at L_4 42

A-22. Total unit force as a function of time--spacecraft is constrained at L_4 42

A-23. Impulse requirement to induce stability at locations in the L_4 region 42

B-1. Moon-centered coordinates 47

B-2. Spherical polar coordinates 47

B-3. Resolution of velocity vector 47

B-4. Osculating ellipse 52

B-5. Velocity required to reach Moon 52

B-6. Earth-to-Moon orbit (schematic) 52

B-7. Orbit in three-dimensions 58

B-8. Earth-Moon system 58

B-9. Restricted three-body problem coordinates 58

B-10. Jacobi-Integral curves of zero velocity 62

B-11. Earth-Moon orbit (x-y projection) 62

B-12. Earth-Moon orbit (x-z projection) 63

B-13. Approach to Moon, Moon fixed coordinates (schematic) 63

FIGURES (Cont'd)

B-14. Lunar approach orbit (x-y projection) 65

B-15. Lunar approach orbit (x-z projection) 65

B-16. Impulse for injection into circular orbit 65

B-17. Optimum altitude for injection into circular orbit 66

B-18. Velocity in circular orbit 66

B-19. Period in circular orbit (by day) 66

B-20. Period in circular orbit (by hour) 67

B-21. Lunar satellite orbits 67

B-22. Minimum altitude as a function of error in injection velocity for 400-km orbit 67

B-23. Precession rates due to J-term in Moon's gravity field--dependence on altitude 72

B-24. Precession rates due to J-term in Moon's gravity field--dependence on inclination (satellite orbit at lunar surface) 73

B-25. Effect of lunar bulge on precession rate 73

B-26. Effect of lunar bulge on precession rate 74

B-27. Dependence of precession rate due to bulge on orbit inclination 75

B-28. Precession rate due to Earth--dependence on distance to Moon's center 75

B-29. Precession rate due to Earth--dependence on inclination 76

B-30. Regression of the line of nodes 76

B-31. Precession of the apses 76

C-1. Location of the Earth-Moon libration points 100

C-2. Libration point coordinate system 100

C-3. Contours of constant thrust vector magnitude in the x-y plane . . 100

C-4. Contours of constant thrust vector magnitude in the y-z plane . . 102

C-5. Contours of constant thrust vector magnitude in the x-z plane . . 102

FIGURES (Cont'd)

C-6. Normalized magnitude and deviation from radial of thrust vector vs $\hat{e}$ 103

C-7. Approximate trajectories (selenocentric) 107

C-8. Approximate terminal velocity increment, $|\Delta\bar{V}|$ vs flight time . . 109

D-1. Conic sections representing a circumlunar trajectory 114

D-2. Circumlunar trajectory in Earth-centered coordinates 114

D-3. Diagram relating the vectors at Points A and B in Fig. D-1 . . . 114

D-4. Trajectories within the Moon's sphere of influence with constant $\bar{V}_{PM}$ and various perigee distances 114

D-5. Representation of the vectors at the points where the circumlunar trajectory enters and leaves the Moon's sphere of influence 115

D-6. Declination of the probe and Moon for the first 80 days past injection 115

D-7. Right ascension of the probe and Moon for the first 80 days past injection 116

D-8. Probe-Earth distance for the first 80 days past injection 116

D-9. Probe-Moon distance for the first 80 days past injection 117

D-10. Earth-probe-Sun angle for the first 80 days past injection 117

E-1. Partial derivatives of doppler for encounter of flight 130

E-2. Partial derivatives of doppler data for heliocentric portion of flight 130

E-3. Early Goldstone doppler residuals 130

E-4. Goldstone doppler residuals at midpoint of mission 132

E-5. Late Goldstone doppler residuals 132

E-6. Early Johannesburg doppler residuals 132

I. INTRODUCTION

Investigators in the field of celestial mechanics have long been aware of the existence of certain points in the space surrounding two bodies orbiting about their mass center at which a third body would experience no net acceleration.

These points arise as a special solution of the restricted three-body problem, in which the orbits of the two primary bodies are assumed to be circular, and the third body has negligible mass (Refs. 1, 2). Three of these libration points lie on the line joining the primary bodies and all are unstable. The remaining two lie at the vertices of equilateral triangles having the primary bodies at the other vertices. In the restricted three-body problem, these equilateral points are stable, i. e., the motion of the third body is such that when disturbed from rest at one of these points, it remains in the vicinity indefinitely.

Because there are more than two bodies in the universe, the conditions of the restricted three-body problem are not precisely satisfied anywhere. However, these conditions are approximated to varying degrees by considering the Sun and one of the planets of the solar system to be the primary bodies. In all but one of these systems, the perturbation of the other planets, particularly Jupiter, are apparently too great to allow stable motion. In the case of Jupiter, however, stable motion near the equilateral libration points has been observed since 1906, when the Trojan asteroids were discovered.

Recently, much interest has been directed toward the corresponding points in the Earth-Moon system, especially after the discovery by Kordylewski (Refs. 3, 4, 5) of faint luminosities in the vicinity of the trailing libration point. The motion of a particle in the vicinity of these libration points has been treated

in a number of studies to varying degrees of sophistication in their consideration of third-body (Sun) and other perturbations (Refs. 6, 7, 8, 9, 10, 11, 12). These studies show that when the perturbing effect of the Sun is taken into account, a particle placed at the assumed position of a stable libration point with zero relative velocity moves away from the libration point in an oscillating motion of increasing amplitude. Several examples of such motion are presented in Ref. 11 and Appendix A, in which it is shown that the amplitude of the motion reaches approximately 150,000 statute miles after about 700 days. It has not been shown that under these conditions the particle continues to move away from the libration point indefinitely; however, if a stable "limit-cycle" does exist, it has not yet been determined.

To take advantage of the unique gravitational characteristics in the vicinity of the libration points, it has been proposed that a spacecraft be placed at a libration point. It is estimated that a trajectory very similar to a lunar transfer could be used for this purpose. For example, a 77-hr trajectory having an Earth injection velocity of 10.9 km/sec at an altitude of 228 km would require a velocity increment of approximately 1.13 km/sec for injection into the orbit of libration point L_4 (Ref. 13). Trajectories having longer times of flight require lower Earth-injection velocities and also lower velocity increments for injection at the libration point; however, such trajectories also exhibit a greater sensitivity to injection errors.

In addition, since objects placed at the libration points have a tendency to wander, it is necessary to continuously or periodically apply corrective acceleration in order to maintain such a spacecraft on station in the immediate vicinity of a libration. In Ref. 13 it is estimated that a continuously applied acceleration of about 3×10^{-6} g (2.94×10^{-5} m/sec^2) would be necessary to maintain a libration point satellite at precisely the desired point. The

programming of the orientation of the corrective acceleration has not been discussed, and it can be expected to be a problem in the implementation of a libration point satellite mission.

It can be assumed that the feasibility of establishing a libration point satellite has been established. However, the problem of maintaining a libration point satellite on station involves more than the usual attitude control requirements. A propulsion system and a specialized navigation system are necessary. Since these systems must function without interruption for the life of the mission, it is felt that this poses a serious reliability problem. Also, it still remains necessary to investigate the utility of such a mission. Several scientific objectives have been mentioned in connection with libration point satellites. Among those are the following:

1. Communications relay
2. Solar-flare observatory
3. Determination of the mass of the Moon
4. Optical and radio astronomical observatories
5. Bistatic radar astronomy
6. Investigation of "dust-cloud" observations
7. Navigation beacon

It is the purpose of this report to briefly discuss the approach to these objectives by means of libration-point satellites, and to compare these whenever possible, with other missions capable of achieving the same objectives. Additional material applicable to the discussion is included in the Appendices.

II. DISCUSSION OF OBJECTIVES AND ALTERNATE MISSIONS

A. Lunar Communication Relays

The overall goal of communications relays is to enable various broadcast points on the Moon to communicate with the Earth and with each other. To achieve this objective, it is necessary that there be direct lines of sight between any two of the communication points, including the Earth, either directly or by way of relays. Most of the points on the near hemisphere of the Moon have direct and permanent contact with the Earth and thus, using the Earth as a relay, with each other. However, this coverage becomes intermittent at the limbs and poles due to libration, and non-existent for most of the far side.

Coverage could be significantly extended by placing relays at the libration points in the Earth-Moon system. Relays placed at the leading and trailing libration points would increase the area of continuous coverage from 41% of the Moon's surface to about 77%, and the area of at least intermittent coverage from 59% to about 89%. Intermittent coverage is caused by the libration of the Moon, and thus approximately corresponds with a one month period.

One difficulty with libration-point relays is that of instability. Without station-keeping corrections, the distance between the actual and ideal relay locations might amount to about 80,000 km in six months. These departures from ideal conditions could degrade the area of continuous coverage by about 7% of the Moon's surface area if they occurred in the most unfavorable possible directions. On the other hand, the oscillations about the libration point make the departures from the ideal position favorable as often as unfavorable, so that the area of at least intermittent coverage would gradually extend over the entire lunar surface.

1. Lunar Orbiters

Another scheme for extending the area of communication coverage on the Moon utilizes lunar satellites as relays. Several difficulties, such as the eclipsing of the satellites by the Moon and the rapid motion of such satellites through the lunar sky, which would not occur in the case of libration point relays, are offset by the fact that lunar satellite relays would be nearer to the surface of the Moon by a factor between 25 and 250, and could thus obtain greater communication bandwidth and information rate per unit weight. Such consideration of efficiency, together with increased orbital stability, favor a low satellite orbit. Geometrical considerations require either high orbits or numerous satellites for proper coverage with the resulting considerations producing optimum altitudes somewhere between 1000 and 10,000 km.

In the case of lunar satellites, three distinct types of variation in coverage occur, all approximately periodic. The first (short-period type) is produced by the motion of the satellites in their orbits and has a period which is a fraction of the orbital period of the satellites, which lie between 3 and 30 hr. The second (long-period variation in communications coverage) depends on the rotation of the Moon with respect to the satellite orbits, as well as the libration of the Moon, and has a period of about a month. Orbits in the plane of the Moon's equator minimize these long-period effects, but are poor at covering the polar regions. A third type of variation which might have a period ranging upward from a few months, results from inaccuracies in orbital placement. Satellites which would ideally be carefully spaced in the same orbit would actually have slightly different periods, so that the faster satellites would gradually catch up with the slower ones and pass them. The resulting imperfect relative positioning of the satellites would degrade the performance of the communication system, particularly whenever two of the satellites were near each other. Thus,

inaccuracies in the major axes of the satellite orbits can have major effects on their relay capabilities.

In addition, the perturbing effects of the nonsphericity of the Moon's gravitational field and of the Earth and Sun would also tend to introduce long-term changes in the parameters of the orbits (Refs. 14, 15) (Appendix B). However, circular orbits of altitudes lower than 10,000 km are expected to remain stable (bound to the Moon's gravitational field) indefinitely.

The guidance requirements necessary to establish a lunar orbit are described in Ref. 16. It is seen that the energy required to establish a lunar orbit is approximately equal to that for a libration point satellite; however, no further energy need be expended, unless it is desired to perform orbital trim corrections.

Finally, an example of the coverage resulting from several simple systems of satellites is considered. System A consists of three satellites equally spaced in a lunar equatorial orbit; system B of six satellites equally spaced in a similar orbit; system C has three satellites equally spaced in a polar lunar orbit; and system D is a combination of systems A and C. Using a system composed of system A and two systems like C in perpendicular orbits, all at altitudes of about 3200 km or more, ideally, at least two satellites would be visible from any point on the Moon's surface at any time. Class one coverage is defined as continuous coverage, where at least one satellite is visible at any time. Class two coverage extends over those areas where at least one satellite is visible at least once every third (or, for system B, sixth) of a satellite orbital period. Class three coverage extends over those areas where at least one satellite is visible at least once a month. Finally, the last three altitudes in Table 1 are the minimum altitudes necessary to achieve class three, two, and one coverage of the entire surface of the Moon.

Table 1. Satellite communication systems

System	Altitude, km	Period, hr	Area of Coverage, (% of total lunar surface area) Class 1	Class 2	Class 3
A	1000	3.56	41.0	86.6	90.6
	3530	9.50	75.0	96.7	89.6
	9630	30.1	95.0	99.3	99.96
B	1300	4.17	75.0	89.4	93.0
	4820	13.2	95.0	97.9	99.3
C	5	1.81	41.0	41.0	100.0
D	720	3.03	41.0	100.0	100.0
	3180	8.58	100.0	100.0	100.0

2. Translunar Libration Point Satellites

For communication between the Earth and the far side of the Moon, a relay satellite stationed near the translunar libration point has been considered as a possibility. Such a satellite would also provide communications between any two points on the far side of the Moon (Ref. 17). Since motion at the translunar libration point is inherently unstable, corrective thrust must be applied to keep a satellite in the vicinity of the libration point for any appreciable period of time. To maintain a direct line of sight to the entire Moon-oriented face of the Earth, a relay satellite must be located away from the Earth-Moon line. At the distance of the translunar libration point (about 65,000 km) behind the Moon, a relay satellite must be stationed at least 3000 km away from the Earth-Moon line to satisfy this condition. To maintain a satellite in a circle of radius 3000 km around the translunar libration point in a plane perpendicular to the Earth-Moon line, it is estimated that a corrective velocity increment of from 125 to 190 m/sec per month is required (Ref. 17).

The injection energy required to place such a relay in the vicinity of the translunar libration point is dependent upon the trajectory; however, it is only slightly higher than the energy required for injection at an equilateral libration point. A more detailed discussion is contained in Appendix C.

B. Solar Flare Observation

Because of their long lifetime characteristics, libration point satellites have been suggested for performing long-term solar-flare observations (Ref. 13). The position of the probe at one of the equilateral libration points would be far enough from the Earth to allow the study of solar plasma streams outside of the influence of the Earth's magnetosphere. Since the study of plasmas is closely connected with the study of magnetic fields, the probe could also be used for measuring the cislunar magnetic field in the vicinity of the libration points, and its variation with the monthly changes in the Earth-Sun-probe geometry. In addition, high-energy particles, such as solar cosmic rays, could also be studied from such a probe.

In the short term, measurement of these phenomena can and has been performed by instrumentation aboard planetary probes (i.e., Mariner 2). For long-term measurement in cislunar space, certain special trajectories appear to be quite suitable. Such trajectories are discussed below.

1. Circumlunar Trajectories

It has been noted above that in order to perform long-term observation of "solar wind", a probe must have a trajectory that exhibits a large Earth-probe distance for sufficiently long periods of time. Th[illegible]equirement is met by a certain class of Earth orbits which acquire interesting [illegible]aracteristics by passage through the Moon's sphere of influence (Ref. 18[illegible] As shown in Appendix D, the first leg of such a trajectory is simply a lunar transfer ellipse that takes it to the vicinity of the Moon. Here, the velocity of the probe is influenced

by the Moon's gravitational field, and the probe leaves the Moon's sphere of influence with some new velocity, magnitude, and direction which depends on the initial velocity of entry into the sphere of influence and the distance of closest approach to the Moon. Since these two quantities are determined by the choice of an appropriate lunar transfer trajectory, a large variety of final geocentric velocities can be obtained by simply "aiming" the incoming trajectory. In that manner, Earth orbits having the desired properties can be established using only the energy required to achieve a lunar transfer trajectory. An example of such an orbit is discussed in Appendix D. It is estimated that for this particular trajectory, the Earth-Moon distance would remain large for at least 160 days.

Other trajectories having the desired properties have been shown to exist in the restricted three-body approximation to the Earth-Moon system, but their behavior in the actual case has not been investigated in detail (Ref. 19).

C. Determination of the Mass of the Moon

It has been suggested in the literature that the motion of a libration point satellite be used to refine the knowledge of the physical constants of the Earth-Moon system, in particular, the mass of the Moon (Refs. 20, 21).

The proposed method is based on the result that the motion of a particle about a libration point is, in the precise restricted three-body problem, a superposition of two periodic motions, the periods of which are related to the masses of the primary bodies (Ref. 1). For the equilateral libration points, these periods would be approximately 28.4 and 91.3 sidereal days. However, because of the eccentricity of the Moon's orbit, the actual motion would contain other periods of oscillation as well as the period of the Earth-Moon system. In addition to these "free" oscillations, a "forced" oscillation would be introduced by the perturbing effects of the Sun, and possibly Jupiter and the other planets. The success of this method would depend on observing the motion of a libration

point satellite and then determining the principal periods of the "free" oscillation. The accuracy with which the mass of the Moon can be determined by this method has not been established; however, it appears that the determination is based on observation of a second order effect, and therefore is not likely to be more accurate than more direct methods described below. It can also be expected that the application of corrective accelerations for station keeping would make the method difficult to implement.

1. Analysis of Planetary-Probe Trajectories (Mariner 2)

The reduction of tracking data from the Mariner 2 flight of 1962 has yielded a new determination of the mass of the Moon that is more accurate by a factor of about 30 than the existing values (Refs. 22, 13).

By using two-way doppler tracking from the Goldstone, California tracking station, it is possible to measure the range-rate between the station and a probe with an accuracy of approximately 1/2 cm/sec (Ref. 22).

During the heliocentric phase of a planetary probe trajectory, the monthly motion of the Earth about the barycenter of the Earth-Moon system is reflected as a periodic variation in the range rate data. When this data is reduced by the weighted least-squares method (Ref. 15), the mass of the Moon is one of the parameters that is estimated. Because of the great accuracy of the range-rate data, it is possible to estimate the mass of the Moon and other physical constants with much greater precision than was possible previously.

The analysis of Mariner 2 tracking data (see Appendix E) has yielded a provisional value for the GM of the moon of $GM_M = 4902.777 \pm 0.2$ km^3/sec^2. Using the value for GM_E from Ref. 23, $GM_E = 398,603.2 \pm 3.0$ km^3/sec^2. The value of the Earth-Moon mass ratio is determined to be $\mu^{-1} = 81.3015 \pm 0.0034$. In view of the preceding discussion it is unlikely that an improvement in the

knowledge of the mass of the Moon could be obtained by observing the motion of libration point satellites.

2. Lunar Satellite Orbit Determination

The mass of the Moon can also be determined as one of the physical constants that is estimated in the determination of the orbits of lunar satellites (Ref. 15). In addition to the parameters of the orbit, the second harmonic coefficients in the Legendre expansion of the Moon's potential function, the mass of the Earth, and the Earth-Moon distance can also be estimated.

Although the opportunity to determine the orbit of a lunar satellite has not yet arisen, the accuracy of lunar orbit (Refs. 24, 25) determination has been investigated numerically. Preliminary studies show that it is unlikely that this method can achieve an accuracy in the determination of the mass of the Moon better than that achieved by the tracking of Mariner 2.

It must be pointed out that the determination of the mass of the Moon is a natural by-product of any lunar satellite mission having as a primary objective any of the numerous objectives that have been proposed for lunar orbiters, such as selenodesy, communications relay, mapping, and others.

D. Optical and Radio Astronomy

It has been suggested (Ref. 13) that a spacecraft placed at one of the stable Earth-Moon libration points would provide a favorable location for optical and radar-astronomy observations. Among the advantages that are ascribed to such a location is the absence of eclipsing effect of the Earth, which allows unobstructed observation of practically the entire celestial sphere, as well as simplifying the power-supply problem by virtue of constant exposure to the Sun's radiation. For optical observation, such a location would be essentially free of interference from light reflected from the Sun.

One of the primary reasons for considering optical observations in space is the need to escape the effects of the Earth's atmosphere, which severely limits the spectrum and resolution of terrestrial observations. It is clear that an astronomical observatory at an Earth-Moon libration point would achieve this purpose; however, it is unlikely that such an observatory would offer any significant advantages over astronomical observatories orbiting the Earth, such as the Orbiting Solar Observatory (OSO) and the Orbiting Astronomical Observatory (OAO). Indeed, it seems that observatories in Earth orbit offer the advantages of much lower injection energy requirements allowing larger payloads in orbit, and a tremendous reduction in communication distance, which would allow either a reduced weight or increased communication rate.

In the case of radar astronomy, the effect of the Earth's environment is not as severe as in the case of optical astronomy; however, there are still advantages to be gained from observations in space. By making observations from above the Earth's ionosphere, radio telescopes can be used at frequencies lower than 10 mc. At the other end of the spectrum, rising above the atmosphere would make possible observation in the range of wave lengths from about 3 cm to the infrared, which is affected by the atmosphere.

As in the case of optical observatories, the much greater communication distance encountered in connection with a libration point observatory seems to favor an Earth-orbit approach, especially since radio noise originating from the Earth in the wave length under investigation would be effectively screened by the ionosphere.

E. Bistatic Radar Astronomy

A bistatic radar system is defined as one having its transmitter and receiver at different locations. In such a system, large transmitting equipment can be located on the Earth, and small receivers on space probes, thus

minimizing the power required aboard the probes. However, the principal advantage of a bistatic radar system is the ability to receive both the signal that reaches the receiver in a direct path, and that which is reflected by the body under study. The reception of both signals could afford automatic calibration of the system, and the characteristics of the reflected signal, such as intensity, polarization, etc., as a function of the angle of incidence would provide information about the reflecting surface and any refracting media (such as atmospheres) that the reflected ray would encounter. Thus, bistatic radar astronomy would be most valuable in the study of the surface and any residual atmosphere or ionosphere of the Moon.

The use of the Earth-Moon libration points as locations for receiving stations of a bistatic radar system do not appear to hold any advantages. In the case of the leading and trailing equilateral points, the distance from the surface of the Moon is the same as that to the Earth, and the more or less fixed location with respect to the Moon would allow only one angle of incidence to be studied. Thus, there is very little improvement over Earth-based monostatic study of the Moon's surface.

Another possibility would be the cislunar libration point located on the Earth-Moon line near the front side of the Moon. Here, the distance to the surface of the Moon is only about 60,000 km, but the location on the Earth-Moon line would allow only angles of incidence very near 90 deg.

The best location for the receiving station for bistatic radar investigations of the Moon seems to be aboard a lunar orbiter. In addition to maintaining a close position with respect to the surface of the Moon, a receiving station aboard a lunar orbiter would be capable of receiving signals reflected over a wide range of angles of incidence, thus realizing the full advantages of bistatic radar.

F. Investigation of "Dust-Cloud" Observations

Kordylewski's discovery (Ref. 3) of luminosities in the vicinity of the trailing equilateral libration point has raised the possibility that there are indeed clouds of particles or dust captured there in the manner of Jupiter's Trojans. Although it has not been established that such capture is possible at the Earth-Moon equilateral libration points (Ref. 12), it would be scientifically interesting to sample the vicinity of either the leading or the trailing equilateral libration point with a probe designed for detection and analysis of material particles. Such a sampling would determine the nature and possibly the origin of any particles in their vicinity, or at least establish their existence. If, as it has been suggested (Ref. 13), these particles are of lunar origin, it may be possible to analyze lunar materials without descending to the surface of the Moon.

Such sampling may conceivably be carried out by means of a planetary probe passing in the vicinity of a libration point on its trajectory to Venus or Mars. However, it is extremely unlikely that during any Mars or Venus opportunity a transfer trajectory would just happen to pass through the vicinity of an Earth-Moon libration point, and in most cases it would be difficult to design the trajectory to pass near a libration point even at a great cost in injection energy. On the other hand, it is not impossible, and future Mars and Venus trajectories should be examined to determine whether or not such a close approach to a libration point is possible. In any case, the probe would remain in the vicinity of the libration point for only a matter of minutes, which would be sufficient for gathering samples, but not for analysis of densities and velocities.

A probe placed in the vicinity of a libration point would be very well suited for sampling and analyzing any dust or debris that may exist. For such a mission, it would not be necessary to use corrective thrust to keep the probe on station as it would be preferable to allow the probe to wander in the vicinity

of the libration point and thus obtain information on the spatial distribution and density of any particles that may be found.

G. Navigation Beacon

In addition to the applications described in the preceding sections, libration point satellites might also be used for purposes of navigation on the surface of the Moon and in cislunar space, although the need for such a navigation beacon has not yet been demonstrated. Ideally, an object that is fixed in the Earth-Moon system would provide a reference in determining one's position relative to the Earth or the Moon. Thus, if the conditions of the restricted three-body problem are assumed, a navigation beacon placed at either or both of the equilateral libration points would remain fixed in the Earth-Moon system, and its position would be known at all times.

However, as shown previously, an object placed at a libration point in the real Earth-Moon system would not maintain its position, but would tend to move around the ideal position in a rather complex motion. Thus, a navigation beacon placed in such a position would have to be maintained on station with a continuously applied corrective acceleration, and its trajectory (or ephemeris) must be known with great precision. In any case, information about the exact position of the libration point beacon in the space around the libration point would have to be obtained by tracking from the Earth, and then transmitted to a navigator on the surface of the Moon, or in cislunar space. The precision with which the orbit of a spacecraft undergoing librational motion in the vicinity of a libration point can be determined is not known; however, the sensitivity of this motion to slight deviations in initial conditions might make precise determination difficult. Also if station-keeping corrections are made, all prior knowledge of the trajectory is corrupted.

Alternatively, lunar orbiters, the orbits of which can be very precisely determined, could also be used for navigation on the surface of the Moon. Communications with the Earth would in this case also be essential; however, this function could be combined with that of a communications relay satellite. Among the disadvantages of lunar orbiters would be their rapid motion and relatively short periods of visibility from the surface of the Moon. The much shorter communications distance to the surface of the Moon would be a definite advantage. A valid comparison of this scheme with the libration point beacon can not be made without further study.

III. CONCLUSION

In the preceding section, the advantages and disadvantages of libration point satellites were discussed in light of various scientific and technical objectives, and an attempt was made to compare their value to that of other missions capable of achieving the same objectives. In all but two cases, it was found that the libration point satellite was probably not the best approach to achieving the objective in question. However, it must be pointed out that libration point satellites are capable of achieving all of the various objectives, although with varying degrees of success. Thus, if it were necessary to choose a mission to achieve one of the objectives mentioned above, in all but two cases the libration point satellite would appear to be a poor choice. However, in the unlikely case of the mission being such as to include all of the objectives, the libration point satellite might well be considered.

To provide a compact presentation of the results, the various comparisons are summarized in Table 2. The advantages and disadvantages of libration point satellites vs alternate missions are listed, and a preference is indicated whenever it is reasonably clear.

ACKNOWLEDGEMENT

The author wishes to express his gratitude to D. J. Alderson for his contributions to the the discussion of lunar communications satellites, and to C. R. Gates for his many helpful suggestions.

Table 2. Comparison of libration point satellites and alternate missions

Objective	Libration point satellite	Alternate missions	Preference
Communications relay	Pro: 1. Only two required 2. Relatively fixed position in Earth-Moon space Con: 1. Incomplete coverage 2. Large communications distance 3. Require station keeping	A. Lunar orbiters Pro: 1. Smaller communications distance 2. Complete coverage Con: 1. Larger number required 2. Rapid motion B. Translunar libration point play Pro: 1. Covers entire far side 2. Smaller communications distance Con: 1. Station keeping required 2. Not suitable for point to point communications on the Moon	No clear preference
Solar flare observation	Pro: 1. Long lifetime Con: 1. Larger injection energy 2. Station keeping required	A Circumlunar trajectories Pro: 1. Lower injection energy 2. No station keeping Con: 1. Shorter lifetime	Circumlunar trajectory
Determination of the mass of the Moon	Pro: 1. Simplicity of observation Con: 1. Questionable accuracy 2. No existing techniques	A. Tracking of planetary spacecraft Pro: 1. Great accuracy 2. Well defined techniques B. Lunar orbiters O. D. Pro: 1. Good accuracy	Tracking or lunar orbiter O. D.

Table 2. Comparison of libration point satellites and alternate missions (Cont'd)

Objective	Libration point satellite	Alternate missions	Preference
Optical and radio astronomy	Pro: 1. Avoids eclipsing and reflecting effects of the Earth Con: 1. Large communications distance 2. Higher energy required for injection (less payload)	A. Earth-orbiting observatories Pro: 1. Shorter communications distance 2. Lower injection energy (higher payload)	Earth-orbiting observatories
Bistatic radar astronomy	Con: 1. Station keeping required 2. Large communications distance 3. Small range of angles of incidence	A. Lunar orbiters Pro: 1. Smaller communications distance 2. Extensive range of angles of incidence	Lunar orbiters
Investigation of "dust-cloud" observations	Pro: 1. Remains on station at libration point for a long period of time	A. Fly-by with planetary spacecraft Pro: 1. Versatile Con: 1. Extremely unlikely 2. Short time in vicinity of libration point	Libration point satellite
Navigation beacon	Pro: 1. Maintains relatively fixed position in Earth-Moon space Con: 1. Complicated motion 2. Station keeping required 3. Large communications distance	A. Lunar orbiters Pro: 1. Orbits can be precisely determined Con: 1. Rapid motion in lunar sky 2. Not suitable for navigation in cislunar space	No clear preference

APPENDIX A

Satellite Motion in the Vicinity of the Stable Earth-Moon Libration Points

B. D. Tapley*

J. W. Lewallen†

ABSTRACT

The motion of a space vehicle in the vicinity of the stable Earth-Moon libration points has been studied using a model which includes the perturbing effects of the gravitational attraction and the radiation pressure of the Sun. The Earth and the Moon are assumed to move in circular orbits about their mass center, and the Earth-Moon orbit plane is assumed to be inclined at an angle of 5° 9' to the ecliptic.

The differential equations of motion in a libration point-centered coordinate system were numerically integrated to determine the behavior of the vehicle.

The results of the investigation indicate that when the effects of the Sun are included, the natural motions of a vehicle placed initially at L_4 or L_5 will not remain near the respective point. Although the vehicle does move on a trajectory about the libration point for at least 700 days, the influence of the Sun causes the vehicle to move through wide departures from the libration point.

The effects of the solar radiation pressure for several area-to-mass ratios are studied and the inpulse requirements necessary to force stability at L_4 or at a point near L_4 are determined.

*Assistant Professor, Department of Engineering Mechanics, The University of Texas.

†Research Engineer, Department of Engineering Mechanics, The University of Texas.

I. INTRODUCTION

In the space that surrounds two bodies which orbit about their mutual mass center, there are five points at which a third body will remain in equilibrium under the gravitational attractions of the other two bodies. The existence of these points was predicted by Lagrange in 1772. As shown in Fig. A-1, three of the points lie on a straight line which joins the mass centers of the first two bodies. The two remaining points lie at the vertices of two equilateral triangles which have the line joining the two bodies as a mutual base.

In establishing the existence of the five libration points, the gravitational attractions of other celestial bodies are neglected. Since, in any realizible physical system, other bodies will be present, the nature of the motion when the third body suffers a small disturbance is of interest.

If the two large bodies move in circular orbits about their mass center, the solution for the motion of a particle of negligible mass can be obtained. A particle of negligible mass is defined to be a particle whose influence on the two large bodies is negligible. If the effects of bodies other than the two original bodies are neglected, these assumptions define the "restricted three-body problem". Complete discussions of this problem and its solution are given in Refs. 1, 2, and 7. The solutions of this problem indicate that, in general, motion about the straight line points is not stable, and natural motion will not persist at these points in a real system. However, the vertex regions are stable and a body that enters either of the two vertex regions with the correct velocity will become trapped there.

The precise conditions assumed for the restricted three-body problem are not present in the solar system. However, the conditions associated with certain planetary configurations approximate these conditions with enough

accuracy to make the restricted three-body solutions of practical value. The motion of Jupiter around the Sun is one example of such a configuration and verification of the stability of the vertex regions was obtained in 1908 when the first of a number of asteroids was discovered near one of the Sun-Jupiter libration points. Subsequent observations revealed that asteroids are trapped in both of the vertex regions.

More recently, the motion of a particle in the vicinity of the libration points associated with the Earth-Moon configuration has been considered in a number of studies (Refs. 6, 7, 8, 9, 21, and 26). Several possible reasons for attempting to establish an artificial satellite at these points are discussed. Each of the investigations neglects the effects of the Sun and the other planets.

In Ref. 10, the influence of the Sun on the stability of the motion at an Earth-Moon libration point is discussed. Lyapunov's Criteria is used to demonstrate that there are points in the very near region of L_4 and L_5 where the motion will not be stable. However, the study assumes that the orbits of the Earth, the Moon and the Sun are coplanar and it neglects the influence of the Sun on the Earth and the Moon. Furthermore, no description of the motion is given and the question of whether or not the particle actually escapes from a trajectory around the libration point is not answered. That is, while the motion may be unstable very near the libration point, stable motion may be possible in another region around the libration point. Obviously, the term "stable" is used here to imply that, if the motion is stable, the particle will remain within a certain region for the period of time during which the motion is observed. The existence of such regional stability is suggested by the reported sightings of two cloud-like objects in the vicinity of the trailing Earth-Moon libration point, L_5 (Refs. 27, 28).

Following the report of these objects, an investigation was started to determine: 1) whether or not a space vehicle placed at either L_4 or L_5 would remain for an indefinite period in the vicinity of the L_4 and L_5 points and 2) what the nature of the motion would be for periods of a few years.

The effects of both the solar gravitational attraction and the solar radiation pressure are included in the analysis. The Earth-Moon orbit plane is assumed to be inclined to the ecliptic at an angle of 5° 9'. However, the eccentricity of the Moon's orbit about the Earth, the effects of the non-sphericity of the Earth and the Moon, and the effects of the other planets are neglected.

II. EQUATIONS OF MOTION

The coordinate system used to describe the motion is shown in Fig. A-2. The Earth and the Moon move in circular orbits about their mass center and the mass center, in turn, moves in a circular orbit about the Sun. The Earth-Moon orbit plane is inclined at an angle of 5° 9' to the ecliptic. Each of the bodies is treated as a mass point.

The (x, y, z) - coordinate system is centered at the Earth-Moon mass center and selected so that the x-axis points toward the Vernal Equinox of Date, the y-axis lies in the Earth-Moon orbit plane and is chosen so that the z-axis points in the direction of the angular velocity vector for the Earth-Moon configuration. The (ξ, η, ζ) - coordinate system is centered at the Earth-Moon mass center and selected so that the ξ-axis always lies along the Earth-Moon line, the η-axis lies in the Earth-Moon orbit plane and the ζ-axis coincides with the z-axis. The (ξ, η) - coordinates rotate about the ζ-axis with the same angular velocity, ω, as the Earth-Moon line. In the rotating (ξ, η, ζ) - coordinate system,

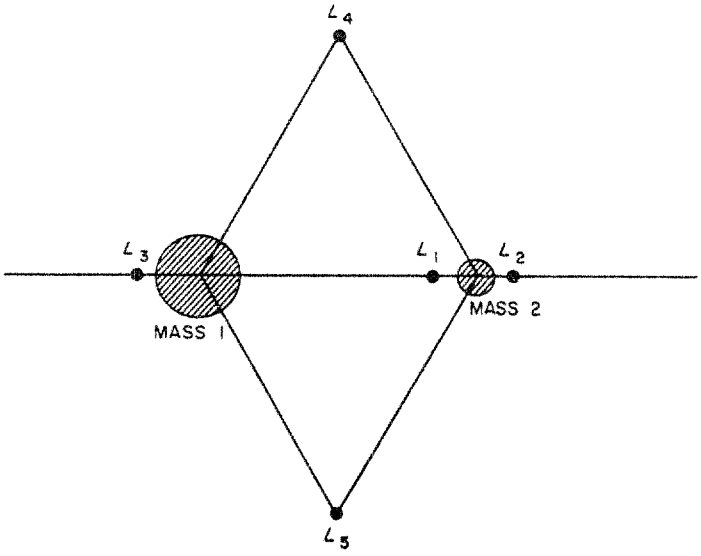

Fig. A-1. Libration points in the restricted three-body problem

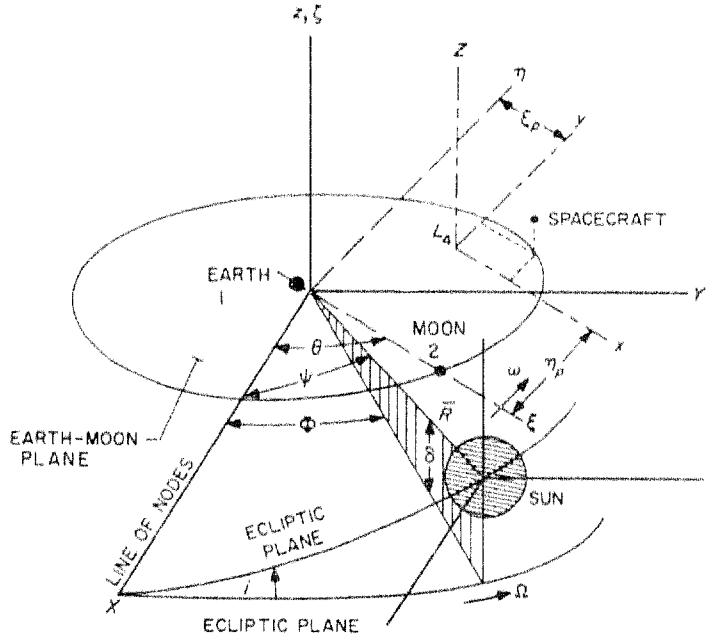

Fig. A-2. Three-dimensional illustration of the coordinate systems and spacecraft location geometry

the differential equations governing the motion of a vehicle of infinitesimal mass are

$$\ddot{\xi} - 2\omega\dot{\eta} - \omega^2\xi = -\frac{\partial V}{\partial \xi} + \frac{\partial U}{\partial \xi} + S_\xi \tag{A-1}$$

$$\ddot{\eta} + 2\omega\dot{\xi} - \omega^2\eta = -\frac{\partial V}{\partial \eta} + \frac{\partial U}{\partial \eta} + S_\eta \tag{A-2}$$

$$\ddot{\zeta} = -\frac{\partial V}{\partial \zeta} + \frac{\partial U}{\partial \zeta} + S_\zeta \tag{A-3}$$

where ($\dot{}$) indicates differentiation with respect to time. V and U are given by

$$V = \frac{Gm_1}{\rho_1} + \frac{Gm_2}{\rho_2} \tag{A-4}$$

$$U = Gm_3\left(\frac{1}{\rho_3} - \frac{\xi\xi_3 + \eta\eta_3 + \zeta\zeta_3}{R^3}\right) \tag{A-5}$$

where G is the Universal Gravitation Constant, and m_1, m_2 and m_3 are the mass of the Earth, the Moon and the Sun, respectively. ρ_1, ρ_2 and ρ_3 are the magnitudes of the distance of the Earth, the Moon and the Sun, respectively from the vehicle, and R is the magnitude of the position vector of the Sun in the (ξ, η, ζ) - coordinates. S_ξ, S_η and S_ζ are the respective components of the solar radiation pressure.

Equations (A-1 to A-3) can be transferred to the libration point-centered coordinate system, (x, y, z), by the following transformations:

$$\xi = x + \xi_p \tag{A-6}$$

$$\eta = y + \eta_p \tag{A-7}$$

$$\zeta = z \tag{A-8}$$

where ξ_p and η_p are coordinates of the libration point and are constant. If the appropriate derivatives of Eqs. (A-4 and A-5) and Eqs. (A-6 to A-8) are substituted along with Eqs. (A-6 to A-8), into Eqs. (A-1 to A-3), the differential equations of motion in the (x, y, z) - coordinate system become

$$\ddot{x} = 2\omega\dot{y} + (x + \xi_p)\omega^2 - (x_3 + \xi_p)\Omega^2 + S_x + \sum_{i=1}^{3} \frac{Gm_i}{\rho_i^3}(x_i - x) \qquad \text{(A-9)}$$

$$\ddot{y} = -2\omega\dot{x} + (y + \eta_p)\omega^2 - (y_3 + \eta_p)\Omega^2 + S_y + \sum_{i=1}^{3} \frac{Gm_i}{\rho_i^3}(y_i - y) \qquad \text{(A-10)}$$

$$\ddot{z} = -z_3\Omega^2 + S_z + \sum_{i=1}^{3} \frac{Gm_i}{\rho_i^3}(z_i - z) \qquad \text{(A-11)}$$

where Ω is the angular velocity of the Earth-Moon mass center around the Sun. The relationship $R^3\Omega^2 = Gm_3$ has been substituted into Eqs. (A-9 to A-11). ρ_i is given by the following expression:

$$\rho_i^2 = (x_i - x)^2 + (y_i - y)^2 + (z_i - z)^2 \; ; \; i = 1, 2, 3 \qquad \text{(A-12)}$$

From Fig. A-2, it can be seen that the coordinates of the Sun, (x_3, y_3, z_3), are determined by the expressions

$$x_3 = R(\cos\psi\cos\theta + \cos i \sin\psi \sin\theta) - \xi_p \qquad \text{(A-13)}$$

$$y_3 = -R(\cos\psi \sin\theta - \cos i \sin\psi \cos\theta) - \eta_p \qquad \text{(A-14)}$$

$$z_3 = R \sin\psi \sin i \qquad \text{(A-15)}$$

where R is the distance between the Sun and the Earth-Moon mass center and i is the inclination of the Earth-Moon orbit plane to the ecliptic. The angular positions of the Sun and the Earth-Moon line with respect to the Vernal Equinox

are given, respectively, by ψ and θ. The angle, θ, is measured in the Earth-Moon orbit plane and ψ is measured in the ecliptic. The relationships defining ψ and θ are:

$$\psi = \Omega t + \psi_0 \tag{A-16}$$

$$\theta = \omega t + \theta_0 \tag{A-17}$$

where ψ_0 and θ_0 are the initial angular positions of ψ and θ.

Equations (A-9 through A-15) were programmed in Fortran 60 compiler language for numerical integration with a standard numerical integration program available from the Computation Center Library at The University of Texas (Ref. 29). The program uses an Adams-Moulton integration scheme employing partial double precision arithmetic. A Runge-Kutta integration procedure is used to provide the starting values for the Adams-Moulton procedure. The computations were performed on the Control Data Corporation 1604 computer at The University of Texas.

The following values were used for the constants in the problem: $m_1 = 4.09407 \times 10^{23}$ slugs, $m_2 = 5.02154 \times 10^{21}$ slugs, $m_3 = 1.36122 \times 10^{29}$ slugs, $G = 2.33546 \times 10^{-19}$ mi^3/sec^2-slug, $\Omega = 1.99082 \times 10^{-7}$ rad/sec, $R = 9.29136 \times 10^{7}$ mi, $i = 5°9'$ and, the Earth-Moon distance, $d = 2.38855 \times 10^{5}$ mi. With the above values, the calculated value for the angular velocity of the (x, y, z) - coordinate system is $\omega = 2.665075637 \times 10^{-6}$. The synodical period and the siderial period of the Moon were taken to be 29.5306 days and 27.3217 days respectively.

III. NATURE OF THE RESTRICTED THREE-BODY MOTION

Since it can be expected that some of the characteristics of the motion in the restricted three-body problem will be present in the case considered here, it is appropriate that the general nature of the three-body motion be reviewed briefly. The differential equations describing this three-body motion can be obtained by setting Ω, m_4, S_x, S_y and S_z equal to zero in Eqs. (A-1 to A-3). The resulting differential equations can then be integrated numerically for various initial conditions to obtain the desired motion.

Figure A-3 illustrates the motion for the initial conditions; $x = y = 10$ mi, $z = \dot{x} = \dot{y} = \dot{z} = 0$. The curls in the motion are identical to those present in the analytical solution obtained after linearizing the differential equations of motion (Ref. 7). The results obtained by numerically integrating the differential equations were found to be in excellent agreement with the results obtained using the analytical solution (Ref. 6). However, regardless of the amplitude of motion for the linearized solution, the resulting motion will continue about the libration point. This is not the case for the actual restricted three-body motion.

Figure A-4 illustrates the motion resulting from the initial conditions $x = 9000$ mi, $y = z = \dot{x} = \dot{y} = \dot{z} = 0$. It can be seen that the motion rapidly diverges from the L_4 region. Hence, for some initial conditions, the actual restricted three-body motion will not be stable.

Figure A-5 shows the motion which results from the initial conditions $\dot{x} = \dot{y} = 10$ ft/sec and $x = y = z = \dot{z} = 0$. It can be noted that the amplitude of motion is much larger than the amplitude of motion for initial displacements. This would suggest that, if an attempt is made to establish a satellite at L_4 or L_5, an error in the velocity components at the libration point will have a more severe effect on the subsequent motion than an error in the displacement.

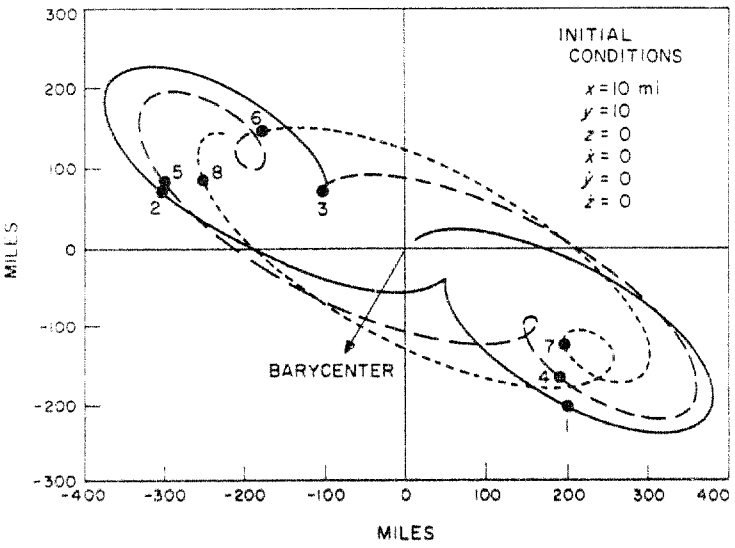

Fig. A-3. Spacecraft motion about L_4 in the restricted three-body problem resulting from an initial displacement error

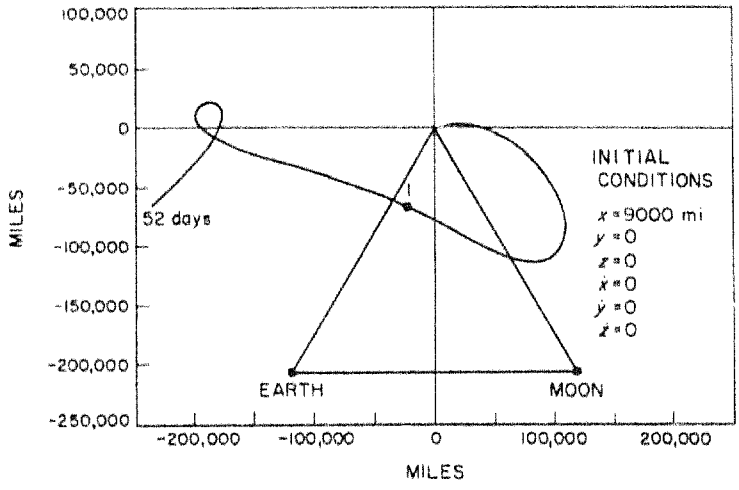

Fig. A-4. Unstable spacecraft motion about L_4 in the restricted three-body problem resulting from a large initial displacement error

It is shown in the linearized solution that the resulting motion is composed of two modes, one with a 28.62-day period and one with a 91.71-day period (Ref. 7). The superposition of these two modes yields the motion illustrated in Figs. A-3 and A-5.

IV. EFFECTS OF THE GRAVITATIONAL ATTRACTION OF THE SUN

If the effects of the Sun's gravitational attraction are included, L_4 and L_5 will no longer be stable points. It is of interest to determine how the perturbations of the Sun influence the motion of a vehicle placed at one of the libration points with zero relative velocity. The projection of the vehicle's motion on the x-y plane is shown in Figs. A-6, A-7, and A-8 for a period of 700 days. The results were obtained by numerically integrating Eqs. (A-9 to A-11) with S_x, S_y and S_z set equal to zero. Note in Fig. A-6 that after eight months, the envelope of motion exceeds 30,000 mi in the x-direction and 20,000 mi in the y-direction. This is about 100 times the envelope of the motion shown in Fig. A-3. Figures A-7 and A-8 indicate that the envelope of motion continues to grow. Furthermore, it does not appear that after 700 days a limiting value for the envelope is being approached. In Fig. A-8, it can be noted that the envelope of motion appears to be warped around a circle centered at the Earth-Moon mass center or Barycenter. The shape of the envelope appears similar to the shape of the periodic orbits reported in Ref. 8. It is interesting to note that the irregular initial motion damps out and that there is an approximate one month periodicity associated with the motion shown in Fig. A-8.

Figure A-9 illustrates the displacement in the z-direction as a function of time for a period of 250 days. The amplitude of motion is increasing with

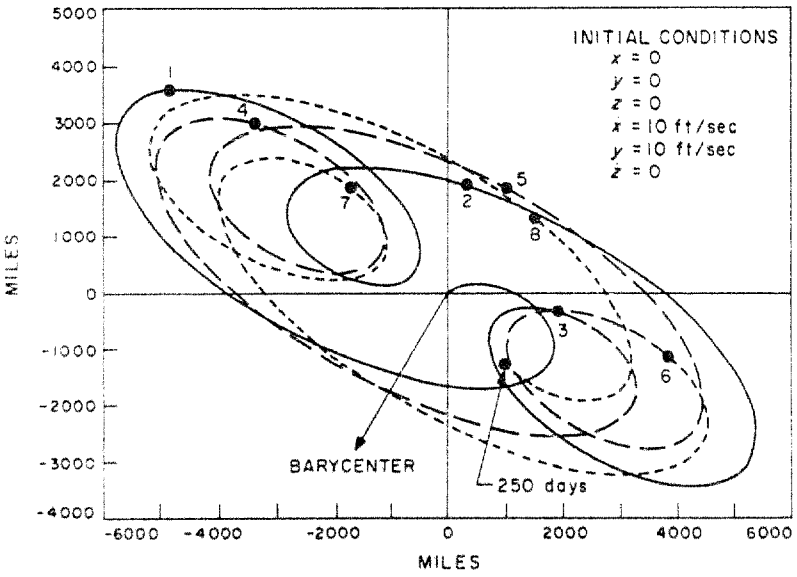

Fig. A-5. Spacecraft motion about L_4 in the restricted three-body problem resulting from an initial velocity error

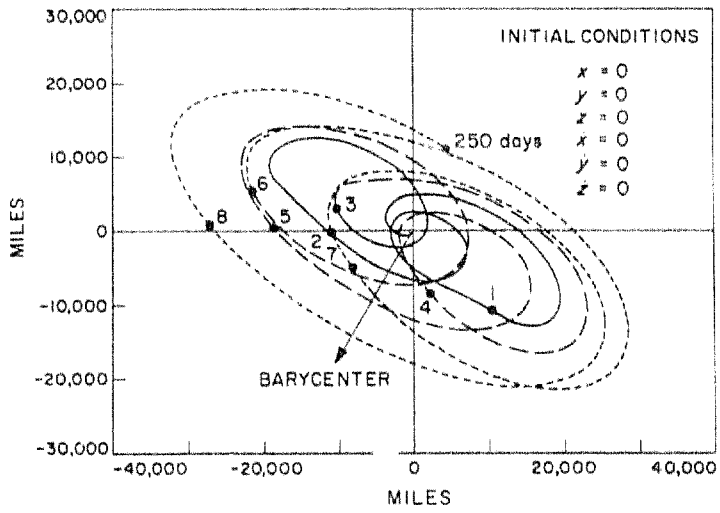

Fig. A-6. Spacecraft motion about L_4 in the very restricted four-body problem resulting from zero initial displacement and velocity errors (250 days)

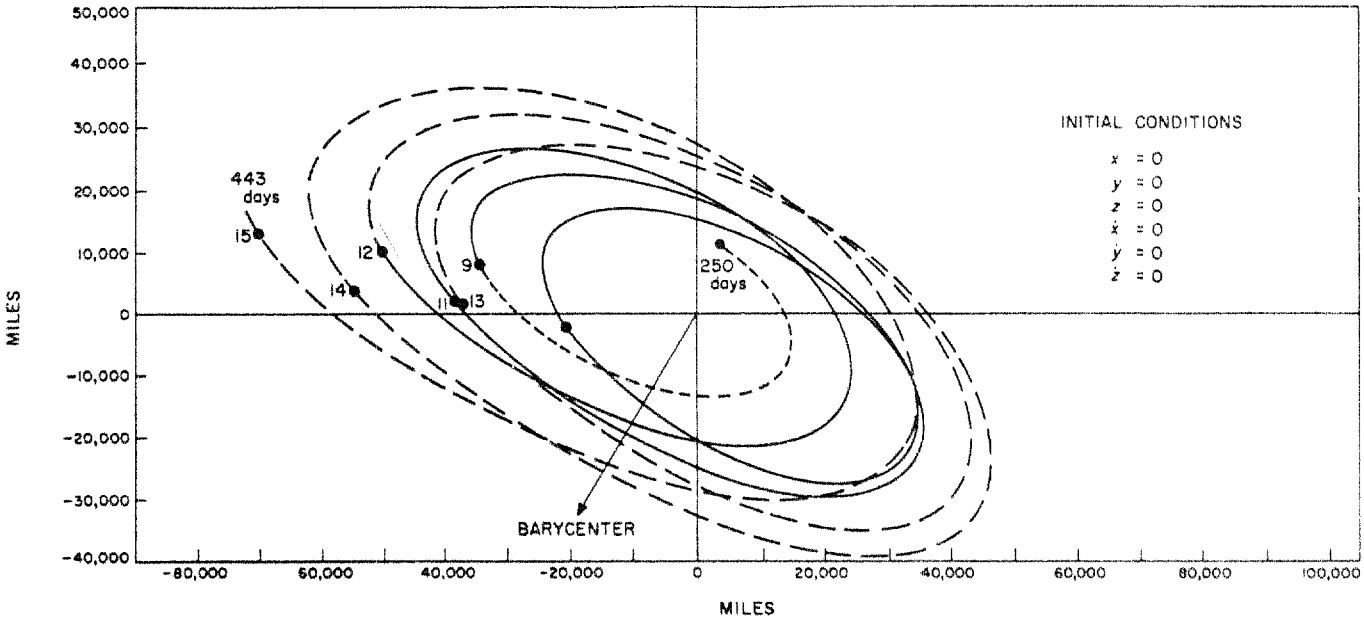

Fig. A-7. Long term spacecraft motion about L_4 in the very restricted four-body problem resulting from zero initial displacement and velocity errors (443 days)

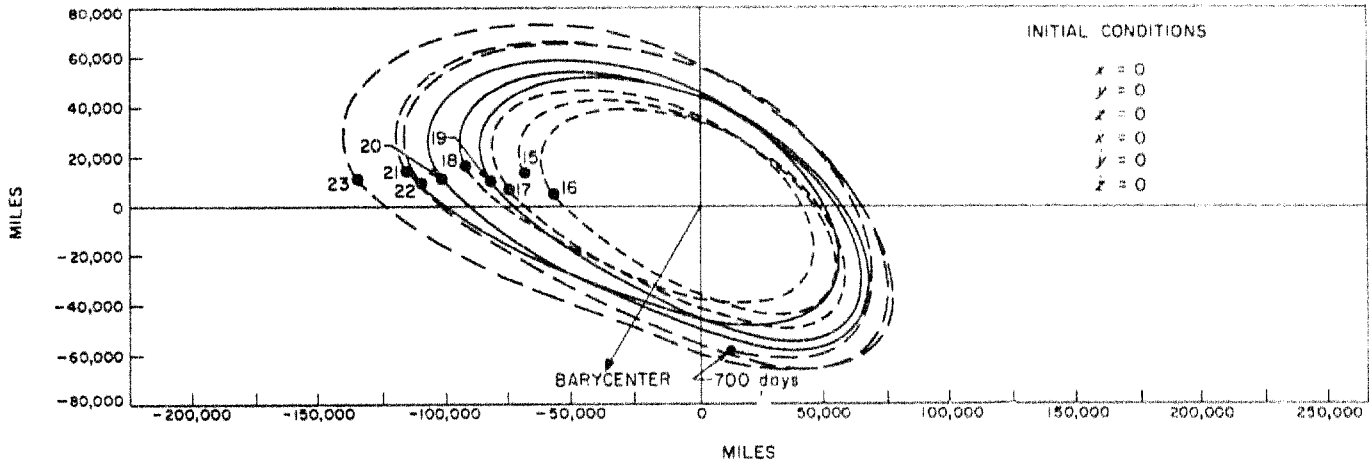

Fig. A-8. Long term spacecraft motion about L_4 in the very restricted four-body problem resulting from zero initial displacement and velocity errors (700 days)

time. The period of the motion in the z-direction is about 27.6 days. This is near the 29.53-day period for the synodical month.

Figure A-10 shows the projection of the motion on the x-y plane for the first 250 days following release with zero velocity at L_5. It can be seen that after this period the envelope of motion is somewhat larger than the envelope of the motion shown in Fig. A-6. This is explained by noting that the Sun is in the same initial position for both cases and, consequently, makes its nearest approach to L_5 one-half revolution sooner than it does for L_4. However, as in the case of the motion started at L_4, the envelope of motion appears to be growing without bound.

Although definite regional instability has not been demonstrated, it is reasonable to expect that unless the trend indicated in these results is reversed the vehicle will ultimately escape from the L_4- or L_5-centered motion.

V. EFFECT OF THE SOLAR RADIATION PRESSURE

In the study reported here, it is assumed that the solar radiation pressure is given by

$$\vec{S} = -k \frac{A}{m} \frac{\vec{\rho}_3}{\rho_3^3} \qquad \text{(A-18)}$$

where $\vec{\rho}_3 = \vec{r}_3 - \vec{r}$, A is the cross-sectional area normal to $\vec{\rho}_3$, m is the mass of the vehicle, and k is a constant. For this study, a value of $k = 4.606191 \times 10^{16}$ slug ft/sec^2 was used. From Eq. (A-18) it is apparent that the effect of the solar radiation pressure will depend on the area-to-mass ratio for the vehicle.

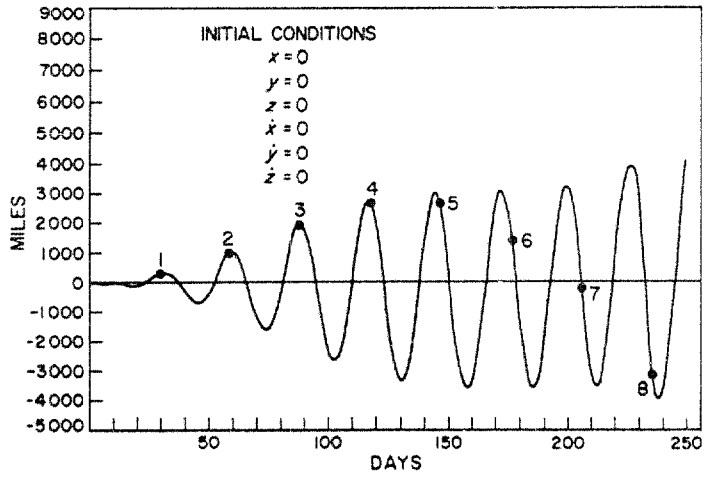

Fig. A-9. Spacecraft motion in the z-direction about L_4 in the very restricted four-body problem resulting from zero initial displacement and velocity errors

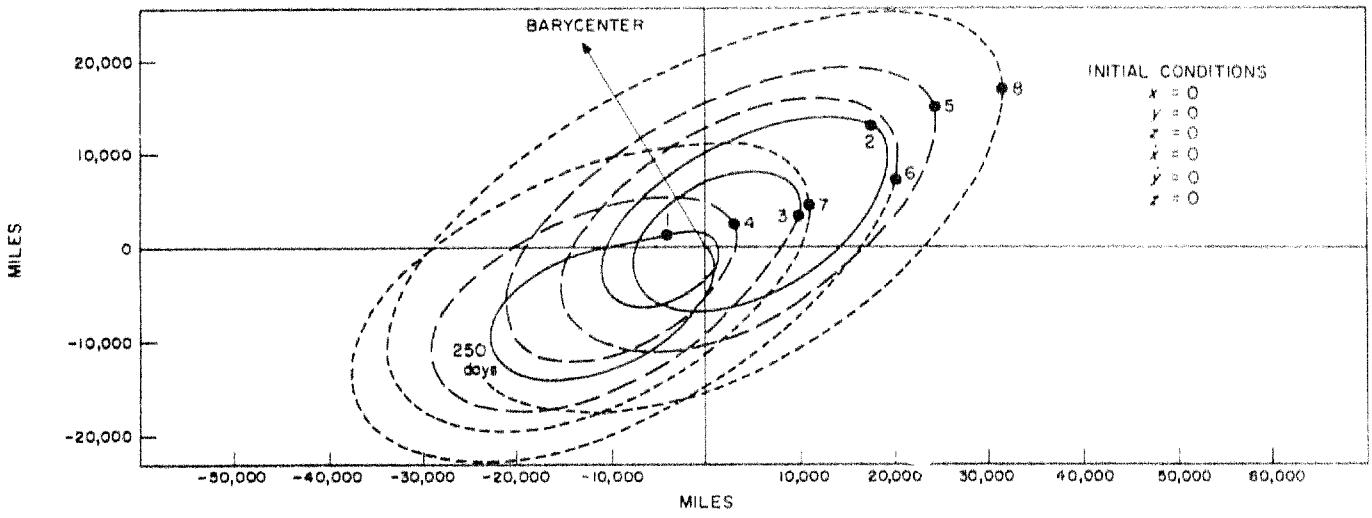

Fig. A-10. Spacecraft motion about L_5 in the very restricted four-body problem resulting from zero initial displacement and velocity errors

Figure A-11 shows the projection of the motion on the x-y plane for a vehicle released with zero velocity at L_4. Results for A/m-ratios of 0 ft^2/slug, 25 ft^2/slug and 50 ft^2/slug are shown. The results were obtained by numerically integrating Eqs. (A-9 to A-11) with the appropriate expressions for S_x, S_y and S_z. In general, it can be seen that the solar radiation pressure causes the vehicle to move farther away from L_4 in a given time. The larger A/m-ratios are associated with large envelopes of motion. The general effect of the radiation pressure is to make the motion less stable. However, if the direction and magnitude of the resultant force due to the radiation pressure could be controlled, it may be possible to bring about a reduction in the envelope of motion or, perhaps, to even stabilize the motion in a small region around the libration point.

VI. LOCATION OF EARTH-MOON-SUN EQUILIBRIUM POINTS

When the effects of the Sun are included, L_4 and L_5 are no longer equilibrium points. It is of interest to locate the equilibrium points for various orientations of the Earth, Moon and Sun. The term "equilibrium" is used here to denote a point where a particle at rest will have zero acceleration in the (x, y, z) - coordinate system. The points can be located by setting $\ddot{x} = \ddot{y} = \ddot{z} = \dot{x} = \dot{y} = \dot{z} = 0$ in Eqs. (A-9 to A-11). For a fixed value of time, the position of the Sun will be specified by Eqs. (A-13 to A-15). Hence, the three resulting non-linear algebraic equations can be solved for the location of the equilibrium points corresponding to the selected configuration.

Figure A-12 shows the x-y coordinates for a 16-day period. The points for A/m ratios of 0 ft^2/slug and 100 ft^2/slug are shown. It is interesting to note that equilibrium points lie along a circle whose center is at the Earth-Moon mass center. This agrees with the general shape of the envelope of motion shown in

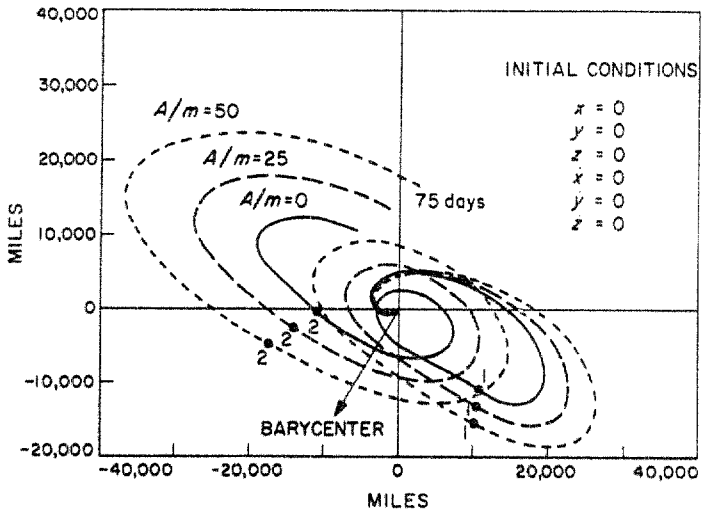

Fig. A-11. Spacecraft motion about L_4 in the restricted four-body problem considering several spacecraft area to mass ratios

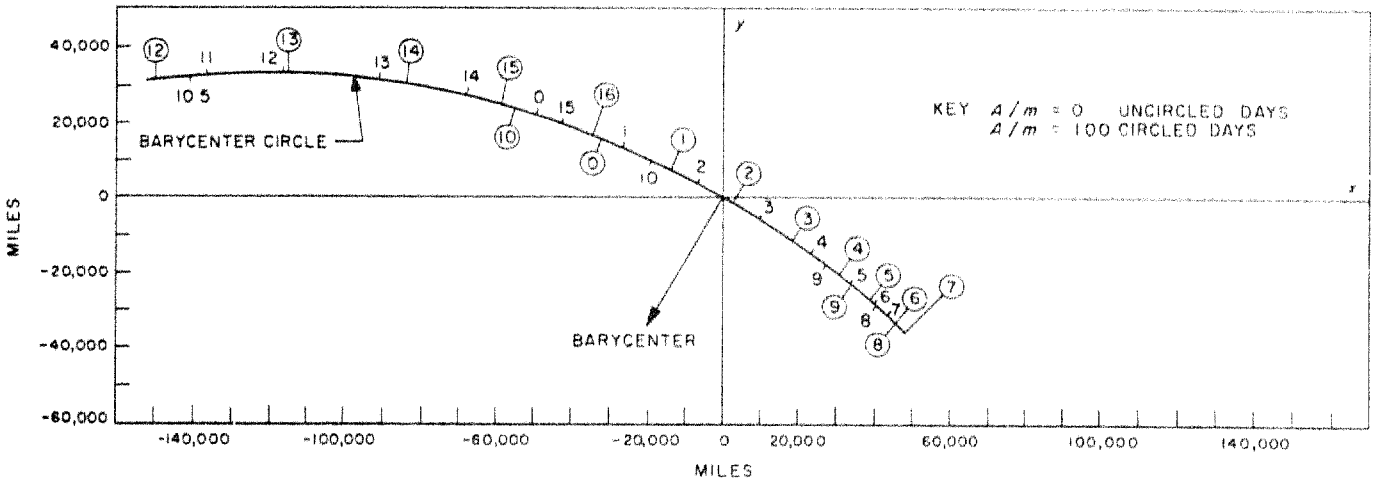

Fig. A-12. The dependent equilibrium point location in the L_4 region

Figure A-8. During the period between 10 and 14 days, the equilibrium point moves more than 140,000 mi away from L_4 in the negative x-direction. The solar radiation pressure changes the locations of the equilibrium points, but they still lie very near to the circle. For A/m = 0 ft^2/slug, the points move along the circle with a period of about 14.7 days, i.e., about one-half of the synodical period. For A/m = 100 ft^2/slug, the period required for the equilibrium point to return to its original position is just over 16 days.

VII. EFFECTS OF THE INITIAL CONDITIONS

Several sets of initial conditions were tried in an effort to find a set which would result in a small envelope of motion. Figure A-13 shows results for $\dot{x} = \dot{y} = \dot{z} = 0$ with the initial position chosen to coincide with the equilibrium point at t = 0, as shown in Fig. A-12. The subsequent motion is considerably less stable than the motion initiated at L_4 and shown in Fig. A-6.

Figure A-14 shows the motion resulting from the conditions $x = y = z = \dot{x} = \dot{y} = \dot{z} = 0$ when t = 2.4 days. This corresponds to the time when the equilibrium point is near L_4. Note that the resulting motion is less stable than the motion shown in Fig. A-6. This indicates that the resulting motion will depend on the initial position of the Sun as well as on the initial position and velocity.

Figures A-15, A-16, A-17, and A-18 show the motion resulting from an initial displacement of zero and with the respective initial velocities of a) 10 ft/sec directly away from the Barycenter, b) 10 ft/sec normal to the Barycenter - L_4 line in the direction of rotation of the coordinate system, c) 10 ft/sec directly towards the Barycenter and d) 10 ft/sec in the opposite direction of case b). It is interesting to note that the envelope of motion for

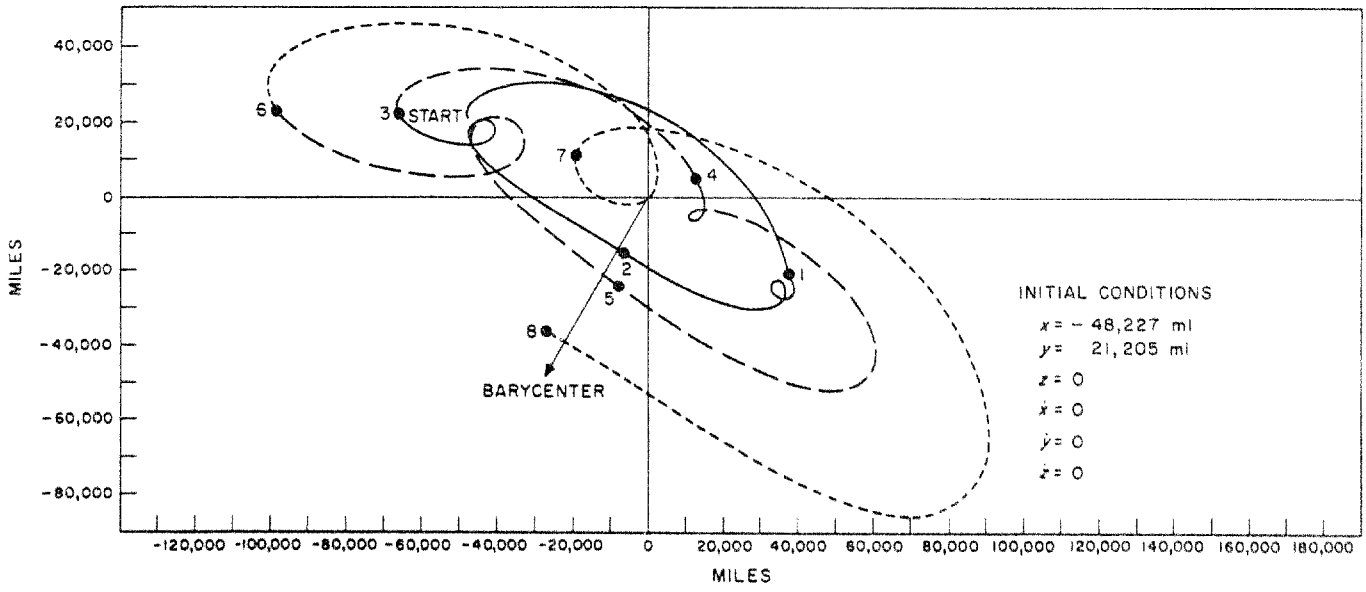

Fig. A-13. Spacecraft motion about L_4 in the very restricted four-body problem with the initial displacement corresponding to a time dependent equilibrium point

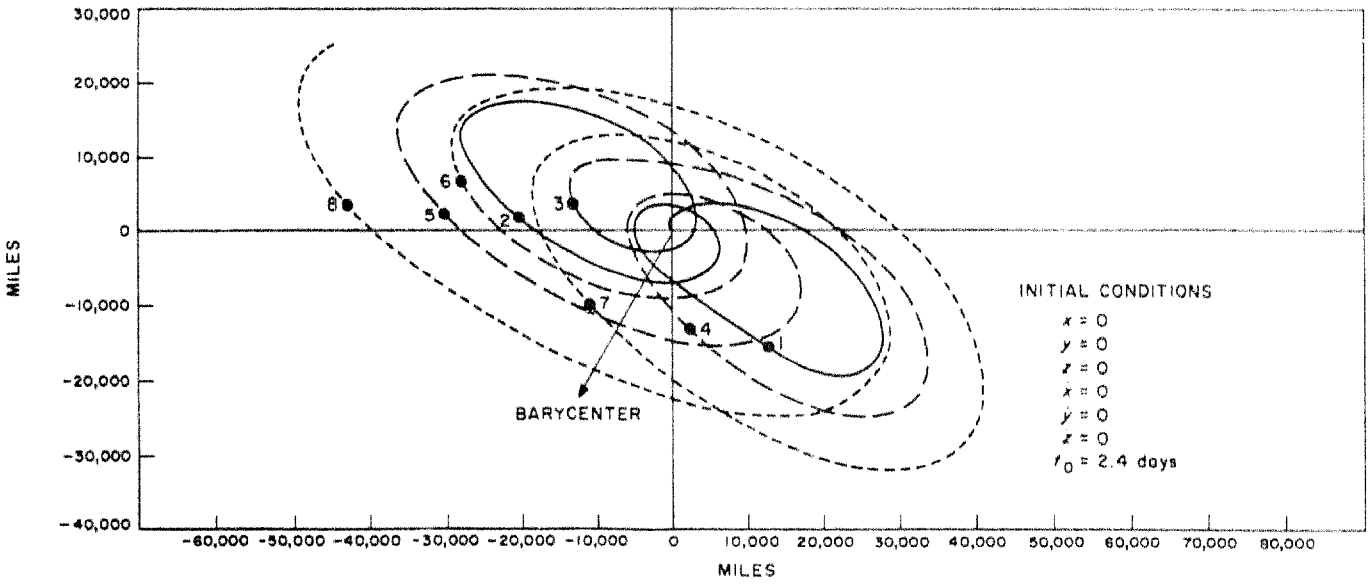

Fig. A-14. Spacecraft motion about L_4 in the very restricted four-body problem with zero initial displacement and an initial time

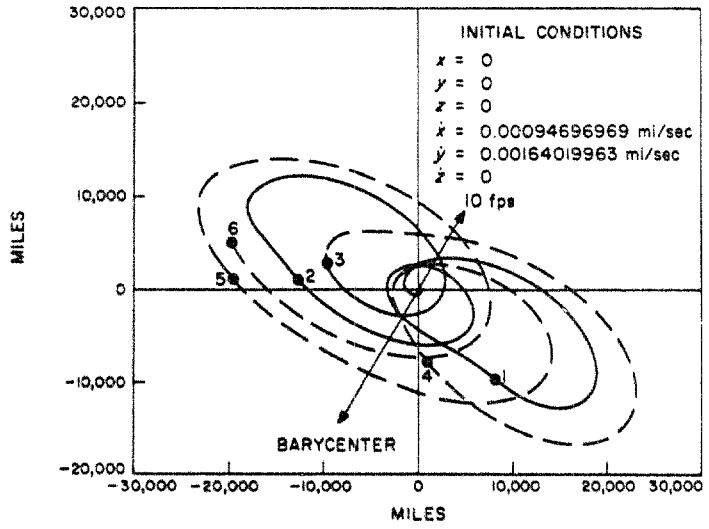

Fig. A-15. Spacecraft motion about L_4 in the very restricted four-body problem with an initial velocity of 10 ft/sec at 60 deg

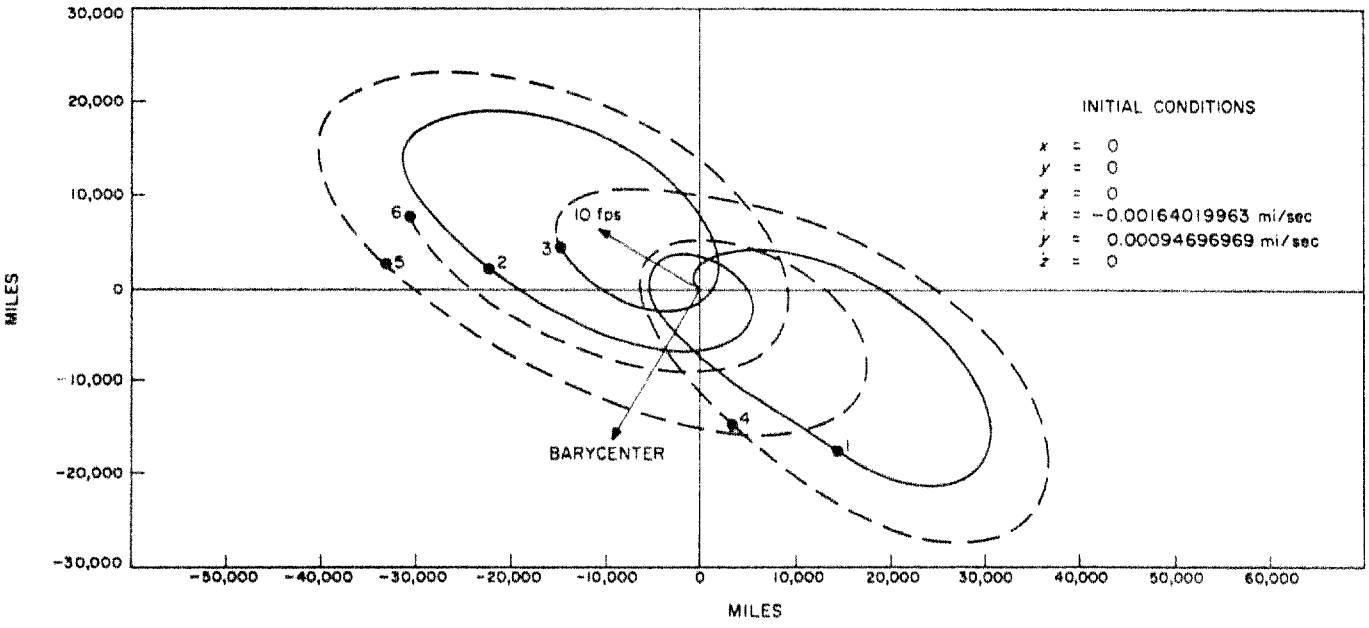

Fig. A-16. Spacecraft motion about L_4 in the very restricted four-body problem with an initial velocity of 10 ft/sec at 150 deg

Fig. A-18 is smaller at any time than the envelope of the motion shown in Fig. A-6 at a corresponding time.

Although a set of initial conditions which would result in a small envelope of motion was not found, several facts pertinent to establishing a vehicle at L_4 were illustrated. First, there is a position of the Sun at the time of arrival of the vehicle at L_4 for which the subsequent motion will have a minimum envelope. Second, to minimize the effects of errors in velocity, the approach should be made normal to the Barycenter-L_4 line. Finally, a negative value for the velocity error in the x-direction is far more detrimental to stable motion than a positive value for relative velocity error. The last two statements follow after observing that the motion shown in Fig. A-18 has a much smaller envelope of motion than either of the other three, and that the motion shown in Fig. A-18 has the largest envelope of motion at any time.

VIII. IMPULSE REQUIRED TO INDUCE STABILITY AT L_4

Figures A-19, A-20, and A-21 indicate the components of the perturbing force per unit mass due to the solar gravitational attraction in the x, y and z-directions respectively, as functions of time. Figure A-22 indicates the magnitude of the total perturbing acceleration due to the Sun as a function of time. In order to force the particle to stay at L_4, this force must be nulled by application of an appropriate thrust. The area under the curve shown in Fig. A-18 represents the magnitude of the specific impulse per unit mass of the vehicle required to force the vehicle to remain at L_4. The value of the impulse required is 2360 lb sec/slug/year. This is represented by a horizontal line in Fig. A-23. Figure A-23 also shows the impulse requirements necessary to force a vehicle to remain at various points around L_4. The angular positions of the points are

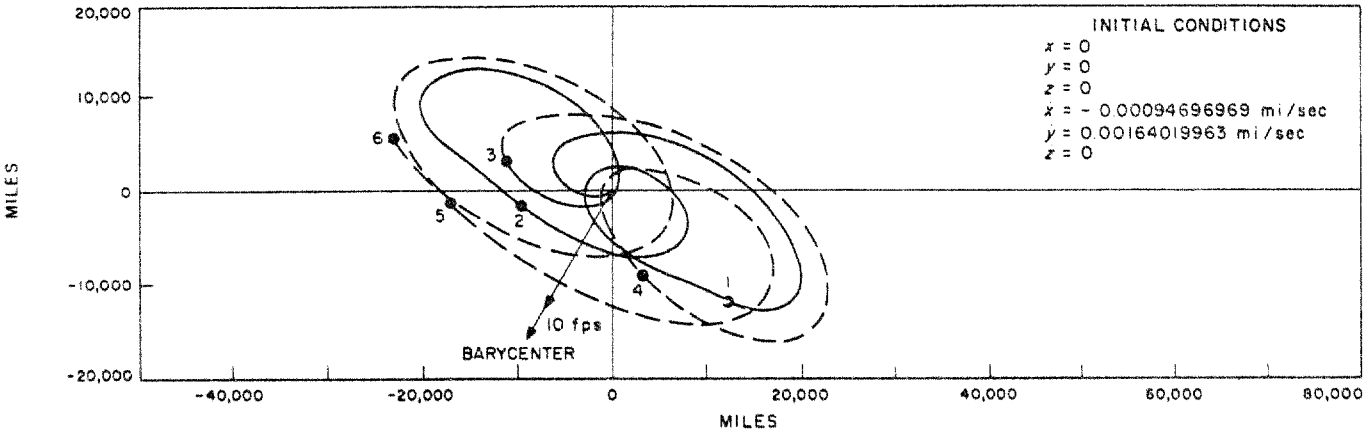

Fig. A-17. Spacecraft motion about L_4 in the very restricted four-body problem with an initial velocity of 10 ft/sec at 240 deg

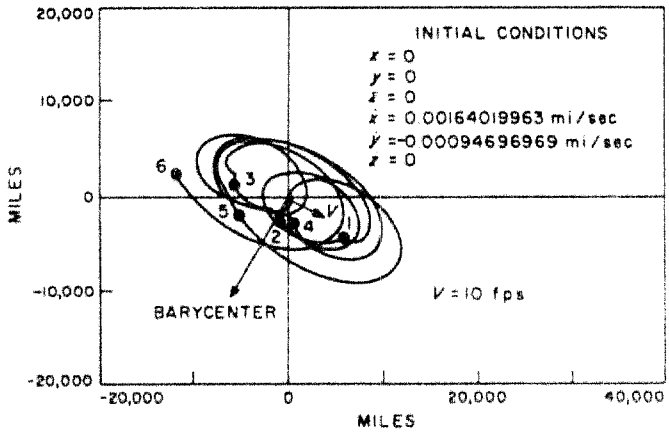

Fig. A-18. Spacecraft motion about L_4 in the very restricted four-body problem with an initial velocity of 10 ft/sec at 330 deg

Fig. A-19. Component of unit force in the x-direction as a function of time--spacecraft is constrained at L_4

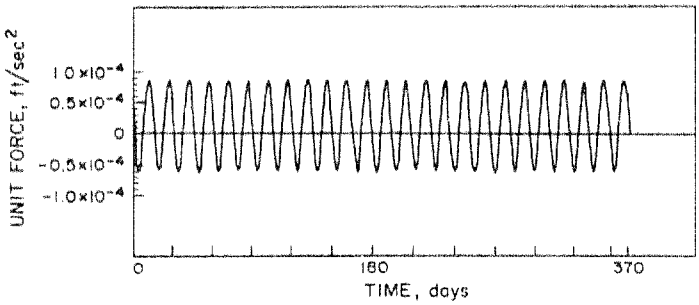

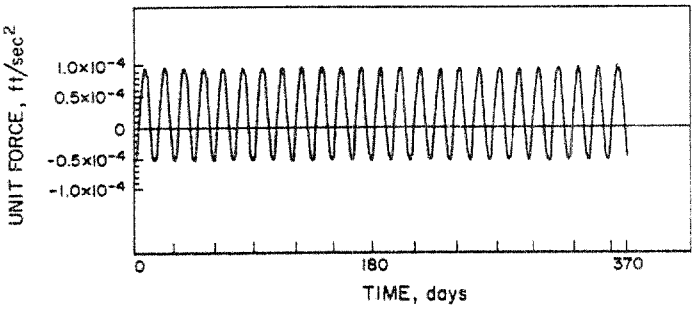

Fig. A-20. Component of unit force in the y-direction as a function of time--spacecraft is constrained at L_4

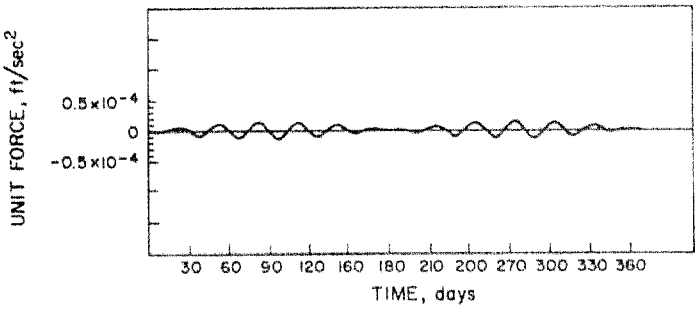

Fig. A-21. Component of unit force in the z-direction as a function of time--spacecraft is constrained at L_4

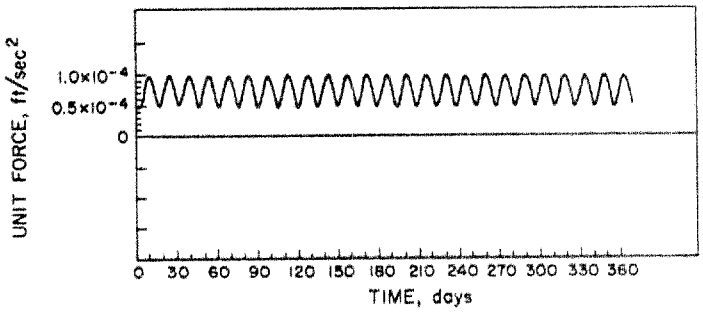

Fig. A-22. Total unit force as a function of time--spacecraft is constrained at L_4

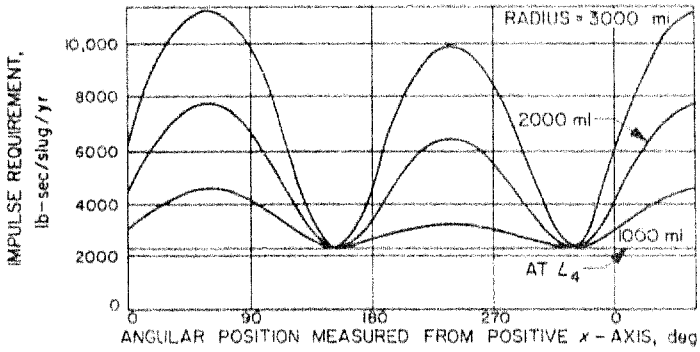

Fig. A-23. Impulse requirement to induce stability at locations in the L_4 region

measured from the positive x-axis and the radial distance is measured from L_4. The L_4-point requires the minimum impulse. At points along the Barycenter Circle no appreciable increase in impulse requirement is found. Along the L_4-Barycenter line, however, extreme increases in specific impulse requirements are necessary as the radial distance is increased. This illustrates again, the desirability of approaching the L_4-point normal to the L_4 Barycenter line during an attempt to establish a satellite at L_4.

IX. DISCUSSION OF RESULTS

While no definite conclusion concerning the stability of the motion about L_4 can be drawn from the results shown, it is obvious that the effects of the Sun cause a vehicle to move through wide departures from L_4, and the application of thrust is required to force a vehicle to remain at L_4.

As the Earth-Moon orbit plane rotates, the L_4-equilibrium point is shown to move along a circle whose center is at the Earth-Moon mass center. At times the displacement of the equilibrium point in the negative x-direction exceeds 140,000 mi.

The effects of the initial position of the Sun and the values of the initial position and the initial velocity are shown to have a decided effect on the motion. For the sets of initial conditions considered here, an initial velocity of 10 ft/sec normal to the line joining the L_4-point and the Barycenter resulted in the smallest envelope of motion.

The impulse requirement for forcing stability at L_4 for a period of one year is found to be 2360 lb sec/slug. In attempting to establish a satellite at L_4, the rendezvous approach should be made normal to the Barycenter-L_4 line to minimize the effects of errors in position and velocity.

The results of the investigation leave unexplained the reported sightings of Kordylewski (Refs. 10, 27), and a detailed investigation of the possible means by which these clouds could have been established is needed.

The results reported here were obtained after neglecting the effects of the eccentricity of the Moon's orbit, the non-sphericity of the Earth and the Moon, and the gravitational attractions of the other planets. A more detailed study including these effects should be made. A study including the first of these effects would seem to be particularly appropriate.

ACKNOWLEDGEMENT

The authors wish to acknowledge the support of this study by the Bureau of Engineering Research at The University of Texas.

APPENDIX B

Characteristics of Lunar Satellite Orbits*

J. Lorell

I. DESCRIPTION OF LUNAR SATELLITE ORBITS

A. General Considerations

In astronomy, a satellite is an object which travels in a more or less circular path around a much more massive body (e.g., the Moon is a satellite of the Earth). The usage herein, no formal definition intended, refers to satellites of the Moon (lunar satellites) as objects traveling in space primarily under the influence of the Moon's gravity, and remaining there for long periods--say of the order of weeks at least. A satellite orbit is the geometrical path through which the satellite travels.

Artificial satellites of the Moon may conceivably have any of a large variety of orbits. The main purpose of the following paragraphs is to describe and catalogue these possible orbits. Primarily, of course, the emphasis is on useful orbits, though the gamut of possibilities is mentioned.

As typically conveived, a lunar satellite follows a nearly circular path around the moon, a few hundred to a thousand miles above its surface. In any single cycle, its altitude may vary from minimum (point of closest approach or periselene) to maximum by a hundred miles or more. If the altitude is constant, the orbit is a circle and is said to have zero eccentricity. Usually, however, there is some variation between minimum and maximum altitude; the orbit is then an ellipse and its eccentricity has some value between zero and one.

*Jet Propulsion Laboratory Technical Memorandum No. 312-164, Feb. 20, 1962.

To best describe the satellite orbit, it is most convenient to distinguish between the motion of the satellite itself on the one hand, and the characteristics and motion of the orbital ellipse on the other hand. To be precise, of course, the orbit is never an exact ellipse. However, it is close to being one, and the fiction of so calling it is extremely useful.

In the following paragraphs, the characteristics of the orbital ellipse are described in detail. From this description, one can deduce general features of the satellite orbital behavior, such as its visibility from Earth, coverage of the lunar surface, stability in orbit, etc.

B. Method of Describing Orbits

1. Coordinate Systems

The most commonly used coordinate systems for orbital work are (a) rectangular coordinates and (b) spherical polar coordinates. Orientation of the axes and the origin of coordinates may be chosen in a variety of ways, according to convenience. For the present purposes, it will be convenient to use the center of mass of the Moon as the origin of coordinates and the Earth-Moon line as the x-axis (see Fig. B-1). The x-y plane is that of the Moon's orbit (which coincides very closely with that of the Moon's equator). Figure B-2 shows the relation between the rectangular coordinates and the spherical polar coordinates of a satellite.

Velocity of the satellite may be represented by its rectangular coordinate components ($\dot{x}$, $\dot{y}$, $\dot{z}$), or it may be represented in one of two spherical polar systems. In the r, ϕ, θ system, the components of velocity are just ($\dot{r}$, $r\dot{\phi}$, $r \cos \phi \, \dot{\theta}$). However, it is sometimes convenient to resolve the velocity vector into components in its own spherical polar system as indicated in Fig. B-3.

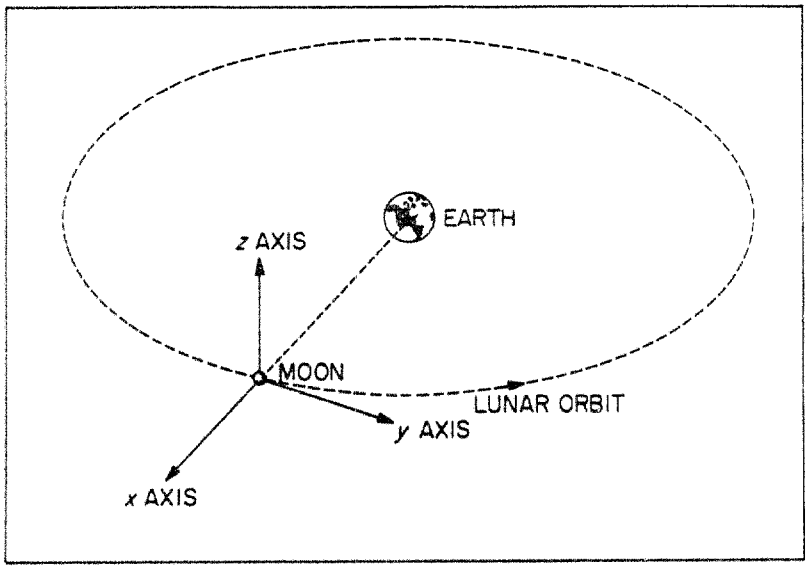

Fig. B-1. Moon-centered coordinates

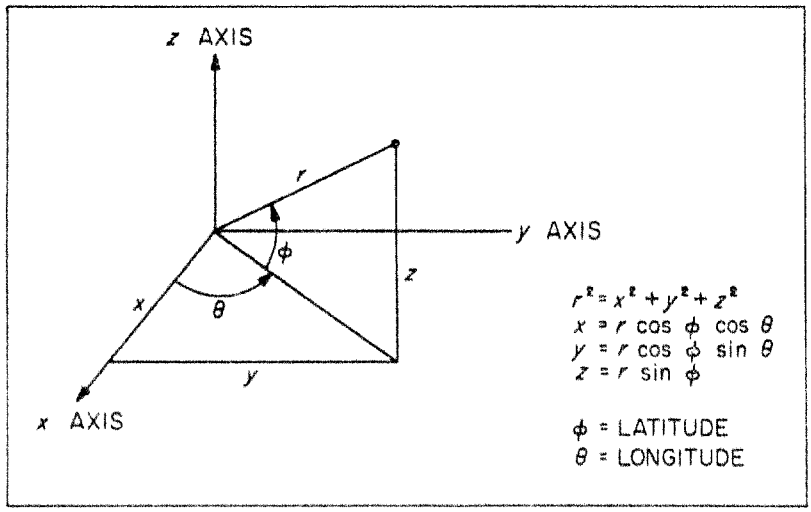

Fig. B-2. Spherical polar coordinates

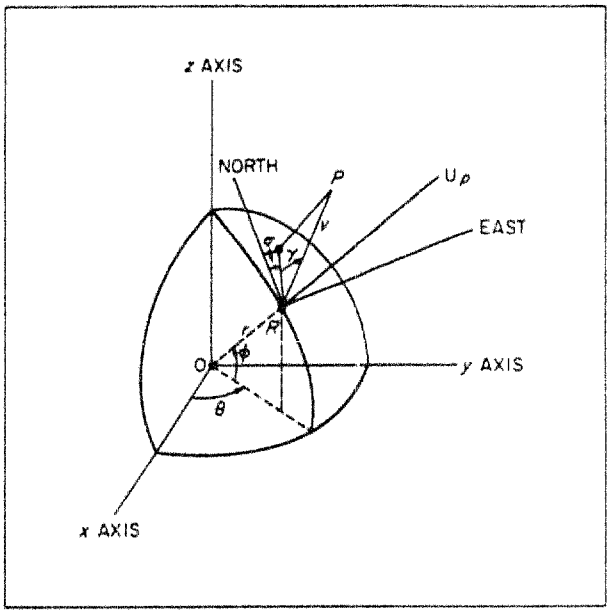

Fig. B-3. Resolution of velocity vector

Here, the velocity vector RP is given in terms of its magnitude v, azimuth angle σ, and elevation angle γ. The azimuth angle can be thought of as the angle measured clockwise from north. These coordinates are compatible with those used in interior ballistics work. Formulas for converting between rectangular velocities and polar velocities are given in Section 'II.

Other coordinate systems are used in the sequel where necessary. For example, in Section C below, the Moon's orbit about the Earth is described in Earth-centered coordinates, with the ecliptic plane as reference. As another example, it is often of interest to consider inertial velocities, in which case a non-rotating coordinate system is used.

It is important to point out before proceeding further that the Moon-centered coordinate system described above is a rotating system, with a rotation rate equal to that of the Moon in its orbit (averaging about 13 deg/day). Thus, any velocities or accelerations given in these coordinates will differ from the corresponding inertial quantities that enter into Newton's laws of motion.

In the following discussion, rates of orbital elements are always referred to in inertial coordinates.

2. Two-body Orbit Elements in the Plane

The coordinate systems of the section above are appropriate for describing the detailed position and velocity characteristics of a satellite. However, for long term description of the motion, it is convenient to focus on the geometrical structure of the orbit and to neglect the motion of the satellite itself. This is particularly useful because in perspective the orbit looks like an ellipse whose shape and position change slowly with the passage of time.

In fact, if the satellite were in an ideal two-body orbit, circling a spherical Moon, undisturbed by the gravity fields of Earth and Sun, its path would be a true geometrical ellipse, whose shape and position would remain constant.

It is of interest, therefore, to understand the characteristics of the two-body motion before proceeding to the more complicated situation.

Consider the dynamics of a small satellite S orbiting a large point mass M, with no forces acting except the gravity field of the large mass (see Fig. B-4). The equations of motion for this idealized situation can be integrated in closed form giving the following expression for r, the radial distance between S and M:

$$r = \frac{p}{1 + e \cos f} \qquad \text{(B-1)}$$

Equation (B-1) represents an ellipse with foci at M and M' as in Fig. B-4. The point M' has no direct physical significance, but is useful in describing properties of the ellipse. In fact, the ellipse has the interesting property that the sum of the distances from M and M' to any point on it is a constant, equal to the major axis, AP.

Some of the parameters which are used to describe elliptic orbits are as follows: (Notation refers to Fig. B-4)

angular momentum (per unit mass) = $h = r^2\dot{f} = x\dot{y} - y\dot{x}$

argument of periselene = ω

eccentricity = $e = 1 - PM/a$ = measure of circularity of ellipse

For a circle, $e = 0$; for an extremely elongated ellipse, e tends to 1.

energy (per unit mass) = $U = 1/2\ v^2 - \mu/r = -\mu/2a$

gravity constant = μ = measure of strength of Moon's gravity field

kinetic energy (per unit mass) = $1/2\ v^2$

major axis = $AP = 2a$

mean angular rate = $n = 2\pi/T$

mean anomaly = nt = angular position corresponding to mean angular rate after time t from periselene

period = T = time in orbit for one complete cycle

periselene = P = point of closest approach to Moon (perigee for Earth satellite, perihelion for orbit about the Sun)

potential energy (per unit mass) = $-\mu/r$

semi-latus rectum = QM = p

time of periselene passage = τ

Fundamentally, it requires only three constants to describe an ellipse in the plane, e.g., a, e, and ω. The scale is given by the semi-major axis, a, the shape is given by the eccentricity e, and the orientation by the angle of periselene, ω. In addition, the time τ at which the satellite passes periselene must be known if time relationships are of concern.

For a fixed ellipse, it is apparent that quantities such as a, e, and ω are constants. However, certain other quantities, which are not obviously constant, turn out to be integrals of the motion -- and hence, constants -- for pure elliptic motion. Thus, the energy U is constant and equal to $-\mu/2a$. Hence, the semi-major axis, a, is a measure of the energy of the satellite. Similarly, the angular momentum, h, is constant and is equal to $\sqrt{\mu p} = \sqrt{\mu a(1-e^2)}$. Together, the two parameters U and h characterize the size and shape of the ellipse.

In addition, the period T (and, thus, the mean angular rate n) is a function of a alone, given by the formula:

$$a^3 = \left(\frac{T}{2\pi}\right)^2 \mu \qquad \text{(B-2)}$$

The relation expressed by Eq. (B-2) is known as Kepler's Third Law.

The energy is particularly useful in characterizing the orbit. It is a measure not only of the scale of the orbit, but of the amount of fuel required to inject a vehicle into it. The expression

$$U = \frac{1}{2} v^2 - \frac{\mu}{r} = -\frac{\mu}{2a} \qquad \text{(B-3)}$$

shows the energy as the sum of kinetic energy $1/2\ v^2$ and potential energy $-\mu/r$. In the case of a circular orbit, Eq. (B-3) becomes

$$U_c = \frac{1}{2} v_c^2 - \frac{\mu}{a} = -\frac{\mu}{2a} \qquad \text{(B-4)}$$

which shows that the velocity in a circular orbit is constant and is given by

$$v_c = \sqrt{\frac{\mu}{a}} \qquad \text{(B-5)}$$

By way of comparing circular orbits of different sizes, it is interesting to note, using Eqs. (B-4) and (B-5), that:

1. the energy is negative
2. the larger the scale of the orbit, the larger (algebraically) is the energy.
3. the larger the scale of the orbit, the smaller is the velocity.

These comments apply in general, even to elliptical orbits of the same shape.

For the purpose of discussing lunar satellites, closed orbits such as the circular and elliptic ones under discussion are of primary interest. However, it is important to understand that non-cyclic orbits that leave the vicinity of the Moon permanently are also possible. A lunar probe launched from the Earth approaches the Moon along such an orbit. In two-body motion, these are the parabolic and hyperbolic cases (see Figs. B-5, B-6).

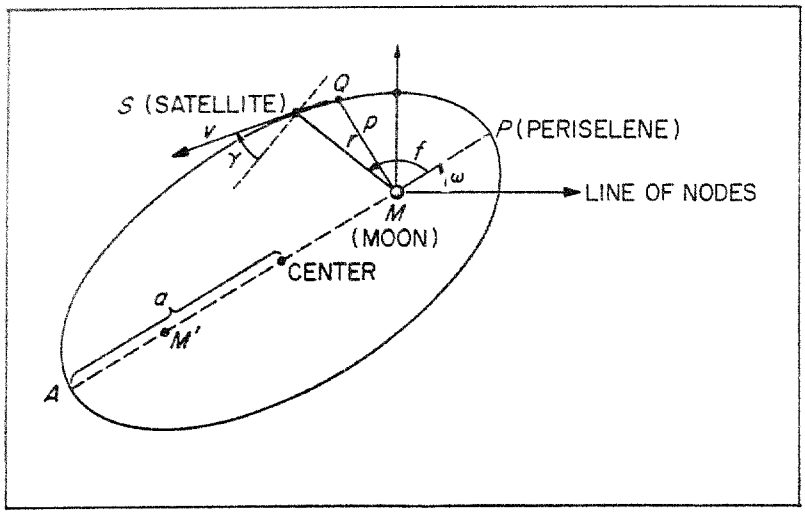

Fig. B-4. Osculating ellipse

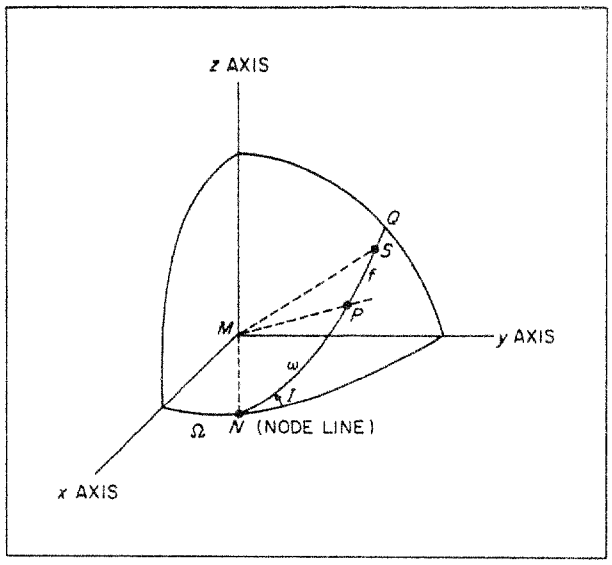

Fig. B-5. Velocity required to reach Moon

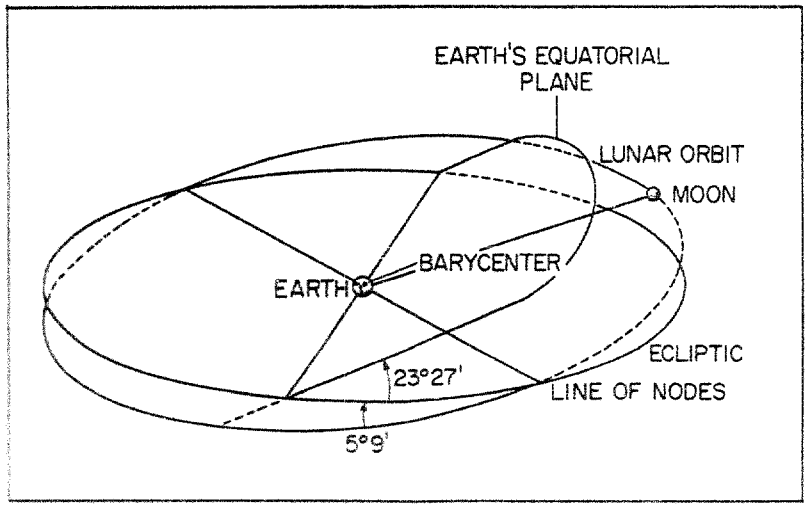

Fig. B-6. Earth-to-Moon orbit (schematic)

Whereas energy in an elliptic orbit is negative, that in a hyperbolic orbit is positive. The motion carries the satellite along an open path which comes to periselene at very high speed and then departs along a direction referred to as the departing asymptote. Obviously, such an orbit has no major axis. The quantity corresponding to the elliptic a is negative. Eccentricities for hyperbolic orbits are greater than unity.

The parabolic case divides elliptic and hyperbolic orbits -- the energy is zero, the eccentricity is unity.

Characteristics of the cases discussed are listed in Table B-1.

Table B-1. Orbit characteristics

Type of orbit	Energy	Eccentricity
Circular	Negative	0
Elliptic	Negative	$0 < e < 1$
Parabolic	Zero	1
Hyperbolic	Positive	$1 < e$

Some of the useful relationships between the parameters of elliptic motion and a summary of the nomenclature are given in Section IV.

3. Two-body Orbit Elements in Three-Dimensions

Location of the orbit in space requires only two additional parameters (beyond those already used). Since the two-body orbit, whether considered in two-dimensions or in three-dimensions is still a planar orbit, the addition of the third dimension makes it necessary only to locate the orientation of the orbit plane with reference to the coordinate system.

In Fig. B-7, the orbit has been projected on the unit sphere centered at M, with P corresponding to the periselene. Here, the argument of periselene, ω, is measured from the line of nodes MN, i.e., the line formed by the intersection of the orbit plane with the x-y plane.

The two angles required for fixing the orientation of the orbit plane in space are Ω and I. The angle Ω locates the line of nodes, while I is the inclination of the orbit plane to the reference plane. Thus, Ω and I are constant.

4. Perturbing Factors and Effects

When the force field affecting a satellite is complicated by a third body or other perturbing influence, the motion is no longer a simple ellipse. However, the motion can be described in terms of the so-called osculating ellipse. In astronomical parlance, the osculating ellipse at any instant along a satellite orbit is the ellipse that would be followed were the perturbing forces suppressed at that instant. As the satellite moves along its orbit, the osculating ellipse changes in size, shape, and position. The smaller the perturbing forces, the smaller these changes. In the limiting case of zero perturbing force, the osculating ellipse remains constant, and, of course, is just the one associated with ideal two-body motion.

What are the forces that cause perturbations? For a satellite of the Moon, the principal ones are (a) irregularity in the Moon's gravity field (i.e., departure from sphericity), (b) Earth's gravity field, (c) Sun's gravity field and (d) solar radiation pressure (important only for very low density satellites). In the case of a close Earth satellite, atmospheric drag is also important, but for the lunar satellite, of course, there is no significant atmosphere. The relative importance of these perturbing factors depends on the nature of the satellite and also on its orbit.

The effect of a perturbing force on a satellite orbit is described in terms of the elements of the osculating ellipse, namely a, e, I, ω, Ω, and τ, and of the integrals of the two-body motion, h and E. For a stable satellite, these quantities are all slowly varying. Celestial mechanics provides formulas (see Section V) for computing directly the rates of variation of the elements from the perturbing force field.

Variations in the osculating ellipse and its elements are often classified as being either of the three types:

Short-period

Long-period

Secular

Short-period variations refer to changes within one orbital period and which leave zero net change. For example, if a lunar satellite had a period of 3 hr, any periodic variations with three-hour periods would be referred to as short period. On the other hand, long-period variations refer to cyclic variations occurring with a period including many orbit cycles. Effects occurring cyclicly with the lunar month would be long period. Secular variations are non-cyclic.

In general, for close satellite orbits, the osculating ellipse is only slowly changing, and the short-period variations are of small amplitude. Thus, the short period variations are of no concern for the present purpose. In fact, most attention will be focused on the secular changes. In dealing with these, it is assumed that the short period effects have been averaged out, so that they do not appear in the results.

C. The Earth-Moon System

1. General Characteristics of the Earth-Moon System

To properly understand the behavior of lunar satellites it is important to understand the environment of such satellites -- namely the Earth-Moon system. Although the Sun and planets can have measureable effects on a lunar satellite orbit, the primary perturbations are due to Moon and Earth.

The Earth and Moon constitute a binary system of two bodies each revolving about the common center of mass, the barycenter, with a period of approximately 28 days (see Fig. B-8). The barycenter, in turn, revolves about the Sun with a period of one year.

Since the Earth is much more massive than the Moon -- by a factor of over 80 -- the barycenter is much closer to the Earth than the Moon, and in fact lies within the interior of the earth at radius of roughly 3000 mi from its center. The Moon's orbit about the Earth is roughly an ellipse with mean distance about 240,000 mi. Its plane is inclined to the ecliptic (plane of the Earth's orbit about the Sun) at an angle of about 5 deg. This plane precesses. so that the line of nodes between it and the ecliptic rotates with a period of 18 yr.

Since the Earth's equator is inclined some 23 deg to the ecliptic, the precession of the lunar orbit plane causes the inclination between it and the Earth's equator to vary between 18 and 28 deg.

Both Earth and Moon are spinning, the Earth with a period of one day, the Moon with a period of one month. Thus, the Moon always presents the same face to the Earth. The plane of the lunar equator is close to that of the lunar orbit.

Both Earth and Moon are nearly spherical, but not quite. The difference from sphericity causes perturbations in the satellite orbit. Those due to the

Earth's asphericity are not important for lunar satellites. However, the orbits of close lunar satellites are appreciably perturbed by the Moon's asphericity.

More detailed information on the Earth-Moon system is given in Section VI, which was assembled partly from information in the 1961 American Ephemeris and Nautical Almanac (Ref. 30).

2. The Restricted Three-Body Problem

Some simplification can be obtained in the study of lunar satellites by using a mathematical model in which the Earth and Moon are point masses revolving about each other in circular orbits. The resulting system neglects the comparatively small perturbations in the lunar satellite orbit due to the Sun, the eccentricity of the lunar orbit, and to the asphericity of the Earth and Moon gravity fields. However, for some purposes such as the study of loosely bound satellites, this model provides a useful tool. The problem of determining the motion of the satellite (assumed to have infinitesimal mass) in this case is called the restricted three-body problem.

The equations of motion (Section VII) for the restricted three-body problem are most simply represented in a coordinate system rotating with the two major bodies. Usually the x-axis is taken along their line of centers with the origin at the center of mass (see Fig. B-9). The y-axis is in the plane of motion and the z-axis normal to this plane forming a right-handed system. Unfortunately, even this comparatively simple set of equations cannot be integrated in closed form. However, there is an integral of the motion, the so-called Jacobi-integral, which is useful for cataloguing the satellite motion.

The restricted three-body problem may be considered as a simple extension of two-body motion, yielding the next step up in complexity. In this sense, the Jacobi-integral is an extension of the energy integral. The energy of the satellite, $U = 1/2\ v^2 - \mu/r$, is no longer constant. Instead, the Jacobi-integral

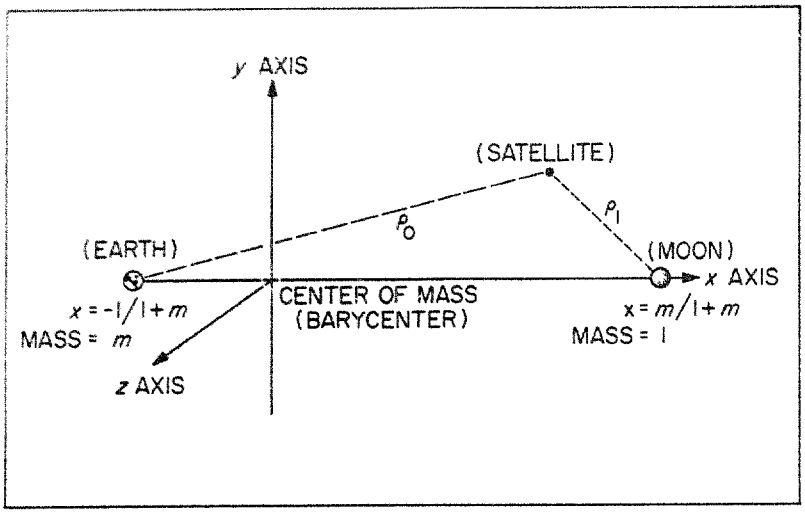

Fig. B-7. Orbit in three-dimensions

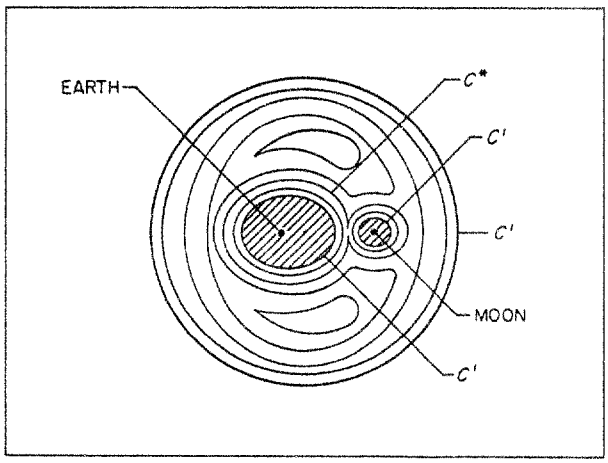

B-8. Earth-Moon system

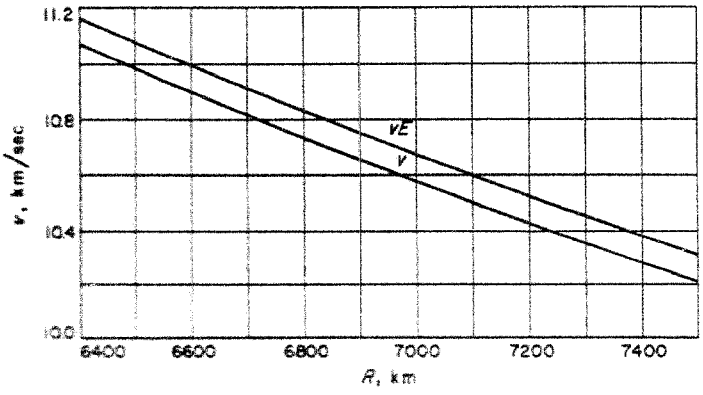

Fig. B-9. Restricted three-body problem coordinates

$$C = -\frac{1}{2}v^2 + \frac{1}{2}(n')^2(x^2 + y^2) + \frac{\mu_0}{\rho_0} + \frac{\mu_1}{\rho_1} \qquad (B-6)$$

is constant. Here n' is the angular rotation rate of the two masses, μ_0 and μ_1 are their gravity field strengths and ρ_0 and ρ_1 the respective distances to the satellite. The usefulness of the Jacobi-integral depends on the fact that to each value of C there corresponds a region in space for which motion is possible. The larger the value of C, the more restricted is the motion. Thus, by evaluating C for a particular satellite, it is possible to identify regions in space that are accessible to it, and other regions that are not accessible. In particular, if for a lunar satellite C is large enough, it will always remain a lunar satellite, and never escape to the influence of the Earth.

3. The Jacobi-Integral for the Earth-Moon System

If, in Eq. (B-6), v is set equal to zero, the resulting equation determines a surface in space. For each value of C there is one such surface (which may of course consist of several separate pieces). If the Jacobi-integral has the value C_1 for a particular orbit, and the corresponding surface is S_1, then the orbit can never penetrate S_1, but must always remain on one side of it. For otherwise, the quantity v^2 would become negative, which is not physically possible.

For satellite orbits close in to the Moon, the value of C (e.g., C') is large and the corresponding surface S forms an approximate sphere about the Moon. Another branch of S, corresponding to C' encloses the Earth. Thus, in this case there are orbits about the Moon and orbits about the Earth all corresponding to C' (see Fig. B-10). But a satellite cannot move between these two orbits if the only forces acting on it are the gravity fields of Earth and Moon.

A third branch of S consists of a cylindrical surface perpendicular to the x-y plane, and enclosing both centers of mass in its interior. Distant orbits outside this cylinder may also correspond to C'.

As the value of C decreases, the surfaces enclosing Earth and Moon grow larger, until for some value (e.g., C^*), they touch. This is the limiting value above which lunar satellites are bound to the Moon, and below which they may escape. However, there is no guarantee that orbits with smaller values of C will eventually leave the Moon.

The value of C^* (Ref. 31) for the Earth-Moon system is

$$C^* = 1.7995302 \times 10^7 \text{ ft/sec}^2$$

$$= 1.6718247 \text{ km/sec}^2$$

Thus, if for a given satellite orbit the value of C is greater than C^*, the satellite will never escape beyond the Moon's influence. If, on the other hand, C is less than C^*, it may (but not necessarily) leave the influence of the Moon and orbit the Earth or follow a complex orbit passing near each body at different times.

A more detailed discussion of the Jacobi-integral, together with sketches of the zero-velocity curves are given in Refs. 31 and 32.

D. Lunar Orbiters

1. Method of Injection from Earth into Lunar Orbit

To place a vehicle into an Earth-satellite orbit requires a velocity of some 7000 m/sec. To effect escape from the Earth requires about 11,000 m/sec. Somewhat less than escape, perhaps 10,500 m/sec is sufficient to reach the distance of the Moon. These velocities are a convenient measure of the energy requirements, and hence of the size of the rocket needed to perform a mission.

Figure B-5 shows the velocity required to reach the Moon's orbit, plotted as a function of launch distance above the center of the Earth. Escape velocity, plotted on the same graph, is seen to be only slightly greater (100 m/sec at 6800 km).

The Earth-to-Moon orbit corresponding to a launch velocity taken from Fig. B-5 is a long ellipse. If the launch is timed properly, this ellipse will pass close to the Moon (see Figs. B-6, B-11, B-12), and the Moon's influence will distort the path. From the point of view of an observer on the Moon (i. e., in Moon-fixed coordinates) the vehicle approaches and passes on a hyperbolic orbit (see Figs. B-13, B-14, B-15), and then continues back toward Earth or escapes into outer space. Only under extremely unlikely circumstances would the vehicle in its ballistic path remain in the vicinity of the Moon.

Thus, to effect injection into lunar orbit, it is necessary to apply a retarding impulse when in the vicinity of the Moon. Assuming minimum energy orbits, the velocity of the vehicle at apogee is close to zero, while that of the Moon is some 1000 m/sec - the moon overtaking the vehicle. Therefore, neglecting the effect of the Moon's gravity field, it requires an impulse of some 1000 m/sec to match the velocities. However, as will be seen in the next paragraph, a much smaller impulse is sufficient to inject into lunar orbit.

In summary then, injection into lunar orbit requires two impulses - an initial impulse of some 10,500 m/sec to inject into an Earth-Moon orbit, and a terminal impulse of something less than 1000 m/sec to inject into lunar orbit.

2. Energy Requirements for Injection into Lunar Orbit

The terminal maneuver which effects injection into lunar orbit is most efficiently made at periselene of the approach hyperbola (Fig. B-13). As noted in the preceding paragraph, the relative velocity between vehicle and Moon before the Moon's gravity field is entered is of the order of 1000 m/sec, a number

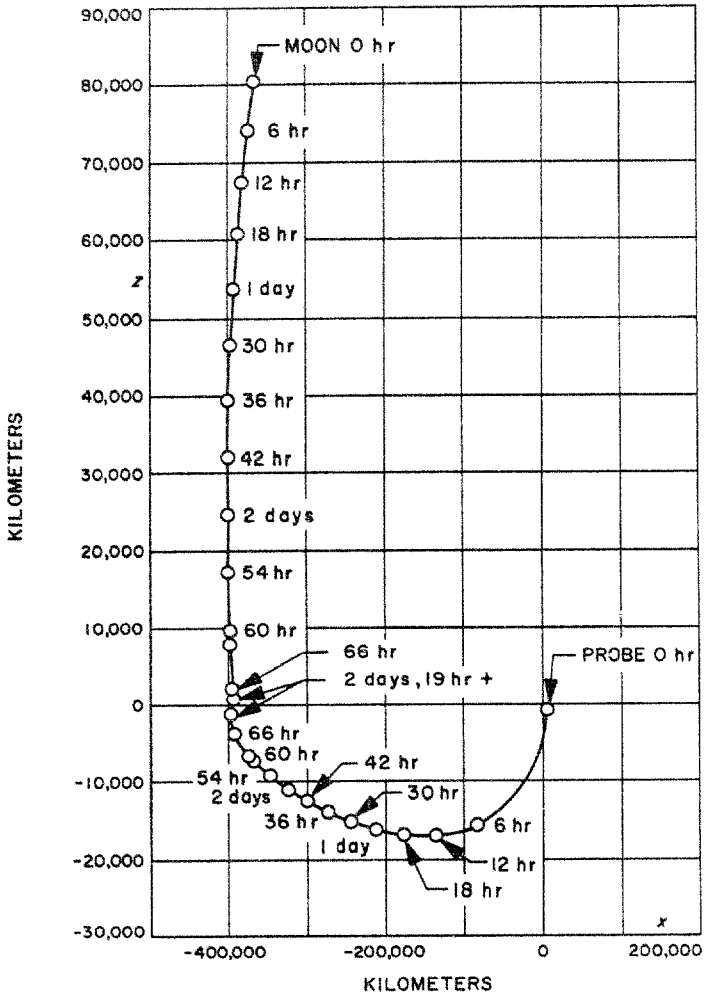

Fig. B-12. Earth-Moon orbit (x-z projection)

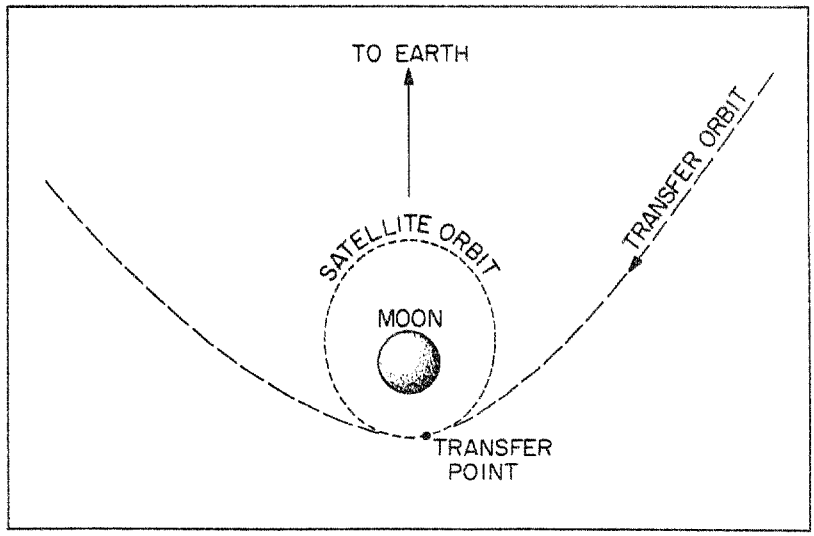

Fig. B-13. Approach to Moon, Moon fixed coordinates (schematic)

sometimes referred to as the hyperbolic excess velocity. As the Moon is approached, the vehicle is accelerated and reaches maximum velocity at the point of closest approach, the periselene (2194 m/sec in the orbit illustrated in Figs. B-14, B-15). This is the point at which the terminal impulse is to be applied, with magnitude sufficient to reduce the velocity to circular velocity (assuming a circular orbit is required). Thus, the periselene distance determines the radius of the satellite orbit. In the orbit illustrated in Figs. B-14, B-15, the periselene distance is about 3000 km from the center of the Moon, and the corresponding circular velocity is 1279 m/sec. Subtracting from the orbital velocity yields 915 m/sec as the velocity impulse required for injection into circular orbit.

Theory predicts that for any given hyperbolic excess velocity, there is an optimum orbit distance for which the retarding impulse is a minimum. Figure B-16 shows the required impulse as a function of orbit distance for several values of the hyperbolic excess velocity. Figure B-17 shows the optimum distance and impulse as a function of hyperbolic excess velocity. Formulas and derivations are given in Section VII.

3. Characteristics of Lunar Satellite Orbits

In general, a lunar satellite remains a satellite indefinitely (i.e., is stable, provided its average distance from the center of the Moon in each revolution does not exceed 25,000 km). For larger orbits, the stability is uncertain, up to perhaps 45,000 km. Beyond 45,000 km the orbit is almost certainly unstable. In this Report, the primary interest is in stable orbits.

Gross characteristics of lunar satellite orbits are shown graphically in Figs. B-18 through B-22.

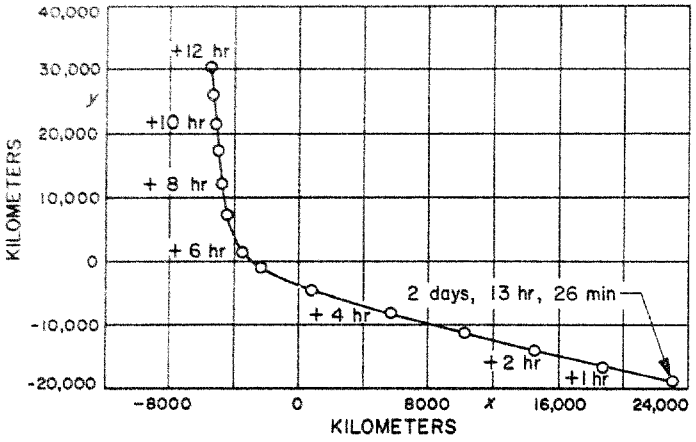

Fig. B-14. Lunar approach orbit (x-y projection)

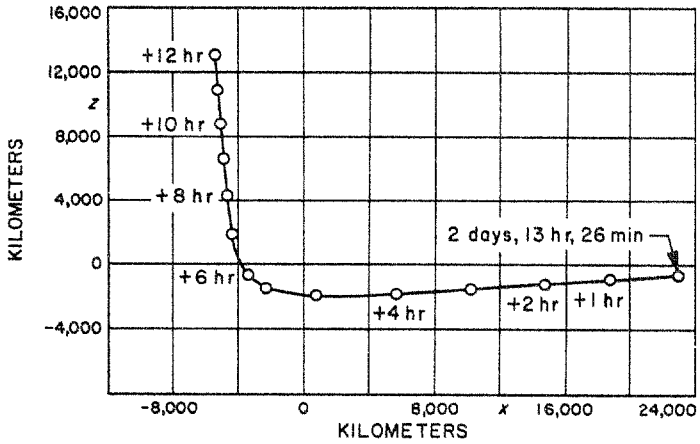

Fig. B-15. Lunar approach orbit (x-z projection)

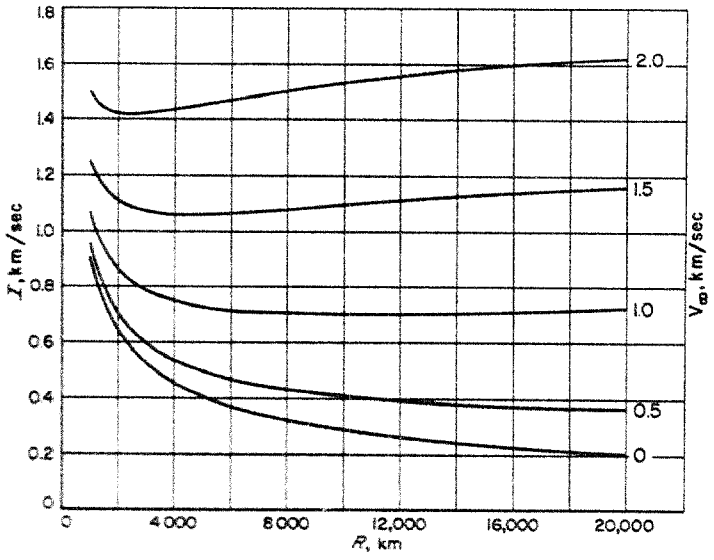

Fig. B-16. Impulse for injection into circular orbit

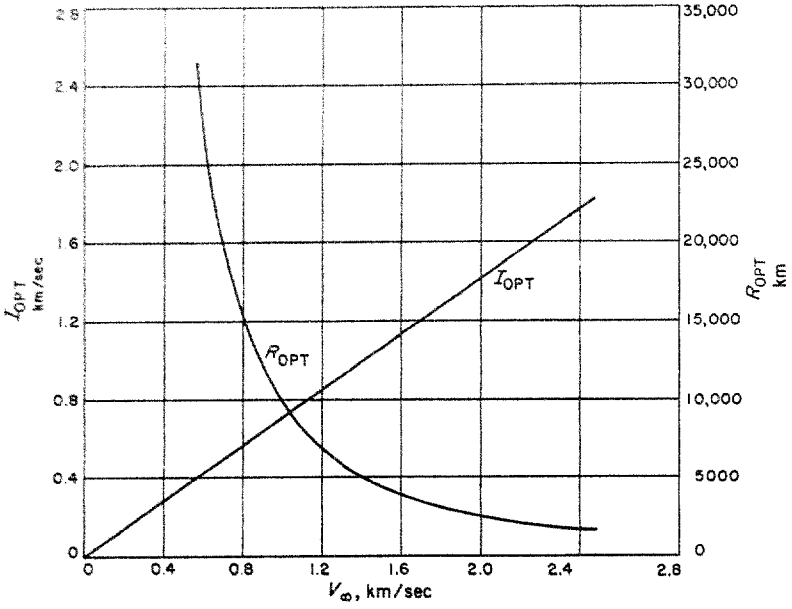

Fig. B-17. Optimum altitude for injection into circular orbit

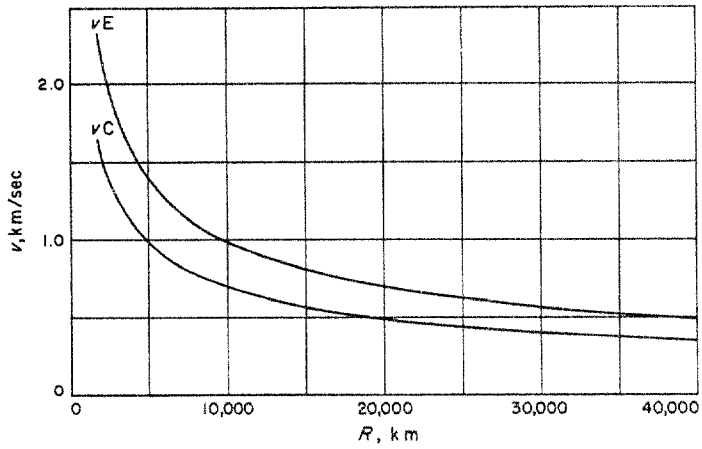

Fig. B-18. Velocity in circular orbit

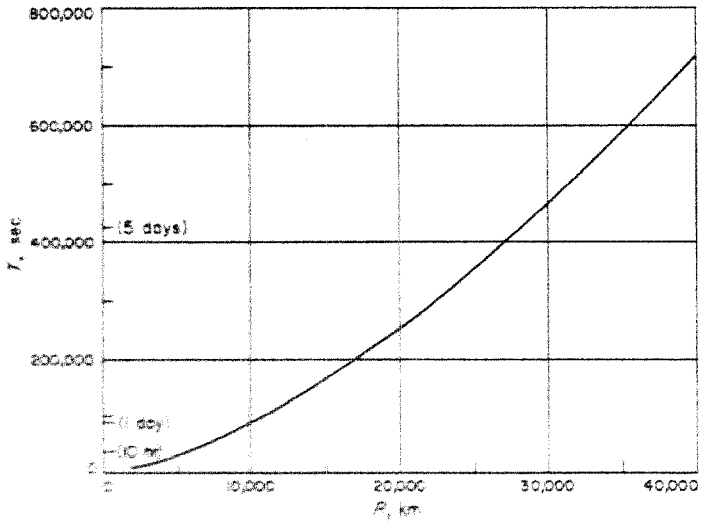

Fig. B-19. Period in circular orbit (by day)

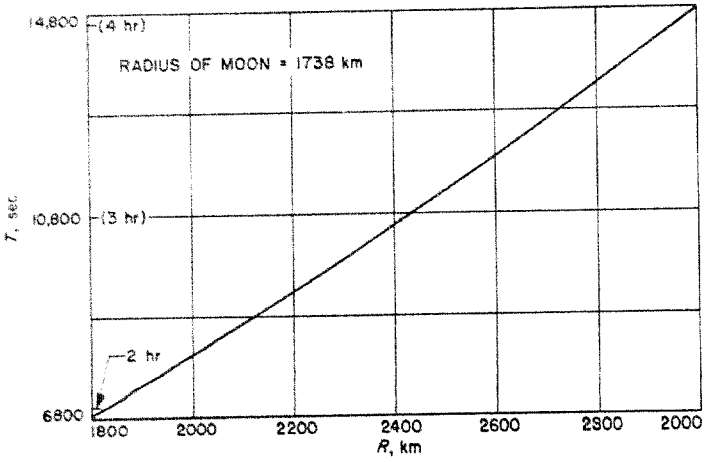

Fig. B-20. Period in circular orbit (by hour)

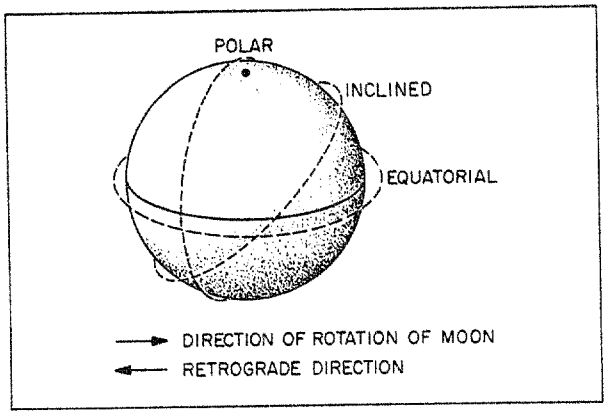

Fig. B-21. Lunar satellite orbits

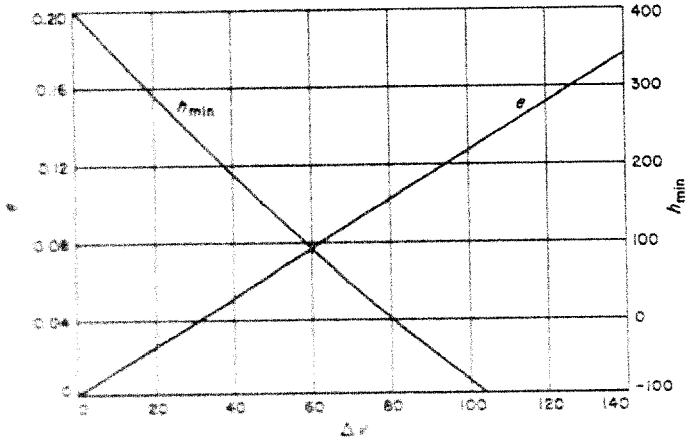

Fig. B-22. Minimum altitude as a function of error in injection velocity for 400-km orbit

Figure B-18 shows escape velocity and velocity in circular orbit as functions of distance from Moon's center. Velocities in elliptic orbits will vary somewhat from these, depending on the eccentricity. However, an estimate of the velocity can be obtained using the expression

$$v^2 = \mu\left[\frac{2}{r} - \frac{1}{a}\right]$$

in which a is the semi-major axis. With r and a in km and v in km/sec, μ has a value of about 4900. In the case of a circle, r is always equal to a and the formula reduces to $v^2 = \mu/a$. The period of an elliptic orbit varies as the three halves power of the semi-major axis, $T \sim a^{3/2}$.

Figures B-19 and B-20 exhibit this relationship for lunar satellite orbits. Close orbits have high velocity and short period. Far-out orbits have low velocity and long period. The period is long not only because the satellite travels a longer path, but because it does so more slowly.

Orbits are often classified according to inclination to the equator. In Fig. B-7, if the equator lies in the x-y plane, then I is the inclination. From geometry it can be seen that the angle I is equal to the highest latitude of the satellite in its orbit - sometimes referred to as the latitude of the orbit (see angle ϕ in Fig. B-3). The extreme cases, as shown in Fig. B-21, are orbits of zero inclination (equatorial orbits) and those of 90 deg inclination (polar orbits).

A lunar satellite in equatorial orbit always passes over the same region of the Moon, i. e., the equator. Since the Moon rotates on its axis with an angular rate of some 13 deg/(earth) day, an equatorial satellite will take slightly longer to go completely around the Moon in the direction of rotation than in the retrograde direction.

Polar satellites, on the other hand, eventually pass over the entire surface of the Moon. Assuming the orbit remains fixed in space (which it does to a first approximation), the Moon rotates beneath the orbit to provide a complete exposure in half a lunar month. For a close orbit with a period of 2 1/2 hr, each successive pass lags the previous one by about 1 1/4 deg in longitude. Thus a satellite on such an orbit sees the lunar surface at steps of 1 1/4 deg, taking fifteen days to see the whole surface.

Of course, half of each orbit is likely to be above the dark or night side of the Moon. To ensure passage of the polar satellite above all portions of the Moon during the lunar day, it would therefore be necessary to allow a full lunar month.

Eccentricity is a measure of the lack of circularity of an orbit. A perfectly circular orbit has zero eccentricity. An extremely elongated elliptic orbit has eccentricity close to, but slightly less than, one. Circular orbits are at a uniform distance from the Moon. Eccentric orbits have one point of closest approach, the periselene, at which the satellite speed is maximum. Thus, a satellite in an elongated orbit spends much more time far from the moon than close-in.

The type of orbit depends, of course, on how the satellite is injected into orbit - i. e., the height above the Moon and the velocity. The sensitivity to injection conditions may be illustrated in terms of a low circular orbit. Figure B-22 shows the minimum distance and eccentricity of a lunar satellite as a function of error in injection velocity for an orbit whose maximum distance above the lunar surface is 400 km. This graph can be used to judge the tolerable error in injection velocity for a 400-km satellite.

4. Effect of Moon's Gravity Field

Were the Moon a perfect sphere of uniform density, it would have a spherically symmetric gravity field with strength varying inversely as the square of the distance from the center of the Moon. In this case, lunar satellites would orbit the Moon in fixed ellipses (except for Earth and Sun perturbations). However, the Moon is not symmetrical. In fact, it not only has an oblateness or flattening at the poles like the Earth, but also a longitudinal asymmetry.

The non-uniformity of the gravity field is best expressed in terms of the gravity potential, which may be approximated by the expression:

$$\Phi = \frac{\mu}{r}\left[1 + \frac{J}{3}\cdot\left(\frac{r_M}{r}\right)^2\left(1-3\sin^2\phi\right) + \frac{H}{5}\cdot\left(\frac{r_M}{r}\right)^3\left(3-5\sin^2\phi\right)\sin\phi\right.$$

$$+ \frac{K}{30}\left(\frac{r_M}{r}\right)^4\left(3 - 30\sin^2\phi + 35\sin^4\phi\right)$$

$$\left. + L\left(\frac{r_M}{r}\right)^2\cos^2\phi\cos 2\theta + \cdots\right]$$

The unit term represents the spherical part of the gravity field. All of the non-spherical effects are incorporated in the dimensionless constants J, H, K, and L.

Oblateness (flattening of the poles) is measured by J which has the value 0.00031 for the Moon as compared with 0.001623 for the Earth. Thus perturbations due to oblateness can be expected to be only one fifth as large for the Moon as for the Earth.

The constants H and K for the Moon are not known well enough to assign values. It is estimated that L is about 0.61×10^{-4}. Of these constants, only L depends on the longitude θ. Thus, L is a measure of the longitudinal bulge.

To find the first order perturbations of an orbit due to the gravity field asymmetry, one refers directly to the planetary equations, as given in

Section V. Substitution of the appropriate harmonic for the perturbing function R yields formulas for the time rates of change of the orbital elements. By averaging these over a period, it is possible to obtain the long period and secular perturbations.

Figures B-23 through B-27 show the secular rates of the orbital elements due to the J and L terms in the Moon's gravity potential. The corresponding formulas are given in Section IX.

5. Effect of Earth and Sun

Perturbations due to Earth and Sun are computed basically in the same manner as those due to the Moon's asymmetry. The appropriate potential is formed and substituted in the planetary equations to give the rates of change of the elements. The appropriate potentials and rate formulas are given in Section X.

The effects of the Earth on lunar satellite orbits is shown in Figs. B-28, B-29. Solar effects are similar, but reduced in magnitude by the factor 144 (see Section X).

Figures B-30 and B-31 compare the effects of Earth and Moon's gravity field on the precession rates Ω and ω. For close in orbits, the Moon's oblateness is dominant until about 2 3/4 Moon radii. At this distance the effects are about equal. Beyond 2 3/4 radii, the oblateness contribution falls off rapidly while the Earth's effect steadily increases. At about 15 to 20 lunar radii (not shown on the figure), the Earth's effect becomes so important as to cause instability in the satellite orbit, and eventual departure from the neighborhood of the Moon.

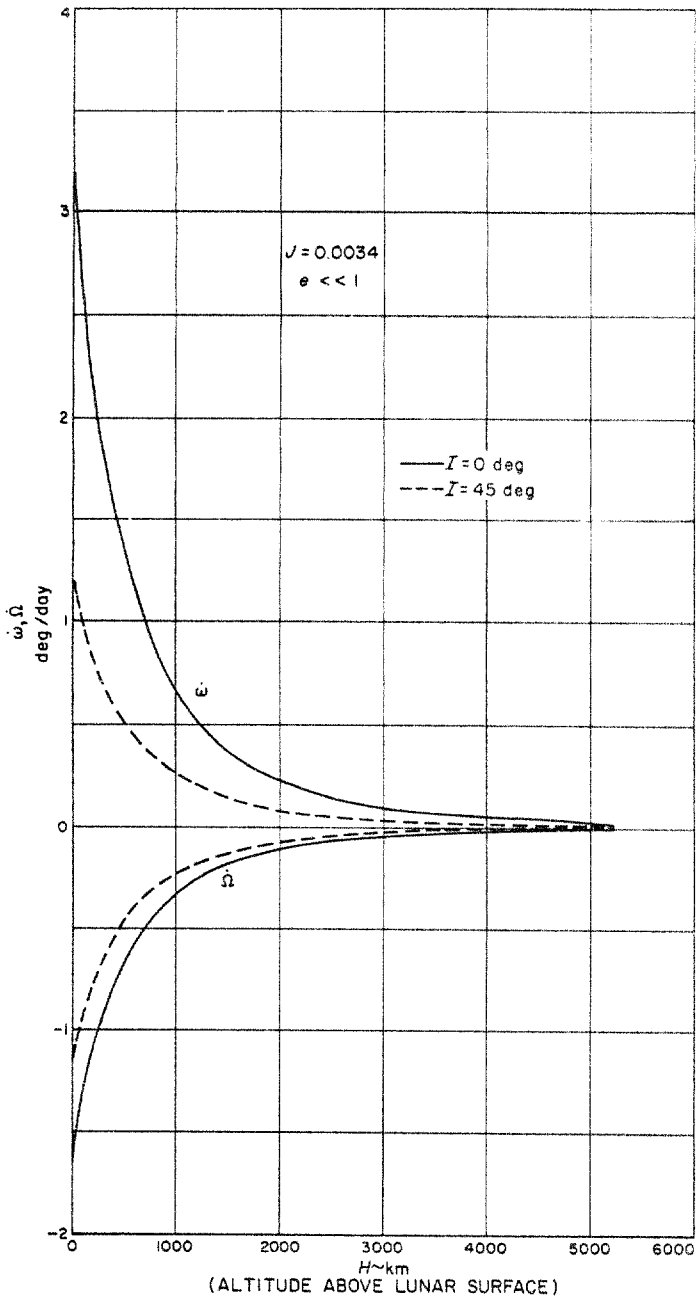

Fig. B-23. Precession rates due to J-term in Moon's gravity field--dependence on altitude

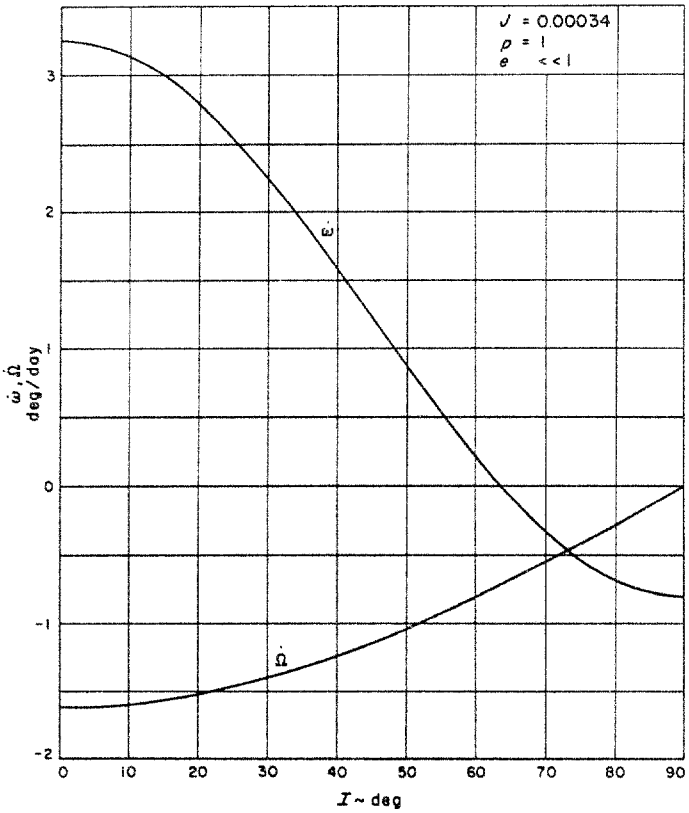

Fig. B-24. Precession rates due to J-term in Moon's gravity field--dependence on inclination (satellite orbit at lunar surface)

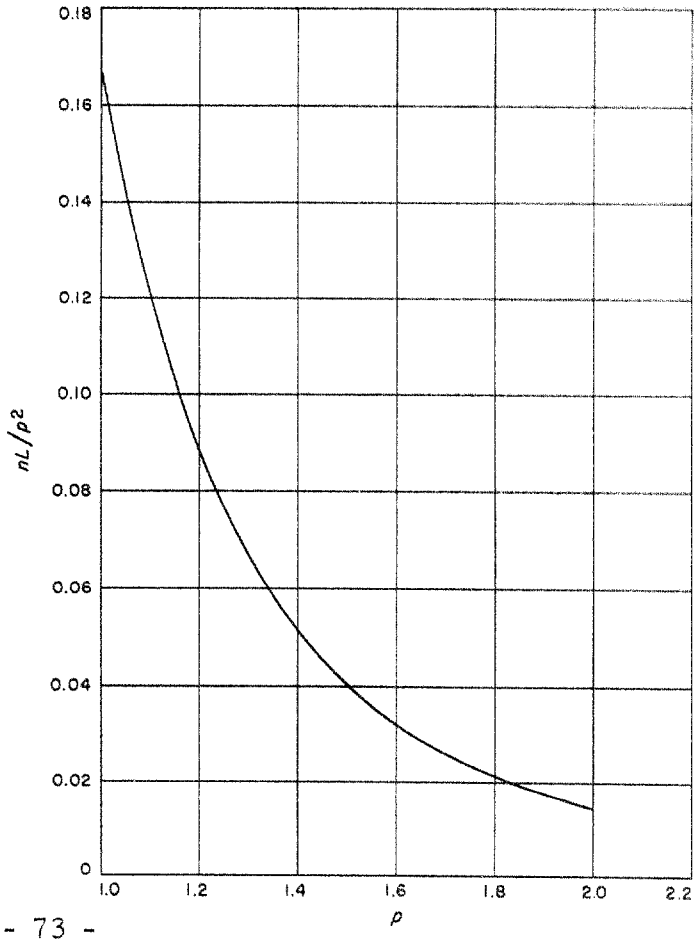

Fig. B-25. Effect of lunar bulge on precession rate

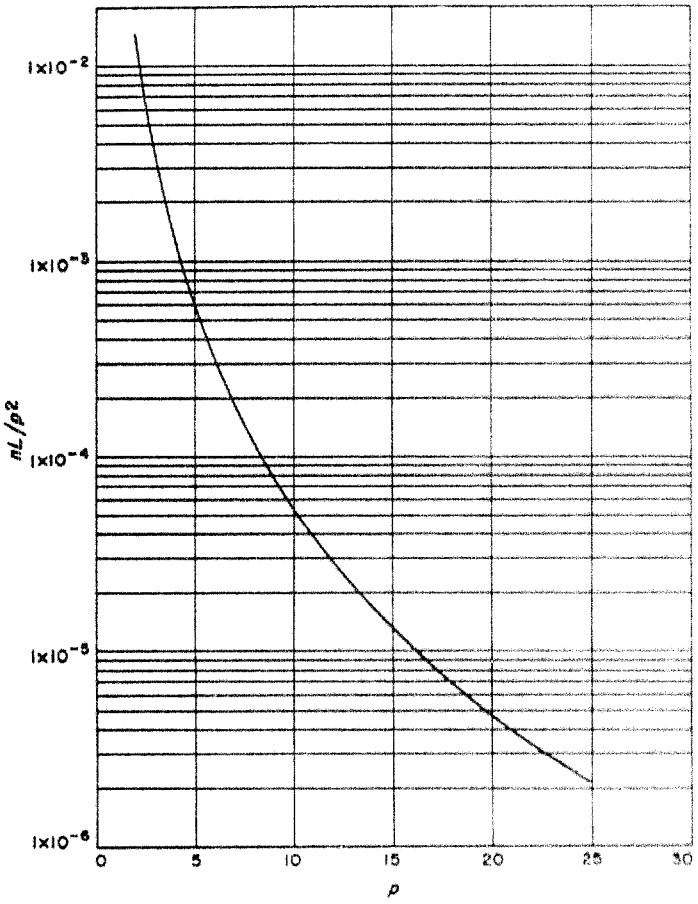

Fig. B-26. Effect of lunar bulge on precession rate

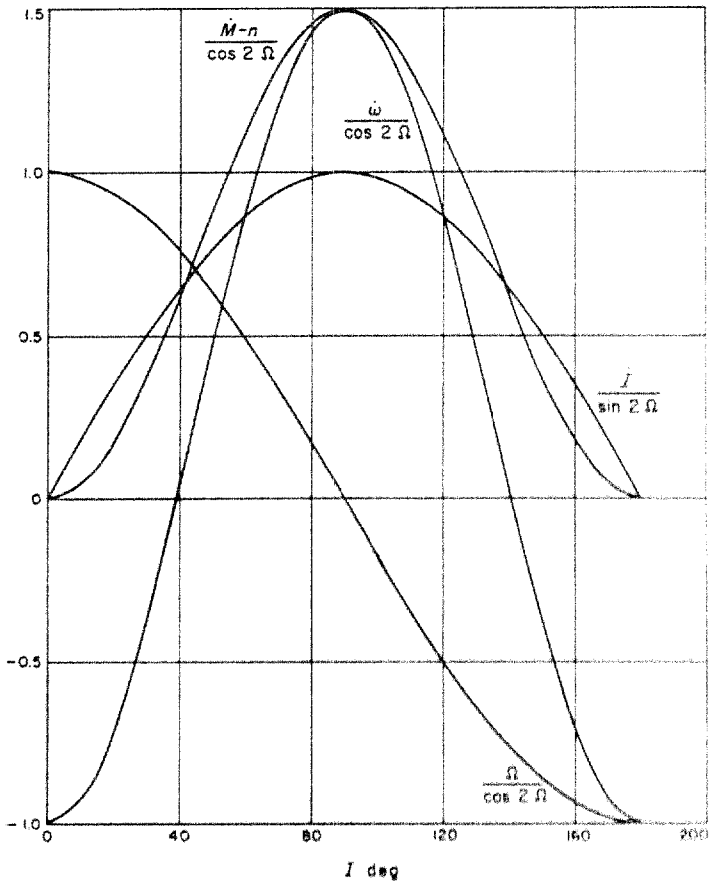

Fig. B-27. Dependence of precession rate due to bulge on orbit inclination

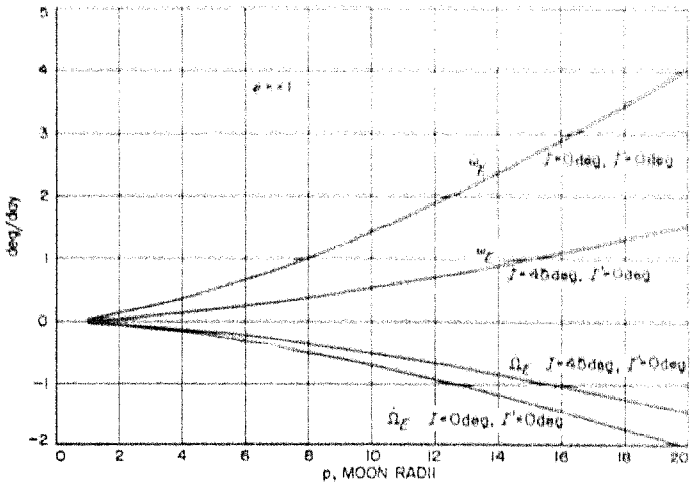

Fig. B-28. Precession rate due to Earth--dependence on distance to Moon's center

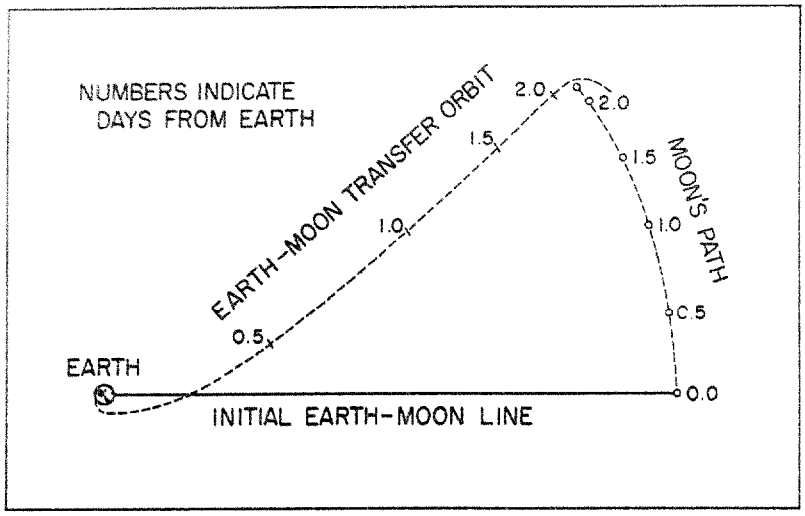

Fig. B-10. Jacobi-Integral curves of zero velocity

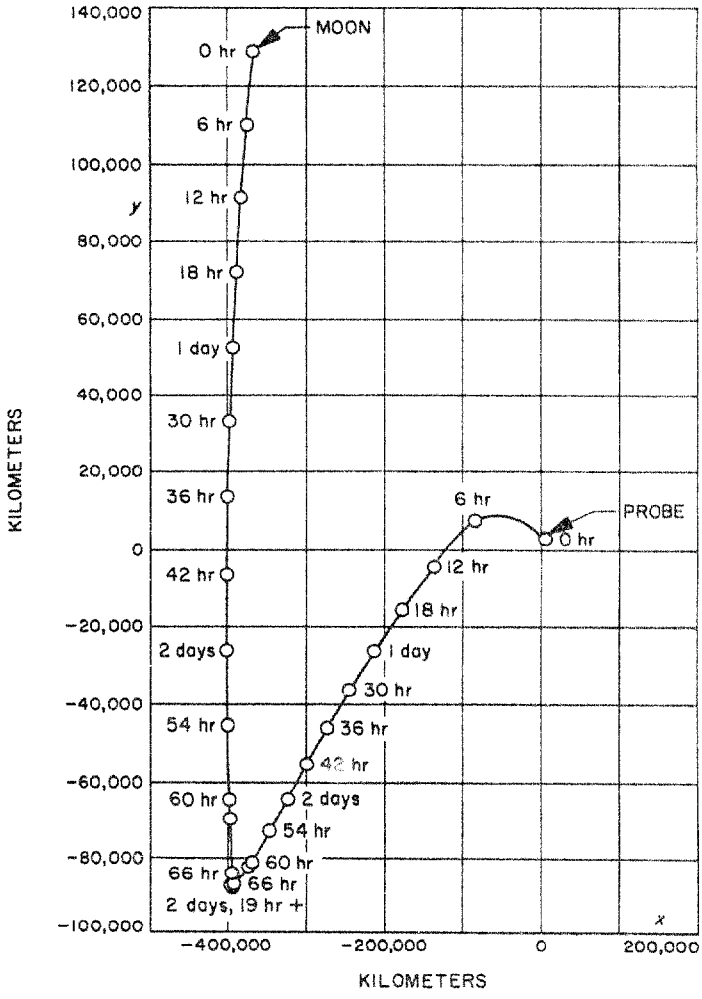

Fig. B-11. Earth-Moon orbit (x-y projection)

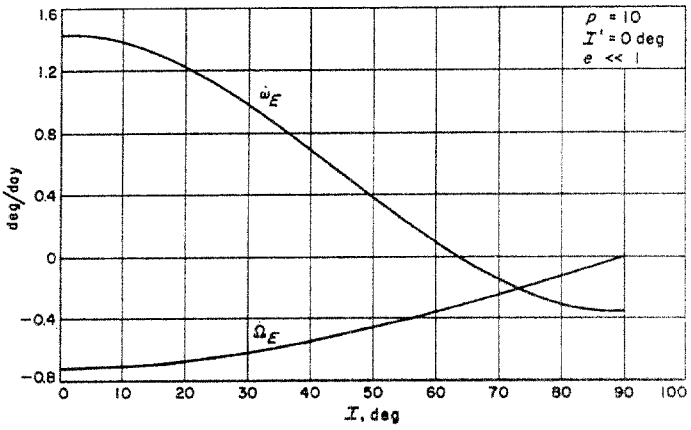

Fig. B-29. Precession rate due to Earth--dependence on inclination

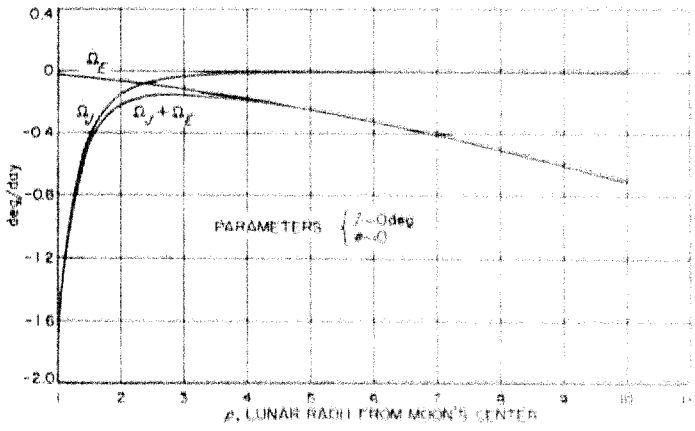

Fig. B-30. Regression of the line of nodes

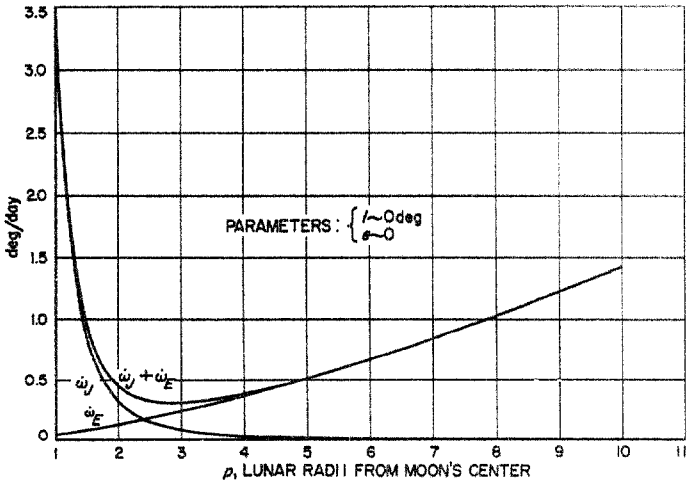

Fig. B-31. Precession of the apses

II. ORBIT DETERMINATION FOR LUNAR SATELLITES

A. The Problem

The problem of finding the orbit of a lunar satellite using Earth-based instruments is parallel in many respects to that of finding the orbits of close-binary-star systems. In both cases, the distance between observer and orbit is large compared with the major axis of the orbit. Therefore, any measurements of angular motion are at best crude. On the other hand, doppler measurements (at optical frequencies for the binary stars and at radar frequencies for the lunar satellite) may be quite precise. Thus, based on this similarity of data, techniques for orbit determination for the lunar satellite can be modeled after techniques developed for binary star.

Some extra leverage on the problem can be obtained, in the case of the lunar satellite, from the fact that the Moon is orbiting the Earth. Effectively, this provides a baseline to obtain range measurements. Without this data, only three parameters of the orbit are determinate; with it, an additional parameter can be computed. A complete description of the orbit requires still additional information.

Of course, if accurate angle data (obtained for example by optical means) is available, then a complete orbit determination can be readily derived.

B. Methods Available

In principle, the Jet Propulsion Laboratory (JPL) orbit determination program designed for use with space probes can be adapted for use with lunar satellites. Modification would be required to take care of the partial derivative computations, and perhaps for a shift of origin of coordinates in the orbit computation. Accurate results might require excessive machine time if the data is

of poor quality and/or long arcs along the orbit need be computed. As an alternative, there is a direct approach to the problem based on the specific types of data available - namely doppler measurements. Deutsch (Ref. 33) suggests the following formulas (also c.f. Ref. 34):

$$e \cos \omega = \frac{\alpha - \beta}{\alpha + \beta} \tag{B-7}$$

$$e \sin \omega = \frac{2\sqrt{\alpha\beta}}{\alpha + \beta} \cdot \frac{\Delta_2 - \Delta_1}{\Delta_2 + \Delta_1} \tag{B-8}$$

$$a \sin I = \frac{T}{4\pi} (\alpha + \beta) \sqrt{1 - e^2} \tag{B-9}$$

yielding values of $\underline{e}$, $\underline{\omega}$, and $\underline{a \sin I}$. Here

α = maximum of $\dot{r}$

β = minimum of $\dot{r}$

r = range

$\dot{r}$ = range rate

$$\Delta_1 = \int_{t_0}^{t_1} \dot{r}\, dt$$

$$\Delta_2 = \int_{t_2}^{t_0} \dot{r}\, dt$$

t_0 = time or $\dot{r}$ maximum

t_1 = time at which $\dot{r}$ = radial velocity of Moon, $\ddot{r} < 0$

t_2 = time at which $\dot{r}$ = radial velocity of Moon, $\ddot{r} > 0$

Since Eqs. (B-7) to (B-9) (which depend on range rate data only) determine only $\underline{e}$, $\underline{\omega}$, and $\underline{a \sin I}$, it is necessary to use other information to get $\underline{a}$ and $\underline{I}$ separately.

The value of $\underline{a}$ may be derived from Kepler's third law, using the equation

$$n^2 a^3 = GM_{\mathfrak{D}}$$

Then, knowledge of the product $\underline{a} \sin I$ yields the value of the inclination, I. This procedure implies prior knowledge of $M_{\mathfrak{D}}$, the mass of the Moon, which in turn limits the accuracy of the results. If, on the other hand, $\underline{a}$ could be evaluated independently of $M_{\mathfrak{D}}$, the procedure could be reversed, and $M_{\mathfrak{D}}$ evaluated by the orbit determination process. The problem, then, is to determine a value of $M_{\mathfrak{D}}$.

Since $\underline{\dot{r}}$ data from one location only determines the product $\underline{a} \sin I$, but not $\underline{a}$ nor $\underline{\sin I}$ separately, other data is needed. For the lunar satellite problem, the additional data derives from the fact that the Moon is in motion around the Earth. Thus, the "observations from coplanar directions" case of Deutsch (Ref. 35) applies.

The coordinate system used for the following formulas is oriented differently than that usually used in lunar computations. The reference plane passes through the center of the Moon, perpendicular to the line of sight from the doppler observing station. The inclination of the orbit is measured with respect to this plane.

Deutsch's formulas for determining $\underline{a}$ depend on observations from two different directions, identified below by subscripts 1 and 2. For each direction separately, it is assumed that the products

$$A_1 = a_1 \sin I_1$$

$$A_2 = a_2 \sin I_2$$

are known. The value of $\underline{a}$ is determined from the equation

$$\left[(2-\sin^2\Gamma_{12})a^4 - (A_1^2+A_2^2)a^2 + A_1^2A_2^2\sin^2(\omega_1-\omega_2)\right]^2 = a^4\cos^2\Gamma_{12}(a^2-A_1^2)(a^2-A_2^2)$$

in which Γ_{12} = angle between two observation directions ($\pm$ angular excursion of Moon). If the angle Γ_{12} is large enough, say at least 5 deg (corresponding to about 12 hr lunar travel), then the limiting factor on the accuracy of the determination of $\underline{a}$ should be Eq. (B-9). Thus

$$\frac{da}{a} \sim \frac{d\dot{r}}{\dot{r}}$$

which, in the case of a lunar satellite, and with a doppler accuracy of 0.2 m/sec, is about 10^{-4}, or a determination of $\underline{a}$ to within 200 m.

C. Application for Astronomical Determination

Aside from the usual reasons for orbit determination, i.e., to locate the satellite for planning maneuvers, for engineering evaluation, and for placing instruments involved in scientific experiments, a precisely determined orbit can also be used for astronomical purposes. Specifically, the Moon's mass, its gravity field, and its distance from the Earth can be measured with greater precision than has been done to date by other means.

The precision with which these quantities may be measured depends on that of the doppler system. For purposes of comparison, two cases are considered,

Case I $\quad d\dot{r} \sim 0.2$ m/sec

Case II $\quad d\dot{r} \sim 0.01$ m/sec

1. Lunar Mass

One method to determine the mass of the Moon, $M_{\leftmoon}$, is from the formula

$$GM_{\leftmoon} = 4\pi^2 a^3/T^2$$

which gives (assuming G is known accurately)

$$\frac{dM_{\leftmoon}}{M_{\leftmoon}} = \frac{3da}{a} \qquad \text{Case I} \quad 3 \times 10^{-4} \qquad \text{Case II} \quad 1.5 \times 10^{-5}$$

as compared with the known value given in Ref. 35:

$$M_{\oplus}/M_{\leftmoon} = 81.35$$

$$\frac{dM_{\leftmoon}}{M_{\leftmoon}} = 0.6 \times 10^{-3}$$

2. Gravity Field Asymmetry

The constants L and J for the Moon's gravity field are given by

$$L = \frac{p^2 (\dot{i} - \dot{i}_E)}{n \sin I \sin 2\Omega'}$$

$$J = -\frac{p^2 (\dot{\Omega} - \dot{\Omega}_E)}{n \cos I} + L \cos 2\Omega'$$

where

$$\dot{i}_E = -\frac{15}{16} \frac{n_3^2}{n} \frac{e^2}{\sqrt{1 - e^2}} \sin 2\omega \sin 2I$$

$$\dot{\Omega}_E = -\frac{3}{4} \frac{n_3^2}{n} \frac{\cos I}{\sqrt{1 - e^2}} \left[(1 - e^2) \cos^2 \omega + (1 + 4e^2) \sin^2 \omega \right]$$

Assuming the orbit determined, the limiting factors on accuracy of L and J are I' and α', the rates of change of inclination and node respectively. It is important also that the values of Ω and I be reasonably far from zero, i.e., an equatorial orbit is undesirable. Present values of $J_{\mathbb{D}}$ and $L_{\mathbb{D}}$ are given to about 1% accuracy. It can be expected that with a lunar satellite, the accuracy can be improved to approximate that obtained for the corresponding Earth constants, which for J is of the order of 4 parts in the sixth decimal digit, i.e.,

$$J_{\oplus} = 0.001623 \pm 4$$

Since $J_{\mathbb{D}} = 0.0003$ according to present estimates, the lunar satellite should be able to yield an order of magnitude improvement.

3. Earth-Moon Distance

The distance from Earth to Moon, D, should be measurable almost directly to give an accuracy of the same order as that for a. Hence*

	Case I	Case II
$dD \sim da$	200 m	100 m

The present value is given as (Ref. 35)

$$384,402 \pm 2 \text{ km}$$

4. Summary of Astronomical Determinations

A close lunar satellite in a non-equatorial orbit should yield accurate values of certain associated lunar constants. In particular, if the order of accuracy of the doppler measurements of the satellite is such as to yield radial velocity measurements with the accuracy

Case I: 0.2 m/sec Case II: 0.01 m/sec

*neglecting uncertainty in the knowledge of the velocity of light.

then the following accuracies can be expected in the lunar constants:

	Case I	Case II	Present
$\frac{dM_{\mathbb{D}}}{M_{\mathbb{D}}}$	3×10^{-4}	1.5×10^{-5}	0.6×10^{-3}
$J_{\mathbb{D}}$, $L_{\mathbb{D}}$	$\pm 4 \times 10^{-6}$		$\pm 1 \times 10^{-5}$
D (meters)	±200	±100	±2000

Note that the value of D depends directly on the value of $R_{\oplus}$ which is given at present to ±100 m.

III. FORMULAS FOR CONVERSION BETWEEN RECTANGULAR AND POLAR COORDINATES

$$x = r \cos \phi \cos \theta$$

$$y = r \cos \phi \sin \theta$$

$$z = r \sin \phi$$

$$\dot{x} = -v \cos \gamma \sin \sigma \sin \theta - v \cos \gamma \sin \phi \cos \sigma \cos \theta + v \sin \gamma \cos \phi \cos \theta$$

$$\dot{y} = v \cos \gamma \sin \sigma \cos \theta - v \cos \gamma \sin \phi \cos \sigma \sin \theta + v \sin \gamma \cos \phi \sin \theta$$

$$\dot{z} = v \sin \gamma \sin \phi + v \cos \gamma \cos \phi \cos \sigma$$

$$r^2 = x^2 + y^2 + z^2$$

$$\phi = \sin^{-1} \frac{z}{r} = \cos^{-1} \frac{\sqrt{x^2 + y^2}}{r}, \quad -\frac{\pi}{2} \leq \phi \leq \frac{\pi}{2}$$

$$\theta = \sin^{-1} \frac{y}{r \cos \phi} = \cos^{-1} \frac{x}{r \cos \phi}, \quad 0 \leq \theta < 2\pi$$

$$v^2 = \dot{x}^2 + \dot{y}^2 + \dot{z}^2$$

$$\rho^2 = x^2 + y^2$$

$$\gamma = \sin^{-1} \frac{x\dot{x} + y\dot{y} + z\dot{z}}{rv}, \quad -\frac{\pi}{2} \leq \gamma \leq \frac{\pi}{2}$$

$$\sigma = \begin{cases} \cos^{-1} \dfrac{\rho^2 \dot{z} - (x\dot{x} + y\dot{y})\, z}{\rho\, r\, v \cos\gamma} \\ \sin^{-1} \dfrac{(x\dot{y} - y\dot{x})\, r}{\rho^2\, v \cos\gamma} \end{cases} \qquad 0 \leq \sigma < 2\pi$$

IV. FORMULAS FOR ELLIPTIC MOTION

$$r = \frac{p}{1 + e\cos f} = a(1 - e\cos E)$$

$$\dot{r} = \frac{n\, a\, e \sin f}{\sqrt{1 - e^2}}$$

$$p = h^2/\mu = a(1 - e^2)$$

$$r_{max} = a(1 + e)$$

$$r_{min} = a(1 - e)$$

$$a = \frac{1}{2}(r_{max} + r_{min}) = \frac{h^2/\mu}{1 - e^2}$$

$$e^2 = 1 + 2Uh^2/\mu^2$$

$$h = r^2\dot{f} = \sqrt{\mu p} = na^2\sqrt{1 - e^2}$$

$$T = \frac{2\pi}{n}$$

$$n^2 a^3 = \mu$$

$$M = n(t - \tau) = E - e\sin E$$

$$U = \frac{1}{2}v^2 - \mu/r$$

$$v^2 = \mu\left(\frac{2}{r} - \frac{1}{a}\right)$$

$$v^2_{circular} = \frac{\mu}{r}$$

$$v^2_{escape} = \frac{2\mu}{r}$$

$$\frac{df}{dM} = \frac{a^2\sqrt{1 - e^2}}{r^2}$$

$$\frac{df}{dt} = \frac{h}{r^2}$$

NOMENCLATURE

a	semi-major axis
C	Jacobi constant
e	eccentricity of orbit
E	eccentric anomaly
f	true anomaly, angle between radius to periselene and radius to satellite, (Figs. B-4, B-7)
h	$r^2\dot{\theta}$, angular momentum
H	coefficient of third harmonic in gravity potential
I	inclination of orbit, (Fig. B-7)
I'	inclination of lunar orbit to ecliptic
J	oblateness coefficient in gravity potential
K	coefficient of fourth harmonic in gravity potential
L	coefficient of longitudinal harmonic in gravity potential
m	81.35, ratio of Earth's mass to Moon's mass
M	mean anomaly
n	mean angular rate of satellite
n'	mean angular rate of Moon in its orbit
p	semi-latus rectum, $a(1 - e^2)$, (Fig. B-4)
r	distance from center of mass of Moon, (Fig. B-2)

r_M	radius of Moon (mean equatorial)
R	perturbing potential
T	period, time for one orbit
U	energy per unit mass, $\frac{1}{2} v^2 - \frac{\mu}{r}$
v	magnitude of velocity, (Fig. B-3)
v_∞	hyperbolic excess velocity
α	angle from Earth-Moon line (extended) to ascending node
γ	velocity pitch angle above horizontal, (Fig. B-3)
θ	lunar longitude, (Fig. B-2)
μ	gravity constant for Moon
σ	velocity azimuth angle, clockwise from north, (Fig. B-3)
τ	time of periselene passage
ϕ	lunar latitude, (Fig. B-2)
Φ	gravity potential
χ	$- n\tau$
ω	angle measured in orbit plane between line of nodes and radius to periselene, (Figs. B-4, B-7)
Ω	longitude of node (Fig. B-7)
r, ϕ, θ	polar coordinate system, (Fig. B-2)
v, γ, σ	velocity polar coordinates, (Fig. B-3)
x, y, z	Moon-centered rectangular coordinate system, (Fig. B-1)
X, Y, Z	barycentric coordinates, (Fig. B-9)

V. LAGRANGE'S PLANETARY EQUATIONS (Ref. 36, p. 69)

1. In terms of the elements a, e, χ, Ω, ω, I:

$$\dot{a} = \frac{2}{na} \frac{\partial R}{\partial \chi}$$

$$\dot{e} = \frac{1}{na^2 e} \left\{ (1 - e^2) \frac{\partial R}{\partial \chi} - \sqrt{1 - e^2} \frac{\partial R}{\partial \omega} \right\}$$

$$\dot{\chi} = -\frac{1 - e^2}{na^2 e} \frac{\partial R}{\partial e} - \frac{2}{na} \frac{\partial R}{\partial a}$$

$$\dot{\Omega} = \frac{1}{na^2 \sqrt{1 - e^2} \sin I} \frac{\partial R}{\partial I}$$

$$\dot{\omega} = \frac{\sqrt{1 - e^2}}{na^2 e} \frac{\partial R}{\partial e} - \frac{\cot I}{na^2 \sqrt{1 - e^2}} \frac{\partial R}{\partial I}$$

$$\dot{I} = \frac{1}{na^2 \sqrt{1 - e^2}} \left\{ \cot I \frac{\partial R}{\partial \omega} - \csc I \frac{\partial R}{\partial \Omega} \right\}$$

2. In terms of the elements a, e, M, Ω, ω, I, (Ref. 37, p. 177) only the first three equations above are different:

$$\dot{a} = \frac{2}{na} \frac{\partial R}{\partial M}$$

$$\dot{e} = \frac{1}{na^2 e} \left\{ (1 - e^2) \frac{\partial R}{\partial M} - \sqrt{1 - e^2} \frac{\partial R}{\partial \omega} \right\}$$

$$\dot{M} = n - \frac{2}{na} \frac{\partial R}{\partial a} - \frac{1 - e^2}{na^2 e} \frac{\partial R}{\partial e}$$

3. In terms of force components. (Ref. 37, p. 178)

If F_1, F_2, F_3 are force components such that F_1 is the component in the radial direction, positive (away from the Moon); F_2 is the component in the plane of motion perpendicular to F_1 and in the direction of motion; F_3 is the out-of-plane component directed so that F_1, F_2, F_3 forms a right-handed system.

Then the planetary equations may be written:

$$\dot{a} = \frac{2}{n r \sqrt{1 - e^2}} \left\{ (e\, r \sin f)\, F_1 + a\,(1 - e^2)\, F_2 \right\}$$

$$\dot{I} = \frac{r \cos (f + \omega)}{n a^2 \sqrt{1 - e^2}}\, F_3$$

$$\dot{e} = \frac{\sqrt{1 - e^2}}{n\, a\, e} \left\{ (e \sin f)\, F_1 + \left[\frac{a(1 - e^2)}{r} - \frac{r}{a} \right] F_2 \right\}$$

$$\dot{\Omega} = \frac{r \sin (f + \omega)}{n a^2 \sqrt{1 - e^2} \sin I}\, F_3$$

$$\dot{\omega} = -\frac{\sqrt{1 - e^2}}{n\, a\, e} \left\{ (\cos f)\, F_1 - (\sin f) \left[1 + \frac{r}{a(1 - e^2)} \right] F_2 + \frac{e\, r \sin (f + \omega) \cot I}{a(1 - e^2)}\, F_3 \right\}$$

$$\dot{M} = n + \frac{1}{na} \left\{ \left[\frac{(1 - e^2) \cos f}{e} - \frac{2r}{a} \right] F_1 - \frac{(1 - e^2) \sin f}{n\, a\, e} \left[1 + \frac{r}{a(1 - e^2)} \right] F_2 \right\}$$

VI. DATA FOR THE EARTH-MOON SYSTEM

1. Mass

$$m_{\odot} = 1.991 \times 10^{33} \text{ g}$$

$$m_{\oplus} = 5.977 \times 10^{27} \text{ g}$$

$$m_{\leftmoon} = 7.34 \times 10^{25} \text{ g}$$

$$\frac{m_{\odot}}{m_{\oplus} + m_{\leftmoon}} = 328452 \text{ (Ref. 38)}$$

$$\frac{m_{\oplus}}{m_{\leftmoon}} = 81.35 \text{ (Ref. 35)}$$

2. Average Distances

Sun-Earth: 149.53×10^{6} km (Ref. 35)

Earth-Moon: 384,402 km = 60.2686 Earth radii (Ref. 35)

Earth-barycenter: 4,668 km = 0.7319 Earth radii

Moon-barycenter: 379,734 km = 59.5367 Earth radii

3. Geometrical Figures

	Equatorial radii, km	Polar radii, km	Inclination of equator to ecliptic	Rate of rotation, rad/sec
Sun	696,000 (Ref. 39)		7° 15' (Ref. 39)	2.90×10^{-6} (Ref. 39)
Earth	6378.15 (Ref. 35)	6356.91 (Ref. 39)	23° 27' (Ref. 39)	7.292×10^{-5} (Ref. 39)
Moon	1738.57 1738.21 (Ref. 35)	1737.58 (Ref. 35)	1° 32'06" (Ref. 35)	

4. Gravity Field ($km^3\ sec^{-2}$)

$$\mu_{\odot} = 1.327154 \times 10^{11}$$

$$\mu_{\oplus} = 3.9863 \times 10^{5}$$

$$\mu_{\leftmoon} = 4.90076 \times 10^{3}$$

$$\Phi_{\oplus} = \frac{\mu_{\oplus}}{r}\left[1 + \frac{J_{\oplus}}{3r^2}(1 - 3\sin^2\phi) + \frac{H_{\oplus}}{5r^3}(3 - 5\sin^2\phi)\sin\phi + \frac{K_{\oplus}}{30r^4}(3 - 30\sin^2\phi + 35\sin^4\phi) + \cdots\right]$$ (Ref. 35, 40)

(r expressed in Earth radii)

$$\Phi_{\mathfrak{D}} = \frac{\mu_{\mathfrak{D}}}{r}\left[1 + \frac{J_{\mathfrak{D}}}{3r^2}(1 - 3\sin^2\phi) + \frac{L_{\mathfrak{D}}}{r^2}\cos^2\phi\cos 2\theta + \cdots\right]$$ (Ref. 40, p. 125)

(r expressed in Moon radii)

$J_{\oplus} = 1623.41 \times 10^{-6}$ (Ref. 35)

$H_{\oplus} = 6.04 \times 10^{-6}$ (Ref. 35)

$K_{\oplus} = 6.37 \times 10^{-6}$ (Ref. 35)

$J_{\mathfrak{D}} = 311 \times 10^{-6}$ (Ref. 41)

$L_{\mathfrak{D}} = 61 \times 10^{-6}$ (Ref. 41)

5. Orbital Elements

	Barycenter w r to Sun	Moon w r to barycenter
gravity constant	1.327154×10^{11} km^2/sec^2	3.890078×10^{5} km^2/sec^2
a	149.6×10^{6} km	379,734 km
e	0.016750	0.05490
greatest distance	152.1×10^{6} km	400,581 km
closest approach	147.1×10^{6} km	358,887 km
average speed	29.77 km/sec	1.0107 km/sec
sidereal period	365.256 days	27.321661 days

	Barycenter w r to Sun	Moon w r to barycenter
n	0.9856 deg/day	13.17639 deg/day
U	$-0.4435 \times 10^{3} km^{2}/sec^{2}$	$-0.5249\ km^{2}/sec^{2}$
h	$4.454 \times 10^{9} km^{2}/sec$	$3.885 \times 10^{5} km^{2}/sec$
I	0 to ecliptic	5.145 deg to ecliptic
$\dot{\Omega}$		-0.052954 deg/day
$\dot{\omega}$		0.111404 deg/day

VII. EQUATIONS OF MOTION FOR THE RESTRICTED THREE-BODY PROBLEM (see Fig. B-9)

Assumptions:

(a) Only three bodies in the system

(b) One body has infinitesimal mass

(c) The two major bodies revolve about their common center-of-mass in circular orbits

Using the rotating coordinate system shown in Fig. B-9, the equations of motion for the infinitesimal mass are: (Ref. 40, p. 254)

$$\ddot{x} - 2n'\dot{y} = (n')^2 x - \frac{\mu_0\left(x + \frac{1}{1+m}\right)}{\rho_0^3} - \frac{\mu_1\left(x - \frac{m}{1+m}\right)}{\rho_0^3}$$

$$\ddot{y} + 2n'\dot{x} = (n')^2 y - \frac{\mu_0 y}{\rho_0^3} - \frac{\mu_1 y}{\rho_1^3}$$

$$\ddot{z} = -\frac{\mu_0 z}{\rho_0^3} - \frac{\mu_1 z}{\rho_1^3}$$

in which

n' = rotation rate of major bodies (and of coordinate system)

ρ_0, ρ_1 = distances to major bodies

μ_0, μ_1 = gravity field strengths

$m = \mu_0/\mu_1$

VIII. OPTIMUM ALTITUDE FOR INJECTION INTO SATELLITE ORBIT

If a space vehicle approaches the Moon from outside its gravity field on a hyperbolic orbit with hyperbolic excess velocity v_∞, its energy with respect to the Moon is

$$U = \frac{1}{2} v_\infty^2 = \frac{1}{2} v^2 - \frac{\mu}{r}$$

If the point of closest approach is at distance $r = a$, then the velocity increment required to enter a circular orbit at altitude a with a single impulse is

$$I = v_a - v_c = \sqrt{v_\infty^2 + \frac{2\mu}{a}} - \sqrt{\frac{\mu}{a}}$$

The problem of optimum altitude is to determine the value of a which minimizes I. This involves adjusting the incoming orbit to vary the point of closest approach without changing the energy.

Setting the derivative of I with respect to a equal to zero, and solving for a yields the required optimum altitude

$$r_{opt} = \frac{2\mu}{v_\infty^2}$$

for which

$$I_{opt} = \frac{\sqrt{2}}{2} v_\infty$$

IX. SECULAR RATES DUE TO J AND L

1. J: (Ref. 42)

$$\dot{a} = 0 \qquad \dot{e} = 0 \qquad \dot{I} = 0$$

$$\dot{\omega} = \frac{nJ}{p^2}\left(2 - \frac{5}{2}\sin^2 I\right)$$

$$\dot{\Omega} = -\frac{nJ}{p^2}\cos I$$

2. L: (Ref. 43)

$$\dot{\Omega} = \frac{n\,L\cos I\cos 2(\Omega - n't)}{p^2}$$

$$\dot{I} = \frac{n\,L\sin I\sin 2(\Omega - n't)}{p^2}$$

$$\dot{a} = 0$$

$$\dot{e} = 0$$

$$\dot{\omega} = -\frac{nL}{p^2}\left(1 - \frac{5}{2}\sin^2 I\right)\cos 2(\Omega - n't)$$

These formulas result from averaging over short period terms only, the averaging parameter being the mean anomaly M. The difference between these formulas and those of Ref. 43 are due to the fact that in Ref. 43 the argument of pericenter, $f + \omega$, was the averaging parameter.

X. SECULAR RATES DUE TO EARTH AND SUN

The Earth and Sun effects can each be represented by the same formulas, with different proportionality constants. In the following formulas, the

appropriate value for n' is given by

$$\text{Sun: } n' = 1 \text{ deg/day}$$

$$\text{Earth: } n' = 13 \text{ deg/day}$$

Thus, the rates $\dot{\omega}$ and $\dot{\Omega}$ are 170 times as large for Earth perturbation as for Sun perturbations. The formulas are (Ref. 44):

$$\dot{a} = 0$$

$$\dot{\Omega} = -\frac{3}{4}\frac{n'^2}{n}\cos I \frac{\left(1+\frac{3}{2}e^2\right)}{\sqrt{1-e^2}}\left(1-\frac{3}{2}\sin^2 I'\right)$$

$$\dot{\omega} = \frac{3}{4}\frac{n'^2}{n}\left(2-\frac{5}{2}\sin^2 I+\frac{1}{2}e^2\right)\frac{1}{\sqrt{1-e^2}}\left(1-\frac{3}{2}\sin^2 I'\right)$$

APPENDIX C

Trajectory and Station-Keeping Near the Translunar Libration Point*

I. INTRODUCTION

It is well known that when the motion of a body in the Earth-Moon system is considered as a restricted three-body problem, certain points are found at which a body experiences no acceleration relative to the Earth-Moon system. Two of these so-called "libration" points form equilateral triangles with the Earth and the Moon, and are stable. The other three, all unstable, are located on the Earth-Moon line, as shown in Fig. C-1 (Ref. 45).

It is the purpose of this study to investigate the problem of placing a body near the translunar libration point and keeping it in a fixed position relative to the Earth-Moon system for a period of time. It has been suggested that a spacecraft placed in such a position might be used as a communications relay station between the Earth and spacecraft orbiting or operating on the far side of the Moon. The problem thus consists of two areas: injection and station-keeping. The injection problem involves the selection of a suitable translunar trajectory and the deboost maneuver near the libration point, while station-keeping requires knowledge of the force-fields near the libration point as well as sensing techniques to determine position relative to the libration point. The problem of station-keeping is discussed first.

*Jet Propulsion Laboratory Technical Memorandum No. 312-287, December 17, 1962.

II. STATION-KEEPING

A. The Force-Field

In the derivation of the analytical expression for the force-field in the vicinity of the translunar libration point the following symbols and constants are used:

$\bar{a}$ acceleration of body in an inertial frame

$\bar{a}_0$ acceleration of libration point

$\bar{f}$ corrective force, thrust

D 1 lunar unit, 3.847527×10^{10} cm

$K = G(m_e + m_m) = 0.052886587$ (lunar units)^3/day^2

$\mu = \dfrac{m_m}{m_m + m_e} = 1/82.45$

ω average angular velocity of the Earth-Moon system, 0.22997084 rad/day

The inertial acceleration of a body expressed in an accelerating and rotating coordinate system is

$$\bar{a} = \bar{a}_0 + \frac{d^2\bar{r}}{dt^2} + \bar{\omega} \times (\bar{\omega} \times \bar{r}) + 2\,\bar{\omega} \times \frac{d\bar{r}}{dt} + \dot{\bar{\omega}} \times \bar{r} \qquad (C\text{-}1)$$

where $\bar{r}$ is the position vector in the coordinate system rotating with an angular velocity $\bar{\omega}$.

This acceleration is equal to the sum of forces per unit mass acting on the body. If these forces are assumed to consist of gravitational forces $\bar{F}_G$ and a thrust force $\bar{f}$, then, for the body at rest in the rotating coordinate system, the

following must be true

$$\frac{\bar{f}}{m} = -\frac{\bar{F}_G}{m} + \bar{a}_0 + \bar{\omega} \times (\bar{\omega} \times \bar{r}) \qquad (C-2)$$

The coordinate system used here is a right-handed cartesian system with the origin at the libration point, and the positive x-axis oriented outward along the Earth-Moon line, as shown in Fig. C-2.

In this coordinate system

$$\frac{\bar{F}_G}{m} = -K(1-\mu)\frac{\bar{r}_E}{r_E^3} - K\mu\frac{\bar{r}_m}{r_m^3} \qquad (C-3)$$

where

$$\bar{r}_E = \left[(1+\ell)D + x\right]\hat{i} + y\hat{j} + z\hat{k}$$

$$r_m = (\ell D + x)\hat{i} + y\hat{j} + z\hat{k}$$

and also

$$\bar{a}_0 = -(1-\mu+\ell)D\omega^2\hat{i} \qquad (C-4)$$

$$\bar{\omega} \times (\bar{\omega} \times \bar{r}) = -\omega^2(x\hat{i} + y\hat{j}) \qquad (C-5)$$

Substituting Eqs. (C-3), (C-4) and (C-5) into Eq. (C-2), the expression for the force required to maintain a body at rest at the point (x, y, z) is found to be:

$$\frac{\bar{f}}{m}(x,y,z) = \left\{\frac{K(1-\mu)\left[(1+\ell)D + x\right]}{r_E^3} + \frac{K\mu(\ell D + x)}{r_m^3} - \left[(1-\mu+\ell)D + x\right]\omega^2\right\}\hat{i}$$

$$+\left\{\frac{K(1-\mu)y}{r_E^3} + \frac{K\mu y}{r_m^3} - \omega^2 y\right\}\hat{j} + \left\{\frac{K(1-\mu)z}{r_E^3} + \frac{K\mu z}{r_m^3}\right\}\hat{k} \qquad (C-6)$$

If it is necessary to describe the behavior of the force-field near the origin, a much simpler expression can be derived. Thus, for small Δx, Δy, Δz about the origin, Eq. (C-6) can be expanded in a Taylor series about the origin as follows:

$$\frac{\bar{f}}{m}(\Delta x, \Delta y, \Delta z) = \frac{\bar{f}}{m}(x, y, z)\Big|_{\substack{x=0\\y=0\\z=0}} + \frac{\partial}{\partial x}\left(\frac{\bar{f}}{m}\right)\Big|_{\substack{x=0\\y=0\\z=0}} \Delta x + \frac{\partial}{\partial y}\left(\frac{\bar{f}}{m}\right)\Big|_{\substack{x=0\\y=0\\z=0}} \Delta y + \frac{\partial}{\partial z}\left(\frac{\bar{f}}{m}\right)\Big|_{\substack{x=0\\y=0\\z=0}} \Delta z + \cdots$$

Retaining only the first-order terms,

$$\frac{\bar{f}}{m}(\Delta x, \Delta y, \Delta z) \cong \left\{ -\frac{2K(1-\mu)\Delta x}{[(1+\delta)D]^3} - \frac{2K\mu\Delta x}{(\delta D)^3} - \omega^2 \Delta x \right\} \hat{i}$$

$$+ \left\{ \frac{K(1-\mu)\Delta y}{[(1+\delta)D]^3} + \frac{K\mu\Delta y}{(\delta D)^3} - \omega^2 \Delta y \right\} \hat{j}$$

$$+ \left\{ \frac{K(1-\mu)\Delta z}{[(1+\delta)D]^3} + \frac{K\mu\Delta z}{(\delta D)^3} \right\} \hat{k}$$

$$\cong A\,\Delta x\,\hat{i} + B\,\Delta y\,\hat{j} + C\,\Delta z\,\hat{k} \qquad (C\text{-}9)$$

where, in lunar units

$$A = -0.39039335 \quad \text{days}^{-2}$$

$$B = 0.11586679 \quad \text{days}^{-2}$$

$$C = 0.16875338 \quad \text{days}^{-2}$$

The force-field described by Eq. (C-7) can be better visualized by considering surfaces of constant magnitude. Thus for a constant value of $|\bar{f}|/m$, Eq. (C-7) yields

$$\left(\frac{|\bar{f}|}{m}\right)^2 = A^2 \Delta x^2 + B^2 \Delta y^2 + C^2 \Delta z^2 \qquad \text{(C-8)}$$

Equation (C-8) describes an ellipsoid having an axis ratio of approximately (1:3.37:2.32 = x:y:z). It is thus apparent that the magnitude of the force increases most rapidly as one moves away from the libration point in the x-direction, and least rapidly in the y-direction.

To obtain a quantitative picture of the force-field, contours of constant magnitude were plotted in each of the three principal planes. For convenience, the equations were first transformed to polar coordinates, as shown below for the x-y plane. Using $\Delta x = \rho \cos \theta$ and $\Delta y = \rho \sin \theta$,

$$\frac{\bar{f}}{m} = \rho \left(A \cos \theta \, \hat{i} + B \sin \theta \, \hat{j}\right) \qquad \text{(C-9)}$$

and thus, for a constant $|\bar{f}|$,

$$\rho = \frac{|\bar{f}|/m}{\left(A^2 \cos^2 \theta + B^2 \sin^2 \theta\right)^{1/2}} \qquad \text{(C-10)}$$

and the direction of $\bar{f}$ is given by

$$\phi = \tan^{-1}\left(\frac{B}{A} \tan \theta\right) \qquad \text{(C-11)}$$

The resulting contours for values of $|\bar{f}|/m$ of 5×10^{-4}, 4×10^{-4}, 3×10^{-4}, 2×10^{-4} and 1×10^{-4} ft/sec^2 are shown in Fig. C-3. The arrows represent the direction of $\bar{f}$ at the corresponding values of the angle θ. Only the first quadrant is shown, as the rest of the contours are symmetrical.

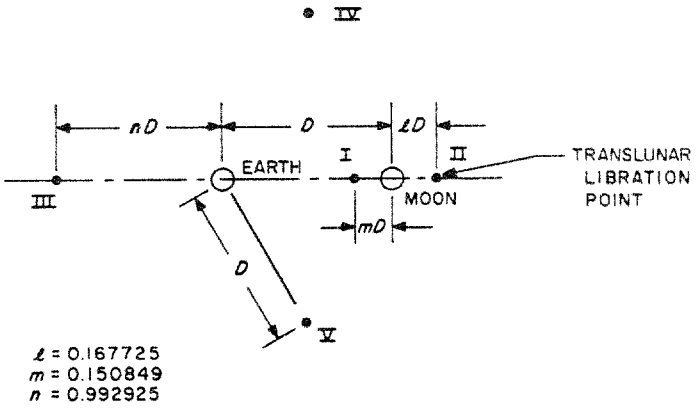

Fig. C-1. Location of the Earth-Moon libration points

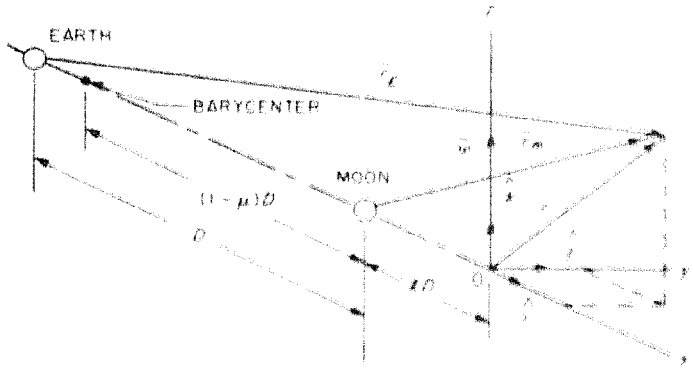

Fig. C-2. Libration point coordinate system

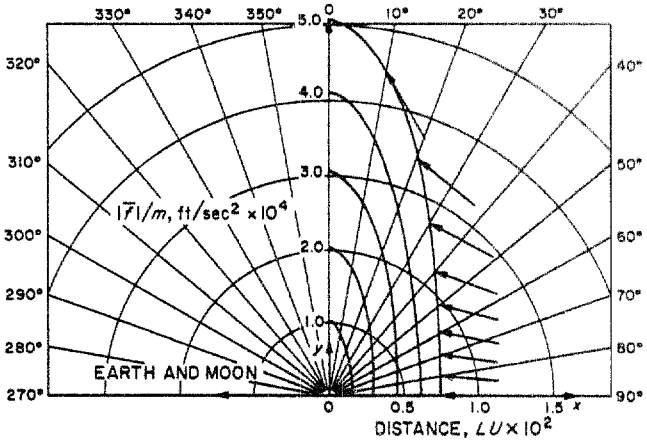

Fig. C-3. Contours of constant thrust vector magnitude in the x-y plane

Similarly, sets of such contours in the x-z and y-z planes are shown in Figs. C-4 and C-5, respectively.

B. Stabilization

In order to maintain a spacecraft in a fixed position relative to the Earth-Moon system near the libration point, some technique is needed to sense its position relative to the libration point and to provide the appropriate corrective thrust force. This problem is here called stabilization.

As an example, it is required to maintain the spacecraft in a position near the libration point such that the entire disk of the Earth would be visible. The locus of all such points nearest the libration point is a circle, essentially in the y-z plane, with a radius distance at which the disk of the Earth appears to be osculant to the disk of the Moon. This distance can be shown to be approximately 3,000 km, or 0.008 lunar units. A circle of this size is shown dotted in Fig. C-4.

The magnitude of the force required to maintain a body at some point on this circle has been computed and is plotted in Fig. C- , together with the deviation of the direction of this force from the radial. From Fig. C-6 it is seen that the magnitude of the required corrective $|f|/m$ varies from a minimum of 1.57×10^{-4} ft/sec^2 in the y-direction to a maximum of 2.29×10^{-4} ft/sec^2 in the z-direction. Assuming that this thrust force is applied continuously, the total velocity increment for one month's station-keeping would vary from a maximum of 629 ft/sec to a minimum of 413 ft/sec, depending on the position of the 3,000-km circle.

This is true only if the spacecraft is maintained strictly in the y-z plane, i.e., if there is no displacement in the x-direction (along the Earth-Moon line). Deviations in this direction are more costly in fuel, since a deviation of only 0.00157 lunar units (585 km) requires a corrective $|f|/m$ of 1×10^{-4} ft/sec^2

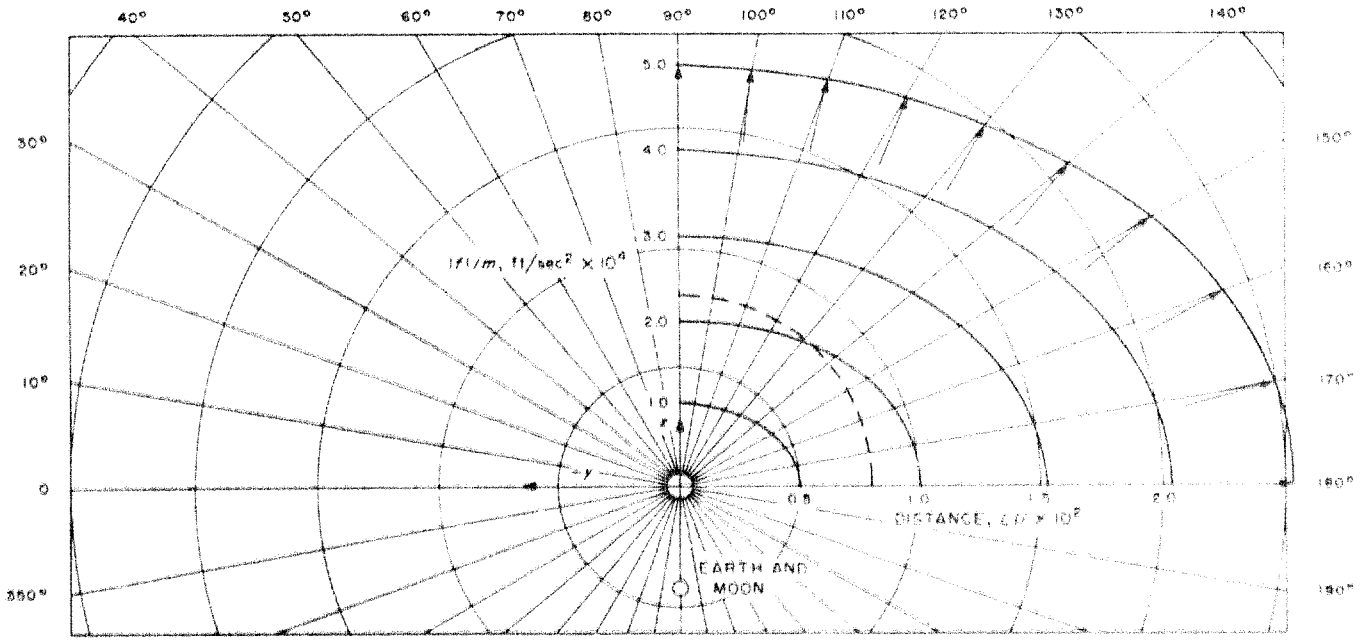

Fig. C-4. Contours of constant thrust vector magnitude in the y-z plane

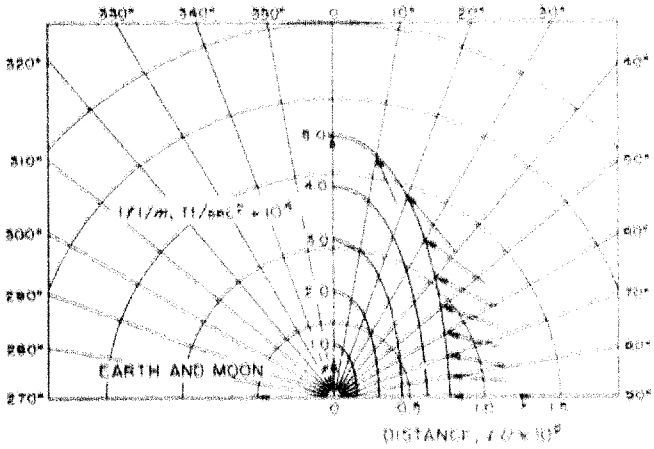

Fig. C-5. Contours of constant thrust vector magnitude in the x-z plane

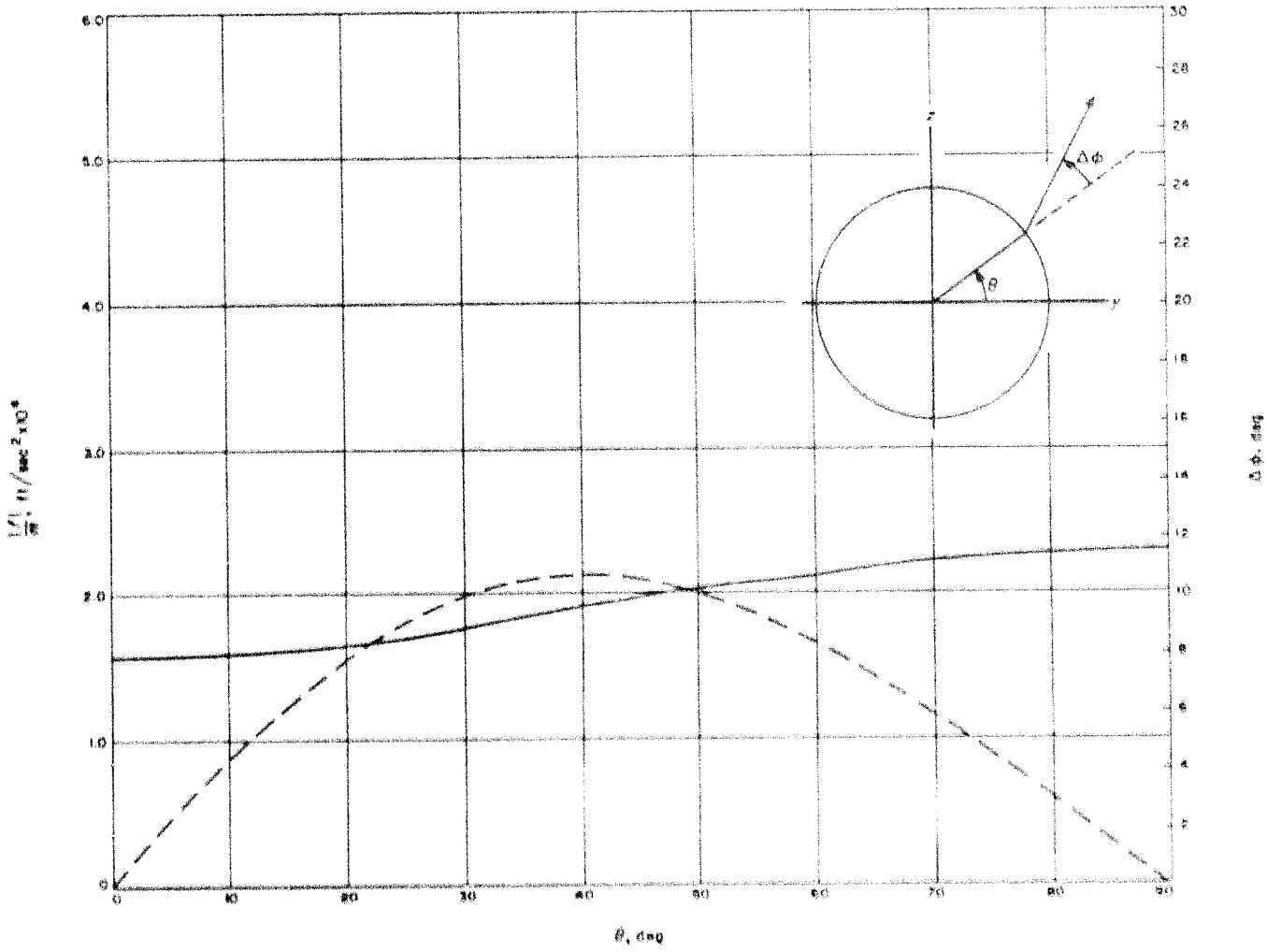

Fig. C-6. Normalized magnitude and deviation from radial of thrust vector vs θ

In addition, even if the spacecraft is constrained to the y-z plane, the direction of the force required to keep it on the 3000-km circle deviates from the radial (central) direction by as much as 11.5 deg.

In view of the preceding, the stabilization problem may be divided into two more or less independent requirements:

a. Restrict the spacecraft to the y-z plane (no x-deviation)

b. In the y-z plane, restrict the spacecraft to the vicinity of a 3,000-km circle about the libration point.

There are two basic approaches to the implementation of these objectives. The most obvious is to determine the exact position of the spacecraft either by Earth-based tracking or by on-board sensing, and then to compute and apply the exact corrective thrust required. The computation may be done on-board or on Earth. In any case, a 3-axis stabilized spacecraft with thrust orientation capability would probably be required. Although this scheme is possible, it does not seem to be the most favorable in terms of complexity.

A simpler approach might be to base the corrections entirely upon sensing information. If one axis of the spacecraft is oriented toward the Earth (also necessary for communications) and another, normal to the first one, in the direction of the libration point (or, the Earth-Moon line), then, since the spacecraft Earth-Moon angle is only about 0.39 deg for any point on the 3,000-km circle, thrust-motors oriented in both directions along this axis can be used to maintain the spacecraft in the y-z plane, with a distance reference provided by an optical sensor measuring the diameter of the Moon's disk. In reality, since the position of the libration point on the Earth-Moon line ($x \neq 0$) depends upon the Earth-Moon distance, the distance to both the Earth and the Moon might have to be measured to obtain deviations in the x-direction.

A predetermined amount of thrust would be applied when the deviation would reach a certain value in either direction, thus keeping the spacecraft in a limit-cycle about $x = 0$.

Similarly, another thrust motor could be oriented along the axis pointing toward the libration point, and this thruster would be actuated when the radial distance of the spacecraft from the libration point would deviate from 3,000 km by some predetermined amount. Position sensing in this case would be accomplished by another optical system that would sense the relative position of the Earth and the Moon, such as the angle subtended by the centers of their disks (approximately 2.4 deg at the desired position). Since the direction of the applied thrust will not in general be in exactly the desired direction, the spacecraft can be expected to move along the 3,000-km circle in some type of a limit-cycle.

The major problem in this scheme appears to be sensing. The illumination of the Earth and the Moon as seen from the station changes from almost total (full) to almost none in the course of a lunar month. It is even possible for the Sun to come into the field of view of the sensors. This problem must be faced if the spacecraft is to remain on station for periods of time in excess of one month.

III. INJECTION

The injection problem consists of placing a spacecraft in the vicinity of the translunar libration point with the same velocity as that of the libration point. Thus, the spacecraft must first be injected into a translunar trajectory that takes it from the vicinity of the Earth to the vicinity of the libration point, and then a terminal maneuver must be performed to change its velocity to that of the

libration point. It is the purpose of this section to investigate the velocity increment requirements for a set of typical trajectories.

For a given launch time and injection C_3, two trajectories passing through the libration point are possible, provided that the C_3 is sufficient. One of these trajectories passes around the leading edge of the Moon, and the other around the trailing edge.

In this discussion, both types of trajectories are considered for four values of injection C_3. All of these trajectories are derived from a 66-hr, 102-deg launch azimuth, Ranger-type vertical impacting trajectory for May 13, 1963. Using this trajectory, vertical impacting cases with flight times of 55, 78 and 86 hr were found. Keeping C_3 constant, injection conditions were then varied to find one leading-edge and one trailing-edge trajectory for each original flight time, except for the 86-hr leading-edge case, which could not be established. The actual flight-times to the libration point are, or course, different.

The approximate projections of these trajectories in the Moon's orbital plane are shown in Fig. C-7. It is noted that the trailing-edge trajectories must pass much closer to the Moon than the leading-edge trajectories. This is necessary to "bend" the incoming trajectory by the required amount, and it also increases the velocity, giving rise to shorter times of flight for the trailing-edge trajectories.

All of these trajectories have different velocities upon arriving in the vicinity of the libration point. In order to remain near the libration point, the final velocity $\overline{V}_0$ must be

$$\overline{V}_0 = \overline{V}_m \frac{(1 - \mu + \ell)}{(1 - \mu)} \qquad \text{(C-12)}$$

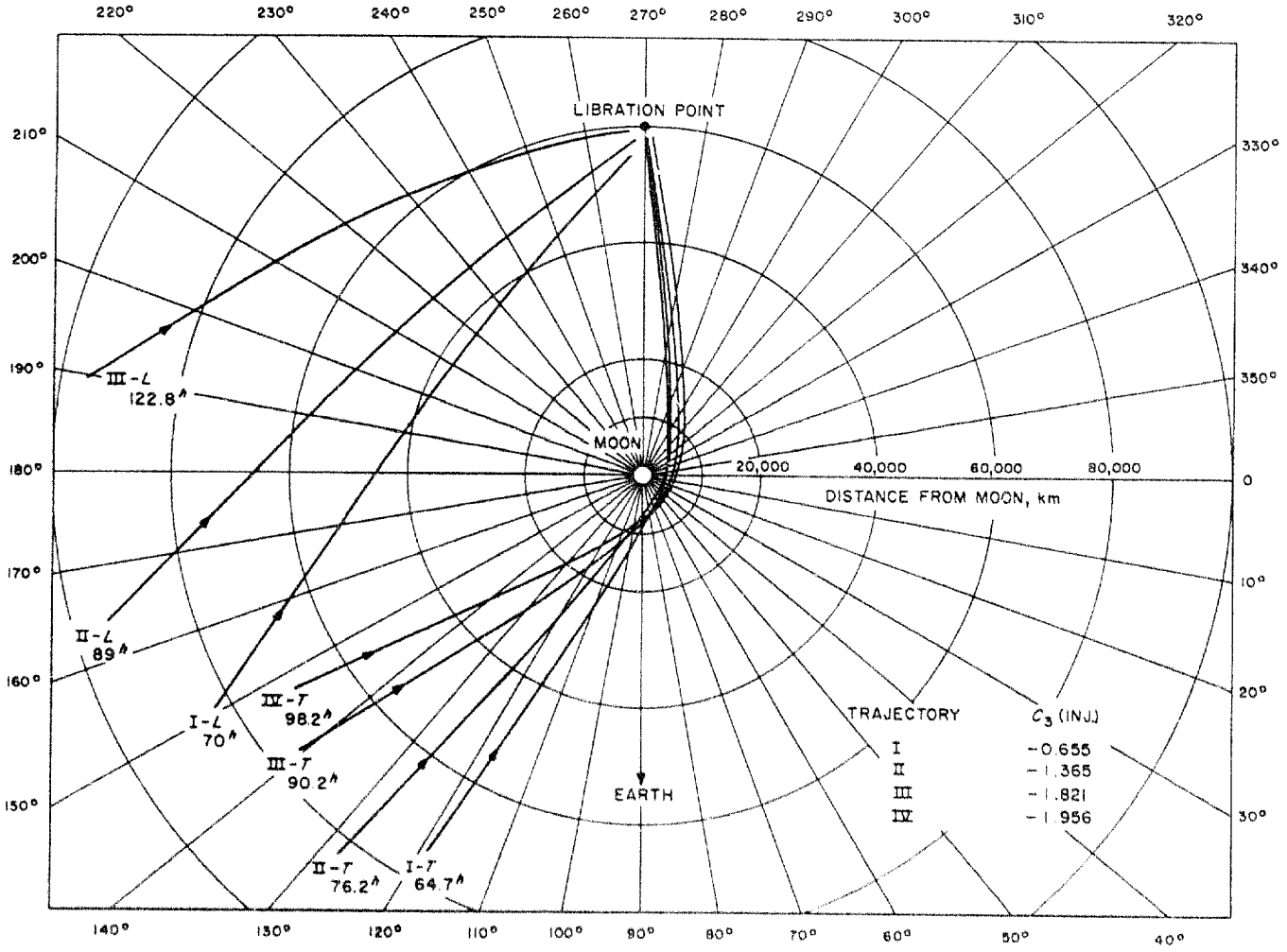

Fig. C-7. Approximate trajectories (selenocentric)

where ℓ and μ are defined in Section II. Thus, if the velocity of a probe approaching the libration point on some trajectory is $\overline{V}$, then the necessary terminal maneuver velocity increment is

$$\Delta\overline{V} = \overline{V}_0 - \overline{V} \qquad (C-13)$$

The values of $\Delta\overline{V}$ were computed for each of the trajectories. The magnitude $|\Delta\overline{V}|$ for both trailing (T) and leading (L) trajectories as well as the angle β between $\overline{V}$ and $\overline{V}_0$ and α between $\overline{V}$ and $\Delta\overline{V}$ are listed in Table C-1.

Table C-1

Trajectory	C_3	T F, hr	$\Delta\overline{V}$,* km/sec	β,* deg	α,* deg
I - T	-0.655	64.7	1.564	56.1	140.4
- L		70.0	1.586	92.1	139.4
II - T	-1.365	76.2	1.282	47.9	135.3
- L		89.5	1.314	88.6	115.5
III - T	-1.821	90.2	1.148	42.6	122.2
- L		122.8	1.169	46.2	41.1
IV - T	-1.956	98.2	1.075	49.6	119.4

* 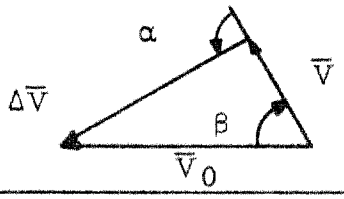

The magnitude of the velocity increment is plotted vs time of flight in Fig. C-8. It can be readily observed that the longer flight time trailing-edge trajectories have the lowest $|\Delta\overline{V}|$ requirements, as well as having lower Earth-injection energy. However, they are more sensitive to injection errors, and possibly would require a greater midcourse correction capability, which is not discussed here.

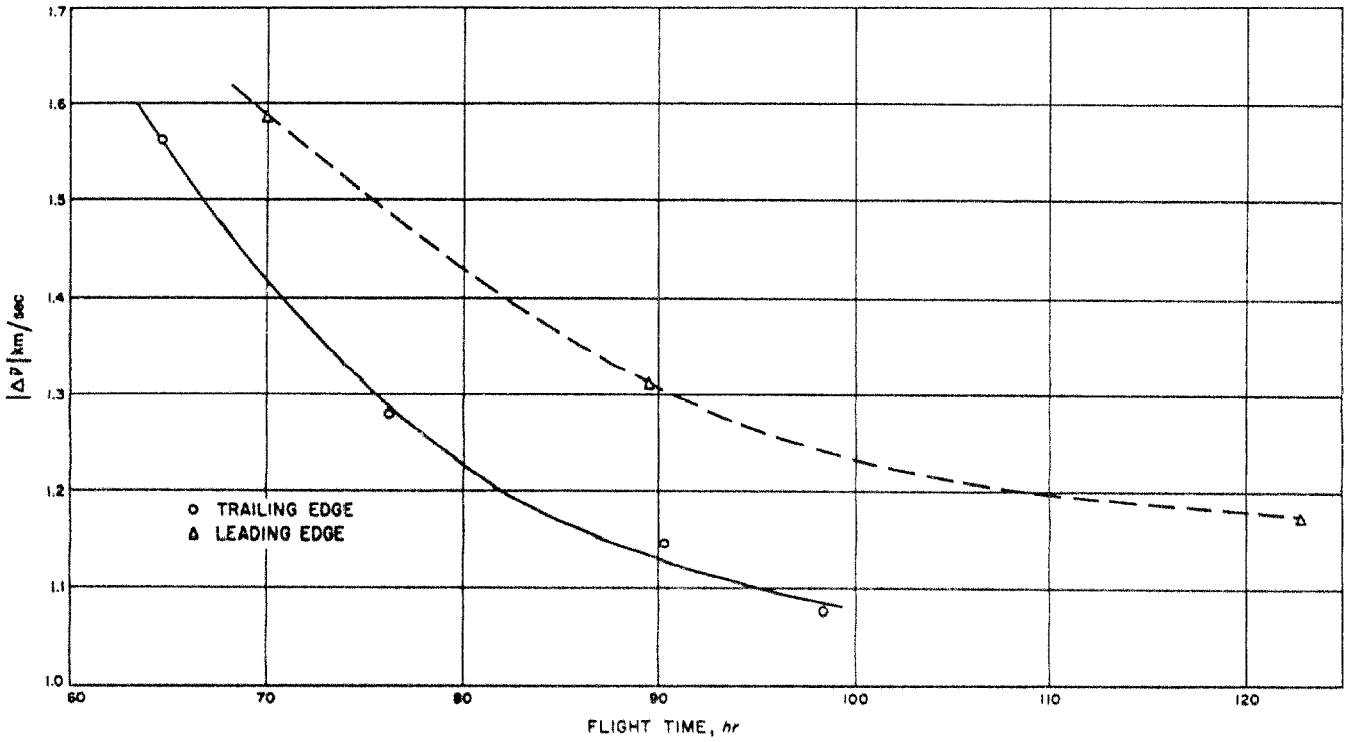

Fig. C-8. Approximate terminal velocity increment, $|\Delta\bar{V}|$ vs flight time

Leading-edge trajectories, in every case, require a greater $\left|\Delta\overline{V}\right|$ and have much longer flight times than the corresponding trailing-edge trajectories, and thus appear to offer no advantages, except possibly a lower sensitivity to errors in the lunar miss parameters.

IV. CONCLUSIONS

From the discussion in the preceding sections it is evident that a spacecraft designed to maintain a station near the libration point should have two propulsion systems. One, a main retro-motor, would be used to supply the large velocity increment necessary for injection. The necessity to orient the thrust of this motor in a desired direction probably dictates a spacecraft with 3-axis attitude control. The second propulsion system could consist of restartable vernier engines to supply the thrust necessary for station-keeping corrections, as discussed in Section II.

Based on the figures derived in Sections II and III, the velocity increment requirement for injection is about 1.1 km/sec (3,640 ft/sec), and the requirement for one month's station-keeping could conservatively be assumed to be of the order of 1,000 ft/sec. Thus, the total for injection and one month's station-keeping is about 5,000 ft/sec. It is interesting to compare these requirements with the capability of the Surveyor lander-spacecraft. This 2100-lb spacecraft carries about 1330 lb of main-retro fuel, 145 lb of vernier fuel, and is attitude controlled. This propulsion system has a total $\left|\Delta\overline{V}\right|$ capability of about 9,000 ft/sec.

These figures suggest that, if a smaller main-retro motor were used with a corresponding increase in vernier capability, the amount of fuel available for station-keeping could be sufficient for five or six months, provided that a Surveyor could be modified to serve as a communications beacon. Although such

a modification may not be the optimal spacecraft for this purpose, it suggests the feasibility of a spacecraft having the propulsion capability necessary for a libration-point station.

APPENDIX D

Conic Approximations Used in Circumlunar Trajectories

W. Kirhofer, Jet Propulsion Laboratory

First estimates can be made for circumlunar trajectories by building up solutions from Earth-centered and Moon-centered conics. In Fig. D-1 a circumlunar trajectory is represented by three conic sections. Here $\overline{V}$ and $\overline{V}'$ are the velocity vectors of the probe relative to the Earth at Points A and B, respectively; $\overline{V}_{PM}$ and $\overline{V}'_{PM}$ are the velocity vectors of the probe relative to the Moon at Points A and B, respectively; and $\overline{V}_M$ is the velocity vector of the Moon relative to Earth. The sphere of influence of the Moon is used to locate the transition points between the Earth-centered (Parts I and III) conics and the Moon-centered (Part II) conics. At the transition points, as shown in Fig. D-1, the Moon's velocity $\overline{V}_M$ must be taken away (Point A) or added to (Point B) the probe's velocity to change from one central body to another. Fig. D-2 shows what the same trajectory would look like in a completely Earth-centered system. Fig. D-3 is a vector diagram relating the vectors at Points A and B in Fig. D-1.

By changing the perigee distance of the Moon-centered conic, the amount of turning or the angle α between $\overline{V}_{PM}$ and $\overline{V}'_{PM}$ can be changed. From Fig. D-3, assuming $\overline{V}_{PM}$ is constant, it can be seen that if α is varied from -180 to +180 deg, all possible $\overline{V}'$ in the two-dimensional representation are achieved. Actually, α is limited to less than ± 180 deg for circumlunar trajectories which preclude lunar impact. Trajectory characteristics relative to the Moon are determined by the orientation of the vectors $\overline{V}_{PM}$ and $\overline{V}'_{PM}$. The vector $\overline{V}'$ is most significant in that it determines the Earth-centered conic after lunar passage.

Figure D-4 shows how the trajectories within the sphere of influence of the Moon change as the perigee distance is varied. If this procedure is extended to three dimensions by varying the magnitude and the direction of lunar perigee, the vectors at A and B in Fig. D-1 must be represented by a three-dimensional figure as shown in Fig. D-5.

Figure D-5 gives a representation of the vectors corresponding to the Points A and B in Fig. D-1 for all trajectories which enter the sphere of influence of the Moon. By using this representation, preliminary decisions can be made as to whether any circumlunar trajectories exist which may be suitable for a particular application.

For example, it was desired that a circumlunar trajectory be used to obtain an orbit about the Earth for which the probe-Earth distance would remain large for a long period of time. Using the representation shown in Fig. D-5, a lunar perigee distance and direction were selected to obtain a $\overline{V}'$ which would result in such an orbit. Some of the characteristics of this circumlunar trajectory are presented in Figs. D-6 through D-10. As seen in Fig. D-8, after the probe's first pass by the Moon, the probe-Earth distance remains large for a long period of time. By extrapolation of the curve shown in Fig. D-9, it is estimated that the probe-Earth distance will remain large for at least 160 days. Figure D-10 shows how the Earth-probe-Sun angle varies with time from injection to provide evaluation of attitude and control considerations.

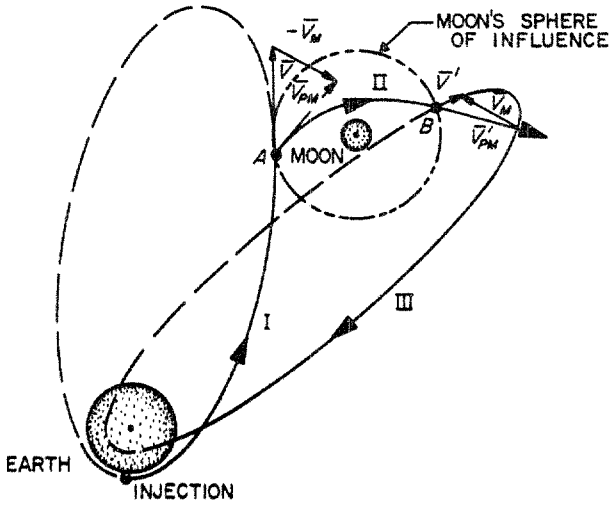

Fig. D-1. Conic sections representing a circumlunar trajectory

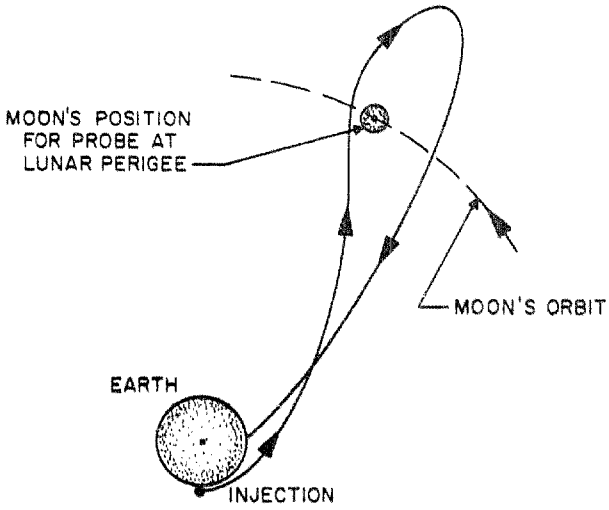

Fig. D-2. Circumlunar trajectory in Earth-centered coordinates

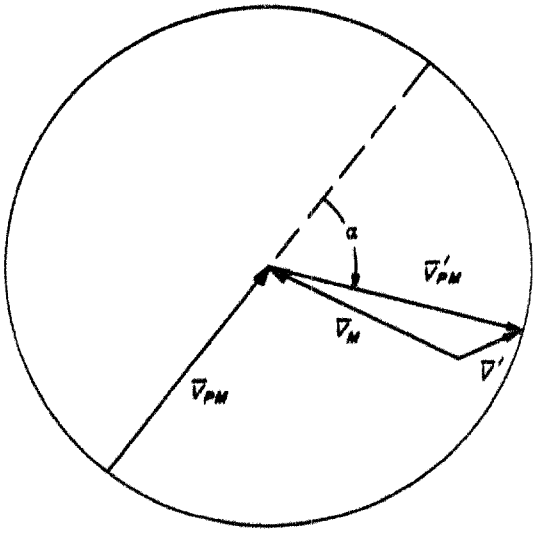

Fig. D-3. Diagram relating the vectors at Points A and B in Fig. D-1

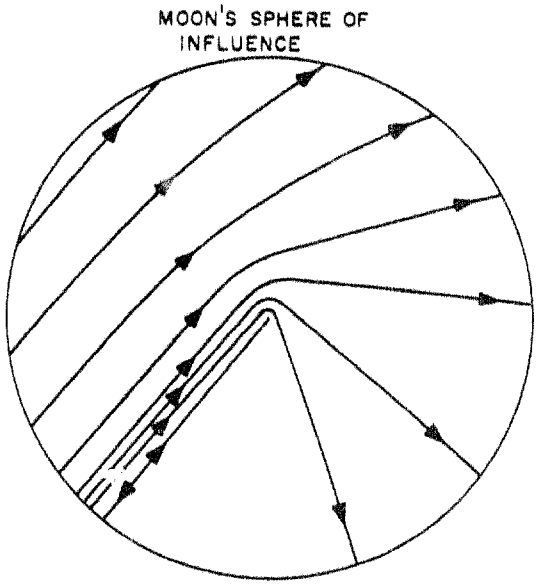

Fig. D-4. Trajectories within the Moon's sphere of influence with constant V_{PM} and various perigee distances

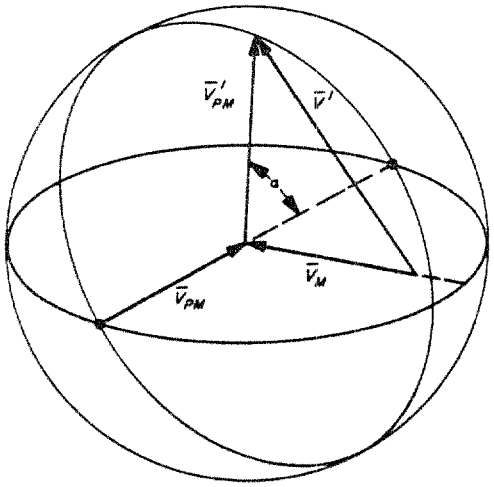

Fig. D-5. Representation of the vectors at the points where the circumlunar trajectory enters and leaves the Moon's sphere of influence

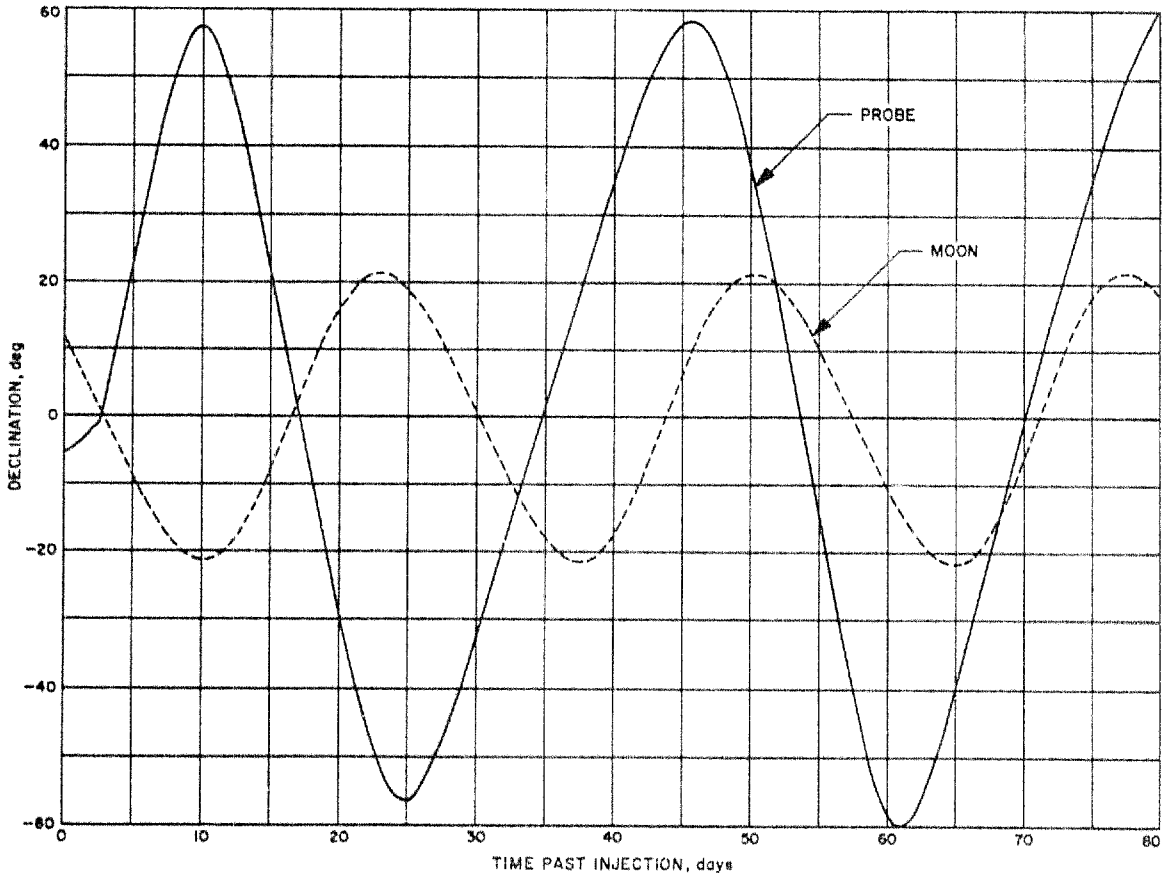

Fig. D-6. Declination of the probe and Moon for the first 80 days past injection

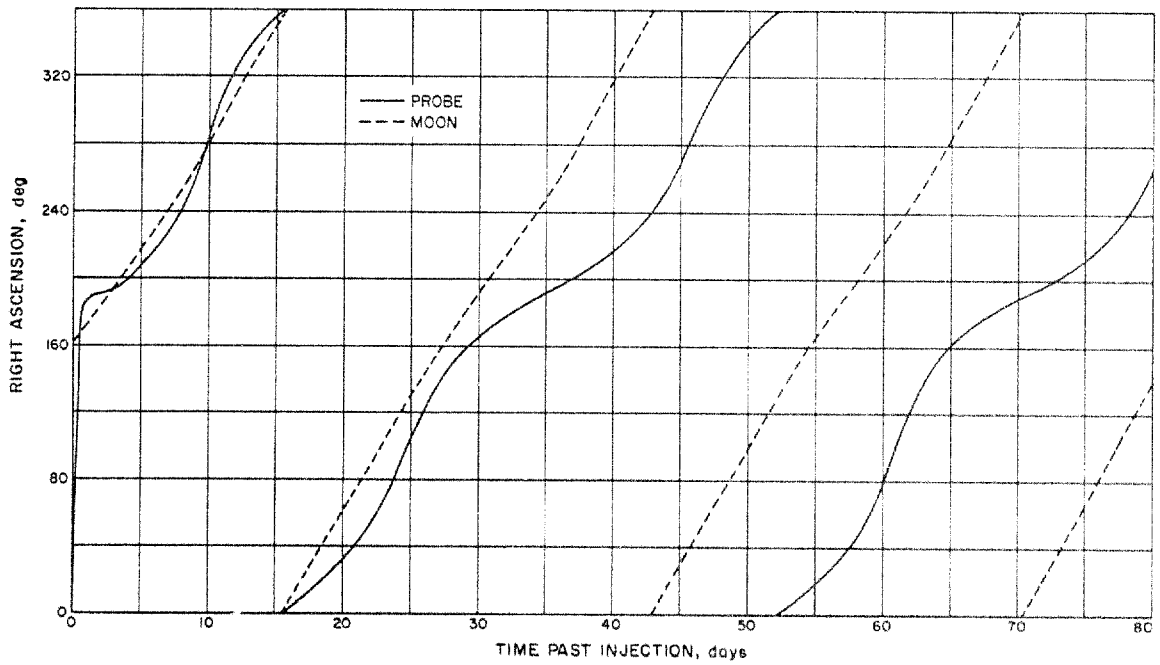

Fig. D-7. Right ascension of the probe and Moon for the first 80 days past injection

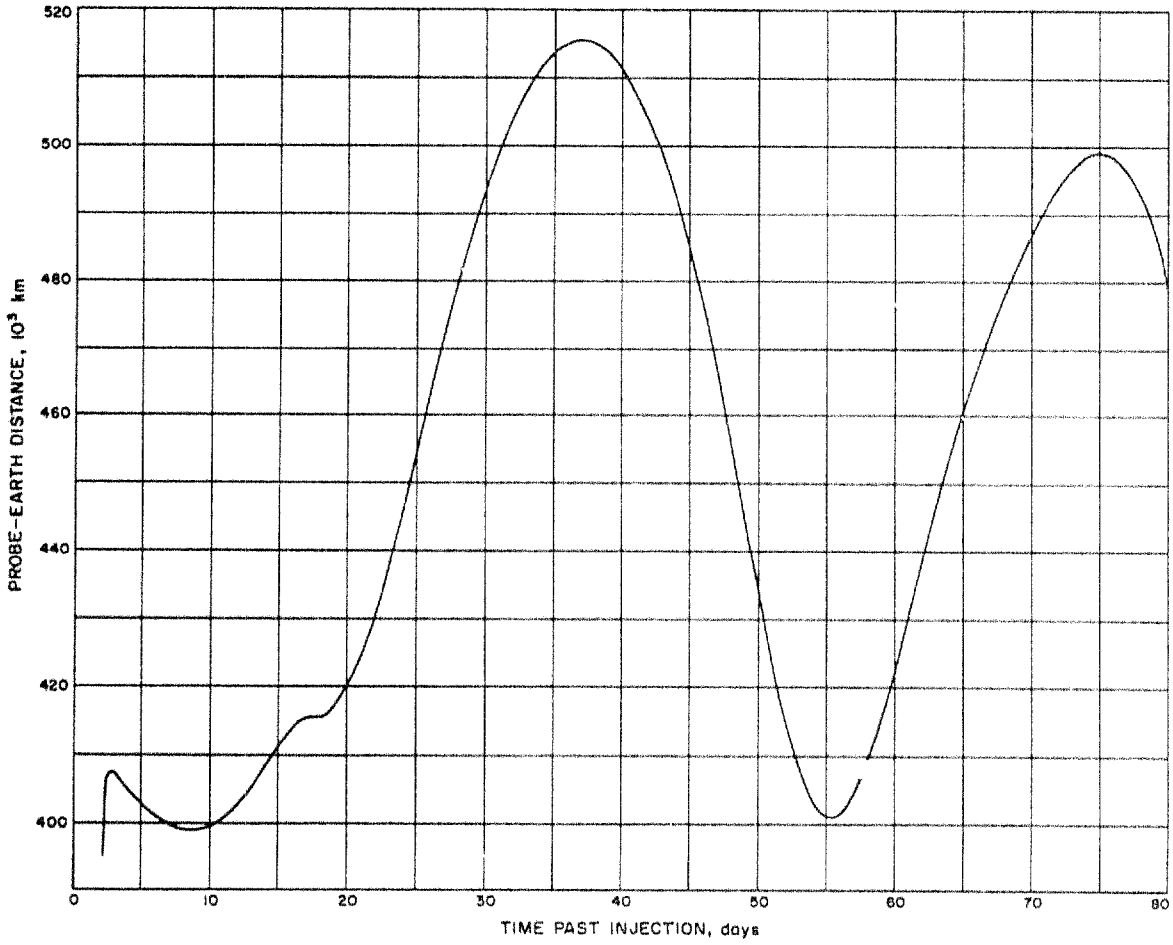

Fig. D-8. Probe-Earth distance for the first 80 days past injection

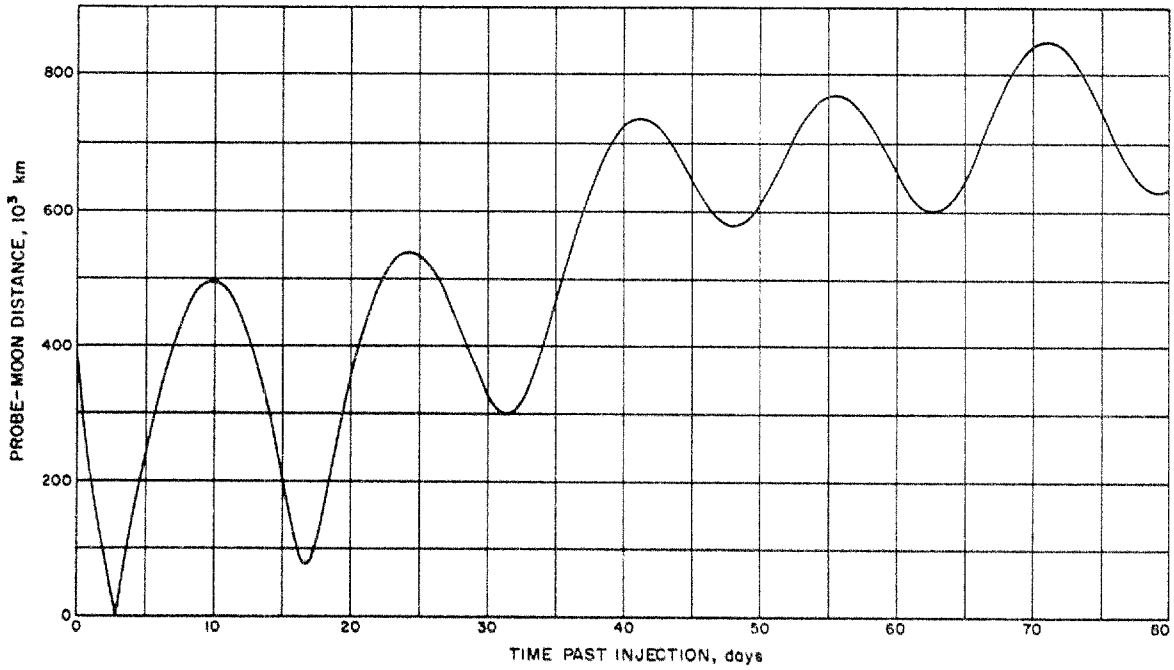

Fig. D-9. Probe-Moon distance for the first 80 days past injection

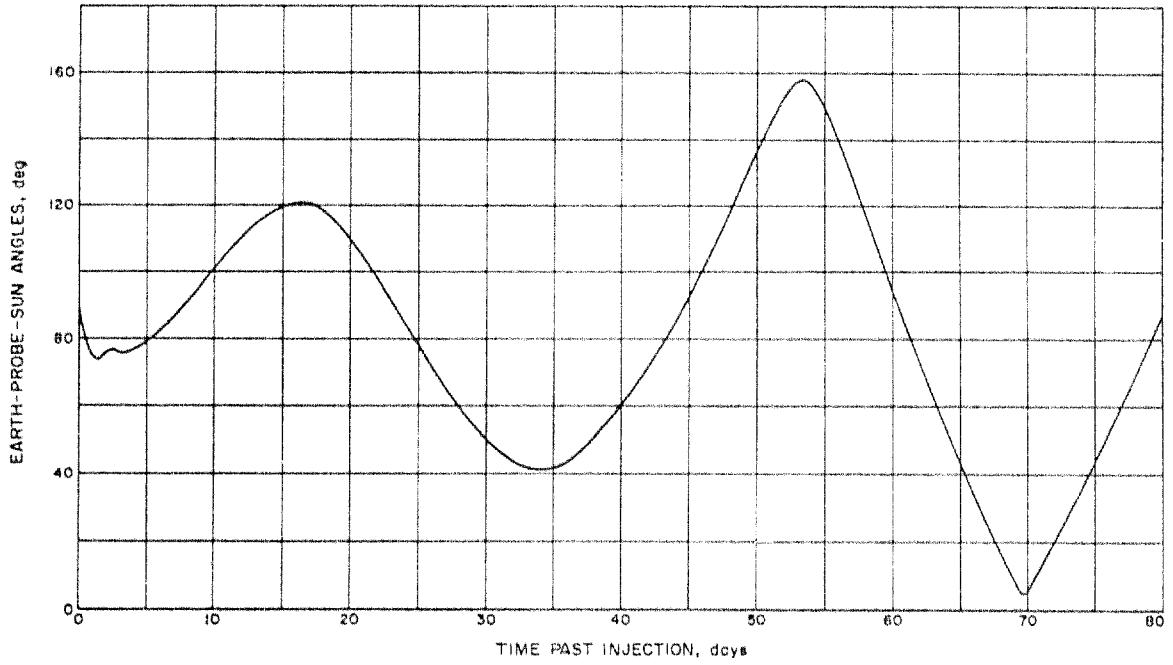

Fig. D-10. Earth-probe-Sun angle for the first 80 days past injection

APPENDIX E

The Evaluation of Certain Physical Constants from the Radio Tracking of Mariner 2*

J. D. Anderson, G. W. Null and C. Thomas Thornton

I. INTRODUCTION

The orbit of the Mariner 2 spacecraft which was launched from the Atlantic Missile Range, Cape Canaveral, Florida, on August 27, 1962, is unique in that it was dominated first by the Earth, then the Sun, and finally the planet Venus. On December 14, 1962, the spacecraft came within about 35,000 km of Venus, and its flight path was deflected by about 40 deg because of its close encounter. In addition, precise two-way doppler data were obtained throughout the 129-day period from launch to January 3, 1963. Fortunately, an atomic reference had been installed at the Goldstone, California, tracking station prior to the launch of Mariner 2, and this piece of equipment allowed the transmitter frequency to be held to better than one part in 10^{11} over the period of an hour. Equivalently the doppler shift in the received signal was measured to an accuracy of about 0.03 cps. In terms of velocity units the corresponding accuracy of the range rate between the probe and station was on the order of 1/2 cm/sec at a received frequency of 960 Mc and a cycle count time of 60 sec.

A combination of the above factors allows the determination of certain constants of the solar system to an accuracy that has been unobtainable in the past. In particular, at least an order of magnitude improvement in the mass of Venus appears possible because of the close approach to the planet. The same order of improvement should be obtained for the mass of the Moon because the periodic component in the data which results from the motion of the Earth about

*Paper presented at the AIAA Astrodynamics Conference, Aug. 19-21, 1963, Yale University New Haven, Conn.

the center of mass or barycenter of the Earth-Moon system is appreciable. The astronomical unit can also be obtained from the data, and its uncertainty is comparable to that of the recent radar determinations from the tracking of Venus.

The purpose of the present paper is to describe the computational methods used in the post-flight reduction of the Mariner 2 data. The basic computer program is the JPL Lunar and Planetary Orbit Determination Program which will be described in detail in a forthcoming JPL technical report. Therefore, all of the formulas used to evaluate the quantities required in the solution for the physical constants are not given here. Hopefully, however, the philosophy of the reduction of the data is clarified, and enough of the computational techniques are given so that the detailed formulas required in the computer program follow naturally from the discussion.

In Section II the form of the weighted least squares estimator is given, and the expressions that evaluate the error on the estimated parameters are listed. A formula for the computation of the two-way doppler observable is given in Section III. To form residuals, this computed value of doppler shift is simply subtracted from the observed value at the time in question. In Section IV the method of finding the coefficients in the equations of condition by a numerical integration of a set of variational equations is described, and finally in Section V three numerical examples of the reduction of a set of Mariner 2 data are given. The first two examples treat data taken before the probe was primarily influenced by Venus while the third considers only the data obtained during the encounter with Venus. An evaluation of the results of the three determinations is also included in Section V.

II. STATISTICAL FORMULAS

The orbital parameters and physical constants are estimated by the method of least squares (Ref. 46). Thus, if the vector $\vec{x}$ represents the parameters which are subject to estimation and $\hat{\vec{z}}$ is a vector representing the data, then the least squares estimate $\vec{x}^*$ of $\vec{x}$ is obtained by minimizing the quadratic form $Q = \delta\hat{\vec{z}}^T \delta\hat{\vec{z}}$. The residual vector $\delta\hat{\vec{z}}$ is given by $\delta\hat{\vec{z}} = \hat{\vec{z}} - \vec{z}(\vec{x})$. Actually, the rigorous sum of squares of the residuals is modified by introducing a diagonal weighting matrix W so that a weight can be assigned to each data point. Also a priori information on the parameter vector $\vec{x}$ is included by treating the a priori values $\tilde{\vec{x}}$ of the parameters as additional observations. In this case the weighting matrix is written as the inverse of the covariance matrix $\tilde{\Gamma}_x$ on the a priori parameter vector. Thus, the quadratic form Q that is minimized to provide an estimate of $\vec{x}$ is $Q = \delta\hat{\vec{z}}^T W \delta\hat{\vec{z}} + \delta\tilde{\vec{x}}^T \tilde{\Gamma}_x^{-1} \delta\tilde{\vec{x}}$ where $\delta\tilde{\vec{x}} = \tilde{\vec{x}} - \vec{x}$ and the corresponding linearized estimation formula is:

$$(A^T W A + \tilde{\Gamma}_x^{-1})\delta\vec{x}^* = A^T W \delta\hat{\vec{z}} + \tilde{\Gamma}_x^{-1}\delta\tilde{\vec{x}} \qquad \text{(E-1)}$$

The vector $\delta\vec{x}^*$ represents the corrections to the nominal values $\vec{x}$ of the parameters (i.e., $\vec{x}^* = \vec{x} + \delta\vec{x}^*$) while the matrix A relates variations in the parameters to variations in the data through the equations of condition $\delta\vec{z} = A\delta\vec{x}$. It is not necessary that the nominal values of the parameters agree with the a priori values and, therefore, the estimation formula Eq. (E-1) can be successively applied until a convergence is attained. The criterion for convergence is the convergence of the function Q which is typically stabilized within the limits of computational accuracy after three or four iterations. Of course, the number of iterations depends on the departure of the initial values of the parameters from the estimate $\vec{x}^*$ that minimizes Q.

In addition to obtaining the estimate of the parameters by Eq. (E-1) the error on this estimate is also required. For this purpose two error expressions are available. The first expression assumes that the weighting matrix W is the inverse of the covariance matrix on the data $\vec{z}$ and that all parameters that sensibly affect the data are included in the solution. Then the covariance matrix Γ_x on the estimated parameters is given by

$$\Gamma_x = (A^T W A + \tilde{\Gamma}_x^{-1})^{-1} \qquad \text{(E-2)}$$

A more general expression admits the possibility that a number of sensible parameters $\vec{y}$ are excluded from the solution. In other words, variational coefficients B are introduced such that $\delta\vec{z} = A\delta\vec{x} + B\delta\vec{y}$, and if the covariance matrix on $\vec{y}$ is Γ_y and $\vec{x}$ and $\vec{y}$ are statistically independent, then the more general parameter covariance matrix Γ_x' is given by

$$\Gamma_x' = \Gamma_x + \Gamma_x A^T W B \Gamma_y B^T W A \Gamma_x \qquad \text{(E-3)}$$

In either case the square roots of the diagonal elements of Γ_x or Γ_x' are taken to form a standard deviation on each parameter. Also Γ_x or Γ_x' is normalized so that all of the diagonal elements are unity. The resulting matrix is thus the correlation matrix on the parameters, and the degree to which various parameters are correlated by a particular data configuration $\hat{\vec{z}}$ is known.

The usefulness of the resulting errors on the parameter estimate is strictly dependent on the reality of the W and $\tilde{\Gamma}_x$ matrices which are constructed from a knowledge of the errors on the data and a priori parameters. Thus, $\tilde{\Gamma}_x$ reflects a confidence in parameter determinations prior to the introduction of the data $\hat{\vec{z}}$. It is customary to express results in terms of probable errors, and thus the construction of $\tilde{\Gamma}_x$ follows naturally from the published values of these errors. It follows that if W is also expressed in terms of probable errors, then the

errors on the estimate of the parameters are in terms of probable errors. This is true only if the ratio of the standard deviation to the probable error is the same for the data, a priori parameters, and estimated parameters. All uncertainties in this paper are assumed given in terms of probable error.

It should be noted that if the a priori information is not used, then, for uniform weighting, an option that makes sense only for the same kind of data, the estimate of the parameters is unaffected by assumptions on the accuracy of the data. Also, the errors on the estimated parameters are proportional to the data errors and can be scaled up and down at will. However, if $\tilde{\Gamma}_x^{-1}$ is not null, then the relative importance of data and a priori parameter errors affects both the parameter estimate and the error expressions. Actually, many options exist in the JPL orbit determination program to aid in the selection of meaningful W and $\tilde{\Gamma}_x$ matrices. These are not described here, although the numerical examples presented in Section V include a specification of the assumptions on W and $\tilde{\Gamma}_x$. After such assumptions are made, the numerical evaluation of $\vec{x}^*$, Γ_x or Γ_x' and the associated correlation matrix is accomplished by the above formulas in a straightforward manner. The description of the computation of the doppler observable $\vec{z}(\vec{x})$ is given in the next section, while the evaluation of the matrix A is described in Section IV. The matrix B can always be extracted from a larger A matrix that includes the variational coefficients for all sensible parameters.

III. DOPPLER RESIDUALS

The doppler residuals are computed by the equation

$$\delta\hat{\vec{z}} = \hat{\vec{z}} - \vec{z}(\vec{x}) \qquad \text{(E-4)}$$

where $\hat{\vec{z}}$ is an (n x 1) vector of observed values, and $\vec{z}$ is an (n x 1) vector of the computed values of $\hat{\vec{z}}$.

Doppler data is coherent, three-way doppler, which is defined as: An electromagnetic signal is transmitted from a point P_1 at time t_1 and reaches a point P_2 at t_2. At P_2 the received signal is multiplied by a constant, k, and instantaneously retransmitted. This second signal is then received at a point P_3 at time t_3. For this experiment P_1 and P_3 are stations on Earth, and P_2 is the position of the spacecraft at t_2.

Let ν_T be the frequency transmitted at t_1, and ν_R the frequency received at t_3, and define

$$\phi(t_3) = \frac{\nu_R}{k\nu_T} = \frac{\nu_R}{b} \qquad \text{(E-5)}$$

The radar equipment is designed so that a quantity $f(t) = a + b\left[1 - \phi(t)\right]$ is continuously received over an interval of time T_c. The constant a is an arbitrary additive frequency used to keep $f > 0$ at all times. Let the total number of cycles counted in this time interval be denoted by N. Then N/T_c is the quantity-designated three-way doppler with a count time T_c, which is measured in seconds so that N/T_c has the dimension cycles per second. The vector $\hat{\vec{z}}$, Eq. (E-4), is composed of n measurements of N/T_c. Each measurement is tagged with the real time T', the midpoint of the count time associated with the measurement.

The components of the vector $\vec{z}$ are computed as follows. For a given count time T_c and a datum time T',

$$\frac{N}{T_c} \triangleq \frac{1}{T_c} \int_{T' - \frac{T_c}{2}}^{T' + \frac{T_c}{2}} f(t)\,dt \qquad \text{(E-6)}$$

The function f(t) is computed as follows:

$$f(t) = a + b\left[1 - \phi(t)\right] \tag{E-7}$$

where a and b are given constants and

$$\phi(t) = \frac{\nu_R}{k\nu_T} = 1 - \frac{\dot{\rho}_1 + \dot{\rho}_2}{c} + \frac{1}{c^2}\left[\dot{\rho}_2^2 + \dot{\rho}_1\dot{\rho}_2 + H\right] \tag{E-8}$$

$$H = \vec{r}(t_2) \cdot \left[\frac{\dot{\rho}_2}{\rho_2}\dot{\vec{R}}_i(t_3) - \frac{\dot{\rho}_1}{\rho_1}\dot{\vec{R}}_q(t_1)\right] \tag{E-9}$$

where

c = speed of light

$\vec{r}(t_2) \triangleq$ geocentric position vector of the spacecraft at t_2

$\dot{\vec{R}}_q(t_1) \triangleq$ geocentric velocity vector of the transmitting station q at t_1

$\dot{\vec{R}}_i(t_3) \triangleq$ geocentric velocity vector of the receiving station i at t_3

$$\vec{\rho}_1 \triangleq \vec{r}(t_2) - \vec{R}_q(t_1) \qquad \dot{\vec{\rho}}_1 \triangleq \dot{\vec{r}}(t_2) - \dot{\vec{R}}_q(t_1)$$

$$\vec{\rho}_2 \triangleq \vec{r}(t_2) - \vec{R}_i(t_3) \qquad \dot{\vec{\rho}}_2 \triangleq \dot{\vec{r}}(t_2) - \dot{\vec{R}}_i(t_3)$$

$$\rho_j \triangleq \left|\vec{\rho}_j\right| \quad (j=1,2) \qquad \dot{\rho}_j \triangleq \frac{\vec{\rho}_j \cdot \dot{\vec{\rho}}_j}{\rho_j} \quad (j=1,2)$$

The time t_3 is the independent variable t; t_2 and t_1 are found from t_3 by an iterative technique. This technique is essentially a light-time correction to the data.

The computation of $\phi(t)$ involves $\vec{r}(t_2)$ and $\dot{\vec{r}}(t_2)$, the geocentric position and velocity vectors of the spacecraft at t_2. These vectors are obtained in the coordinates of data from the trajectory program (Ref. 47). Corrections to the data because of atmospheric refraction are applied to the computed values of the range rates $\dot{\rho}_1$ and $\dot{\rho}_2$.

IV. EQUATIONS OF CONDITION

The method of computing the variational coefficients in the equations of condition $\delta\vec{z} = A\delta\vec{x}$ is accomplished by solving a system of differential equations in the coefficients that relate trajectory variations at time t to variations at some epoch t_0. In other words, designate the position and velocity of the spacecraft at time t by the vector $\vec{X}$. This vector is obtained as the solution to the spacecraft equations of motion which can be written in the form $\dot{\vec{X}} = \dot{\vec{X}}(\vec{X}, \vec{Y}, t)$ where $\vec{Y}$ is a vector of physical constants. The variation in $\dot{\vec{X}}$ can be obtained by differentiating these equations of motion with respect to each position and velocity component and each physical constant. Time variations are ignored. Thus, formulas are available for the elements of the matrices Φ and Θ defined by $\delta\dot{\vec{X}} = \Phi\delta\vec{X} + \Theta\delta\vec{Y}$. On the other hand, the solution to the equations of motion gives $\vec{X}$ in terms of the initial conditions $\vec{X}_0$ at time t_0 and the physical constants so that $\vec{X} = \vec{X}(\vec{X}_0, \vec{Y}, t)$. Therefore, the variation in $\vec{X}$ can be written $\delta\vec{X} = U\delta\vec{X}_0 + V\delta\vec{Y}$, and by differentiating this variation with respect to time, one obtains $\delta\dot{\vec{X}} = \dot{U}\delta\vec{X}_0 + \dot{V}\delta\vec{Y}$. For the two expressions for $\delta\dot{\vec{X}}$ to be equal for arbitrary variations $\delta\vec{X}_0$ and $\delta\vec{Y}$, it is necessary that the following differential equations be satisfied:

$$\dot{U} = \Phi U \tag{E-10}$$

$$\dot{V} = \Phi V + \Theta \tag{E-11}$$

The numerical solution to the equations of motion, the computation of the Φ matrix and the numerical solution to Eq. (E-10) are all described by Holdridge (Ref. 47). Initially U is the unit matrix $U(t_0) = I$, and V is null so that $V(t_0) = 0$. Once U(t) has been obtained the solution to Eq. (E-11) is computed in terms of U by numerical quadrature integration of the following formula:

$$V(t) = U(t) \int_0^t U^{-1}(\tau)\Theta(\tau)d\tau \qquad \text{(E-12)}$$

It is easily shown by direct substitution that this is a solution to Eq. (E-11). The computation of the matrix Θ is accomplished by evaluating formulas that represent partial derivatives of the equations of motion of the spacecraft with respect to physical constants.

It still remains to obtain the variation in the observables $\vec{z}$. Partition the A matrix into two parts corresponding to the variation of $\vec{z}$ with respect to the orbital initial conditions X_0 and the physical constants Y, respectively. That is, let $\delta\vec{z} = A_1\delta\vec{X}_0 + A_2\delta\vec{Y}$ so that $A = (A_1 \vdots A_2)$. Now, by Section III the doppler observable can be written in terms of the position and velocity $\vec{X}$ of the spacecraft and also in terms of physical constants $\vec{Y}$ that enter explicitly in the formula for $\vec{z}$. Thus in general, $\vec{z} = \vec{z}(\vec{X}, \vec{Y}, t)$, although any explicit dependence on the time is unimportant in what follows because of the neglect of time variations. The variation in $\vec{z}$ is, therefore, given by $\delta\vec{z} = G\delta\vec{X} + H\delta\vec{Y}$ where the matrices G and H are obtained by differentiating the expression for the doppler data with respect to $\vec{X}$ and $\vec{Y}$. Again by equating two expressions for the same variation $\delta\vec{z}$, the formulas for A_1 and A_2 are $A_1 = GU$ and $A_2 = GV + H$ and the required matrix A assumes the following form:

$$A = (GU \vdots GV + H) \qquad \text{(E-13)}$$

In practice, the vector $\vec{Y}$ contains all of the physical constants that enter either into the trajectory computation or the data computation. Thus, if a constant enters only in the data computation, then the row of the V matrix that corresponds to that constant is zero. An example of this sort of constant is the velocity of light or the geocentric coordinates of the station. Similarly a constant such as

the mass of Venus that does not enter explicitly in the doppler formula will have a corresponding zero row in the H matrix.

Plots of the partial derivatives computed by the above technique are given in Figs. E-1 and E-2. Figure E-1 shows the partial derivatives of the doppler observable during the heliocentric portion of the flight for an initial epoch eight days after launch (just after the midcourse maneuver of September 5, 1962). Figure E-2 shows partial derivatives during the Venus-centered portion of the flight for an epoch on December 7, 1962, which was seven days before closest approach to Venus. Closest approach occurred at 20^h UT on December 14, 1962. These partial derivatives have been scaled so that each curve represents the doppler perturbation in cps caused by the indicated perturbation in the parameter. The conversion between doppler and range rate is given by 1 cps = 0.156 m/sec. The definitions of the plotted parameters are

GM_m = universal gravitational constant multiplied by the mass of the Moon

ϵ = a constant relating to solar pressure. The solar pressure force on the spacecraft is of the form $F = K(1 + \epsilon)/r^2$ where r is the distance from the Sun, K is a constant and F is directed radially away from the Sun

A_E = astronomical unit

M_V = mass of Venus in solar mass units

V. NUMERICAL EXAMPLES

The first example illustrates a least-squares solution for data taken before the Venus encounter period. Only data from the Goldstone, California, station are used, and in addition 90% of this data is neglected by selecting every

tenth doppler measurement as data. As a result 518 measurements are used in this example with the first measurement occurring on September 5, 1962, and the last on December 1, 1962. The count time T_c for the data is 60 sec.

The parameters selected for adjustment by the least-squares method are the selenocentric gravitational constant GM_m (the universal gravitational constant times the mass of the Moon), the astronomical unit A_E, the geocentric radii R and longitudes λ of the Goldstone transmitter (Station 3) and receiver (Station 2), and the six geocentric equatorial coordinates of data ($X_0, Y_0, Z_0, \dot{X}_0, \dot{Y}_0, \dot{Z}_0$) for the spacecraft position and velocity at the epoch t_0. The station latitude $\emptyset$ is not included in the solution because a separation of the radius and latitude is impossible with the Mariner 2 data. In other words, the data essentially measure the rotational velocity of the station about the Earth's polar axis, or equivalently the quantity R cos $\emptyset$ is obtained from a combination of the data with the known angular velocity of the Earth's rotation. An additional parameter ϵ is added to the solution to account for a heliocentric inverse square perturbative force arising from solar radiation pressure. In other words the area-to-mass ratio of the spacecraft is relatively large (about 2.16×10^{-11} km^2/g or 10^9 times the same ratio for the Earth), and the solar radiation pressure imparts a perturbative acceleration on the order of 10^{-10} km/sec^2 at one astronomical unit. For comparison, the total acceleration is about 6×10^4 times this number. The parameter ϵ represents a percentage change in the nominal value of the acceleration caused by radiation pressure.

The input values of the parameters are the following:

t_0 = September 5, 1962, $0^h23^m32^s.000$ (UT)

$X_0 = -1.4243704 \times 10^6$ km

$Y_0 = -1.9397521 \times 10^6$ km

$Z_0 = -0.10293568 \times 10^6$ km

$$\dot{X}_0 = -1.7445233 \text{ km/sec}$$

$$\dot{Y}_0 = -2.4233963 \text{ km/sec}$$

$$\dot{Z}_0 = -0.10989823 \text{ km/sec}$$

$$\epsilon = 0.383$$

$$GM_m = 4900.7589 \text{ km}^3/\text{sec}^2$$

$$A_E = 1.4959900 \times 10^8 \text{ km}$$

$$R_2 = 6372.0327 \text{ km}$$

$$\phi_2 = 35^\circ.20598$$

$$\lambda_2 = 243^\circ.15175$$

$$R_3 = 6372.0165 \text{ km}$$

$$\phi_3 = 35^\circ.11654$$

$$\lambda_3 = 243^\circ.19539$$

$$c = 299792.5 \text{ km/sec (speed of light)}$$

In this example and those that follow, any constant that is not stated explicitly is given the value specified by Clarke (Ref. 23). With the above values of the parameters, the weighted sum of squares of the residuals is $\delta\vec{\hat{z}}^T W \delta\vec{\hat{z}} = 649.73$. A uniform weighting is assumed in the first two examples given here, and each data point is assigned a probable error of 0.0569 cps or equivalently 0.009 m/sec in range rate. If this figure is multiplied by the square root of 10 to allow for the selection of every tenth measurement, then the equivalent error on each measurement, if used without a selection process, is 0.03 m/sec. This is about a factor of six times the estimate of the actual random error on the data, but an allowance is thus provided for possible systematic error sources.

The only exceptions to a uniform weighting is for measurements taken at a low elevation angle where the refraction correction is unreliable. These data are effectively weighted so that they do not influence the solution for the parameters. Figures E-3, E-4, and E-5 show residual plots for Goldstone for data

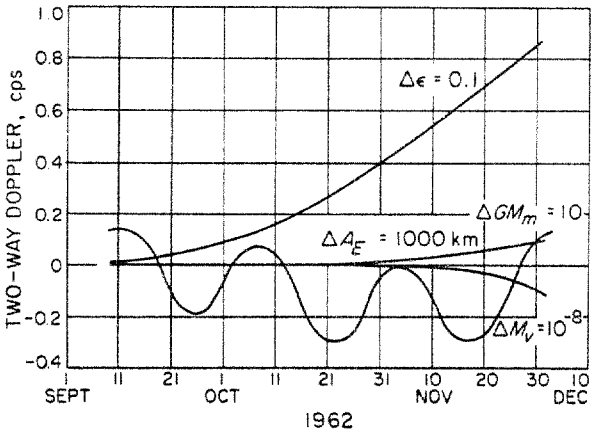

Fig. E-1. Partial derivatives of doppler for encounter of flight

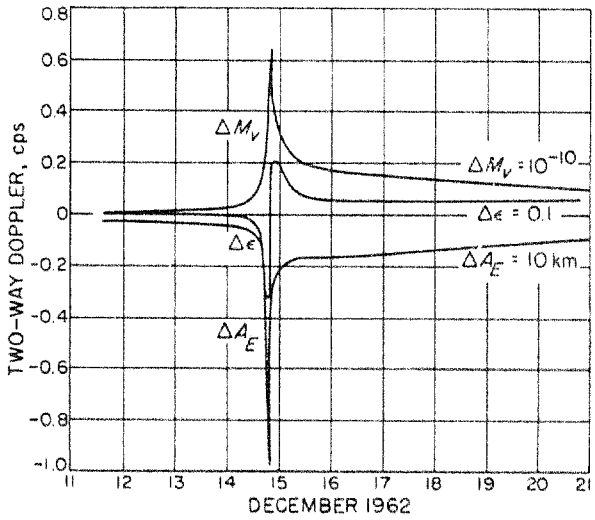

Fig. E-2. Partial derivatives of doppler data for heliocentric portion of flight

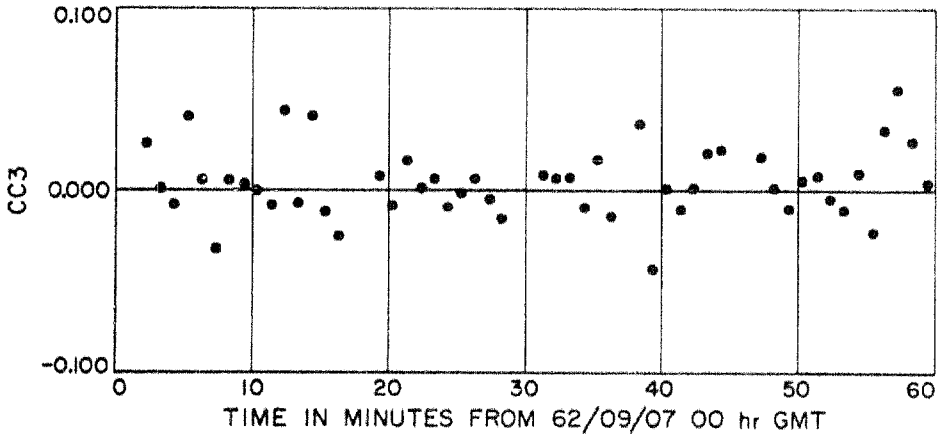

Fig. E-3. Early Goldstone doppler residuals

taken respectively near the beginning, middle, and end of the heliocentric portion of the flight. The ordinate CC3 is the doppler residual in cps. These plots would seem to indicate that the errors assigned to the data are not overly optimistic in the sense of being too small. For comparison, an early pass of data taken from the Johannesburg DSIF station (Station 5) is shown in Fig. E-6. These data are not used in the solution, but the residuals can be computed from the fit to the Goldstone data. The relatively large scatter in the points is attributed to the lack of an atomic reference for the transmitter frequency.

An application of the formulas of the preceding sections without the introduction of a priori information on the parameters ($\tilde{\Gamma}_x = 0$) yields the following corrections and probable errors:

$$\delta X_0 = -160 \pm 108 \text{ km}$$

$$\delta Y_0 = -113 \pm 141 \text{ km}$$

$$\delta Z_0 = 2216 \pm 251 \text{ km}$$

$$\delta \dot{X}_0 = -0.0856 \pm 0.04 \text{ m/sec}$$

$$\delta \dot{Y}_0 = 0.108 \pm 0.03 \text{ m/sec}$$

$$\delta \dot{Z}_0 = -0.582 \pm 0.111 \text{ m/sec}$$

$$\delta_\epsilon = 0.530 \pm 0.12$$

$$\delta GM_m = 2.016 \pm 0.20 \text{ km}^3/\text{sec}^2$$

$$\delta A_E = 16892 \pm 4640 \text{ km}$$

$$\delta R_2 = -170.6 \pm 18.2 \text{ m}$$

$$\delta \lambda_2 = -0^\circ.00177 \pm 0^\circ.00043$$

$$\delta R_3 = -168.6 \pm 17.3 \text{ m}$$

$$\delta \lambda_3 = -0^\circ.00171 \pm 0^\circ.00044$$

The new weighted sum of squares of the residuals is now reduced to 67.43. A large variation in the astronomical unit occurs because a perturbative force has been neglected in these examples. This force results because of a

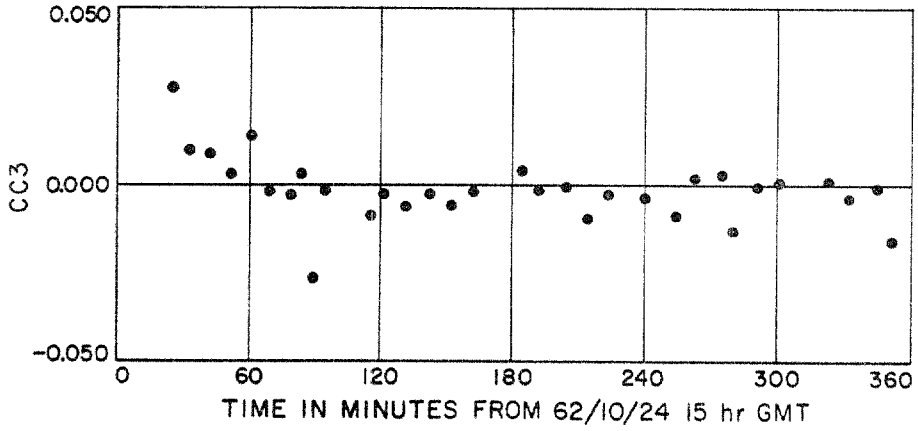

Fig. E-4. Goldstone doppler residuals at midpoint of mission

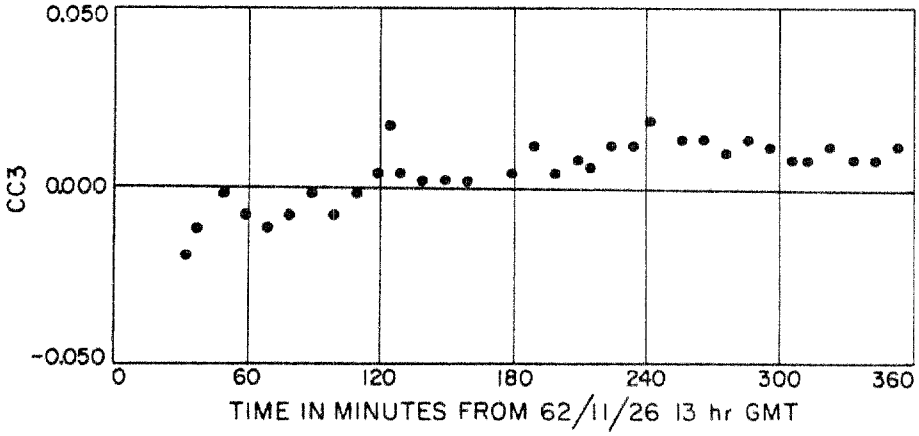

Fig. E-5. Late Goldstone doppler residuals

Fig. E-6. Early Johannesburg doppler residuals

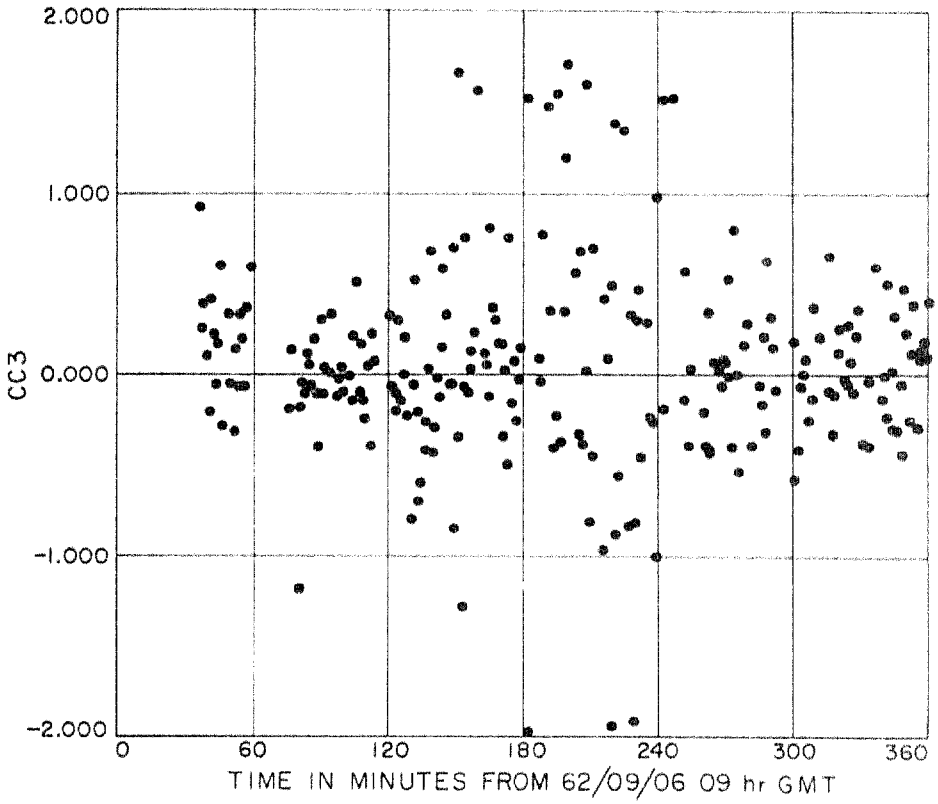

slow leak in the attitude control system which operates by releasing cold nitrogen gas from a number of jets. As a result a perturbative acceleration of about 3×10^{-11} km/sec^2 (about one-third the magnitude of the solar radiation pressure) is imparted to the spacecraft throughout the duration of the mission, and because this effect is neglected, other parameters absorb the gas leakage perturbation to some degree. Clearly some of the effect is thrown into the solar radiation coefficient ϵ. However, the correlation matrix given in Table E-1 indicates a fairly strong correlation (-0.75) between the coefficient ϵ and the astronomical unit, and therefore, the astronomical unit would be expected to absorb some of the gas leak perturbation as well.

The correlation of A_E and ϵ arises because a variation in the astronomical unit must also result in a variation in the mass of the Sun if the well-known periods of the Earth and planets are to remain constant. Therefore, the inverse square heliocentric distance effect of the astronomical unit on the trajectory looks very much like the inverse square effect of radiation pressure so long as the spacecraft is dominated by the Sun (see Fig. E-1). As a result the solution given above provides practically no information on physical constants with the notable exception of the mass of the Moon. In this case the correlations with other parameters are all small, and a variation in the trajectory has little effect on GM_m. Here the doppler data are measuring the monthly motion of the Earth above the center of mass or barycenter of the Earth-Moon system (see GM_m curve in Fig. E-1), and variations in the trajectory have practically no effect on this measurement.

As a second numerical example the same input values of the parameters are used as before, but the astronomical unit is dropped as a parameter for adjustment. Because the astronomical unit can no longer absorb some of the gas leak perturbation, the expected result of this example is a fairly significant

Table E-1. Correlation matrix of estimated parameters

X_0	Y_0	Z_0	$\dot{X}_0$	$\dot{Y}_0$
0.99999999 00	0.96520441 00 0.99999999 00	-0.81608672 00 -0.82121404 00 0.10000000 01	-0.85505868 00 -0.89405078 00 0.56217142 00 0.10000000 01	0.84143814 00 0.89278047 00 -0.52519772 00 -0.99388224 00 0.10000000 01

$\dot{Z}_0$	ϵ	GM_m	A_E
-0.90310363 00 -0.93536808 00 0.62124607 00 0.86011139 00 -0.88869873 00 0.10000000 01	0.70740512 00 0.80383706 00 -0.41863089 00 -0.96346607 00 0.97215246 00 -0.80063977 00 0.10000000 01	-0.20143232 00 -0.19435844 00 0.20803739 00 0.22959995 00 -0.20667874 00 0.90344363-01 -0.18169434 00 0.10000000 01	-0.36452017 00 -0.43841335 00 0.25862856 00 0.70996388 00 -0.66715355 00 0.26610538 00 -0.75017612 00 0.28883922 00 0.99999999 00

R_2	λ_2	R_3	λ_3
0.69345473 00 0.70728159 00 -0.70537353 00 -0.54139221 00 0.53461257 00 -0.62413774 00 0.44942844 00 -0.13767263 00 -0.20239079 00 0.99999997 00	-0.47995839 00 -0.62711255 00 0.30677602 00 0.75731903 00 -0.76258093 00 0.61741365 00 -0.84248237 00 0.14715431 00 0.63193730 00 -0.31985184 00 0.99999999 00	0.70654134 00 0.71906652 00 -0.70420323 00 -0.55255681 00 0.54822414 00 -0.64746739 00 0.46047395 00 -0.11787525 00 -0.18919596 00 0.48365797 00 -0.32536693 00 0.10000000 01	-0.47320807 00 -0.62209836 00 0.28952056 00 0.76235378 00 -0.76839046 00 0.60928615 00 -0.84936448 00 0.16066238 00 0.65323931 00 -0.30900698 00 0.91680225 00 -0.31293735 00 0.10000000 01

difference from the previous solution for ϵ and those parameters that are highly correlated with the radiation pressure coefficient. The variations given below generally support such a conclusion. However, the important point is that the relatively independent mass of the Moon changes only by an amount equal to its probable error while other highly correlated parameters change by as much as four times their estimated error. Therefore, the solution for GM_m is probably not significantly degraded by the gas leak effect. The sum of squares of the residuals after convergence of Q is 79.86 for this second example, and thus by a comparison with 67.43 for the first example, the fit to the data has not been degraded appreciably.

$$\delta X_0 = -15.5 \pm 101 \text{ km}$$

$$\delta Y_0 = 115 \pm 127 \text{ km}$$

$$\delta Z_0 = 1982 \pm 241 \text{ km}$$

$$\delta \dot{X}_0 = -0.188 \pm 0.028 \text{ m/sec}$$

$$\delta \dot{Y}_0 = 0.182 \pm 0.023 \text{ m/sec}$$

$$\delta \dot{Z}_0 = -0.689 \pm 0.107 \text{ m/sec}$$

$$\delta_\epsilon = 0.859 \pm 0.086 \text{ m/sec}$$

$$\delta GM_m = 1.803 \pm 0.19 \text{ km}^3/\text{sec}^2$$

$$\delta R_2 = -157.3 \pm 17.9 \text{ m}$$

$$\delta \lambda_2 = -0.^\circ00277 \pm 0.^\circ00034$$

$$\delta R_3 = -156.7 \pm 17.1 \text{ m}$$

$$\delta \lambda_3 = -0.^\circ00276 \pm 0.^\circ00034$$

From the first example the estimated value of GM_m is

$$GM_m = 4902.775 \pm 0.20 \text{ km}^3/\text{sec}^2$$

The corresponding value for the mass of the Earth M_E is from Clarke (op. cit.).

$$GM_E = 3.986032(\pm 0.000030) \times 10^5 \text{ km}^3/\text{sec}^2$$

and the mass ratio of the Earth to the Moon is

$$\frac{GM_E}{GM_m} = \mu^{-1} = 81.30155 \pm 0.0034$$

Finally for a third example, a fit to all the Goldstone doppler data during the encounter period of the flight from December 7 to 20, 1962, is given. The count time T_c for the encounter data is normally 600 sec, and therefore, the data sampling rate is the same as for the above two heliocentric examples. Thus, the weights for the data are the same as before, and again measurements at a low elevation angle are discarded by applying small weights. In addition a measurement occasionally occurs with a count time shorter than 600 sec, and the corresponding error on such a measurement is increased by a factor of $\sqrt{600/T_c}$ or, what amounts to the same thing, the standard weight is multiplied by the factor $T_c/600$. The total number of measurements used in this encounter example is 610.

The mass M_V of Venus in units of the solar mass is added to the parameter list in this example, but the mass of the Moon is dropped, and its value from the first example above is used in the trajectory computation. The initial values of the parameters are

$$t_0 = \text{December 7, 1962, } 0^h \text{ (UT)}$$
$$X_0 = -3.6494745 \times 10^7 \text{ km}$$
$$Y_0 = -2.9910919 \times 10^7 \text{ km}$$
$$Z_0 = -0.94548403 \times 10^7 \text{ km}$$

$$\dot{X}_0 = -7.3401189 \text{ km/sec}$$

$$\dot{Y}_0 = -10.825346 \text{ km/sec}$$

$$\dot{Z}_0 = -5.4161879 \text{ km/sec}$$

$$\epsilon = 0.383$$

$$M_V = 2.4471118 \times 10^{-6}$$

$$A_E = 1.4959900 \times 10^{8} \text{ km}$$

The station coordinates are taken from the solution of the first example. The initial sum of squares of the residuals is 49835, and the corrections to the parameters are the following. Again the a priori matrix $\tilde{\Gamma}_x$ is assumed null.

$$\delta X_0 = -134.5 \pm 106 \text{ km}$$

$$\delta Y_0 = -58.5 \pm 179 \text{ km}$$

$$\delta Z_0 = 225.4 \pm 43 \text{ km}$$

$$\delta \dot{X}_0 = 0.110 \pm 0.161 \text{ m/sec}$$

$$\delta \dot{Y}_0 = -0.059 \pm 0.228 \text{ m/sec}$$

$$\delta \dot{Z}_0 = -0.358 \pm 0.046 \text{ m/sec}$$

$$\delta_\epsilon = 0.592 \pm 0.22$$

$$\delta M_V = 6.317(\pm 0.24) \times 10^{-10}$$

$$\delta A_E = 244 \pm 278 \text{ km}$$

$$\delta R_2 = -24.0 \pm 16.5 \text{ m}$$

$$\delta \lambda_2 = -0^{\circ}0001 \pm 0^{\circ}00038$$

$$\delta R_3 = -24.0 \pm 16.5 \text{ m}$$

$$\delta \lambda_3 = 0^{\circ}0001 \pm 0^{\circ}00038$$

The new sum of squares of the residuals is 86.20. The correlation matrix for this solution is shown in Table E-2. Again the gas leak is present as a perturbing force, but now because of the relatively short interval over which data are taken, the radiation pressure can absorb practically all of a radial perturbing

Table E-2. Correlation matrix of estimated parameters

X_0	Y_0	Z_0	$\dot{X}_0$	$\dot{Y}_0$
0.10000000 01	-0.47611232 00 0.10000000 01	0.90533835 00 -0.17179116 00 0.10000000 01	-0.74674425 00 0.94012643 00 -0.47412299 00 0.10000000 01	0.75884523 00 -0.93395624 00 0.49608308 00 -0.99945072 00 0.10000000 01

$\dot{Z}_0$	ϵ	M_V	A_E
-0.88383915 00 0.63995212 00 -0.84739782 00 0.81810140 00 -0.83411209 00 0.10000000 01	0.81805885 00 0.87415753 00 -0.56740189 00 0.97775859 00 -0.98063353 00 0.84229464 00 0.99999999 00	-0.76468217-01 0.67585243 00 0.24963430 00 0.54735706 00 -0.53160518 00 0.10921155 00 0.50262720 00 0.99999999 00	-0.32767197 00 -0.67449725 00 -0.58230696 00 -0.38369286 00 0.36620133 00 0.63413529-01 -0.25295767 00 -0.66774978 00 0.99999999 00

R_2	λ_2	R_3	λ_3
-0.57443364-01 0.37632449-02 -0.25764921-01 0.28534785-01 -0.25283753-01 -0.16596697-03 0.45740775-01 0.60210604-01 0.39962482-01 0.10000000 01	0.20891538-01 -0.20821640-01 -0.27957654-01 -0.19216209-01 0.28763327-01 0.47566533-01 -0.47582622-01 -0.14097147 00 -0.25526828-02 0.10682547 00 0.99999998 00	-0.57407453-01 0.36930172-02 -0.25739808-01 0.28470474-01 -0.25212098-01 -0.21565546-03 0.45607173-01 0.60201785-01 0.40003871-01 0.33646668 00 0.11032300 00 0.10000000 01	0.20952987-01 -0.20879724-01 -0.27886989-01 -0.19281795-01 0.28831718-01 0.47473002-01 -0.47646284-01 -0.14096949 00 -0.25444084-02 0.10248328 00 0.87433820 00 0.10597927 00 0.10000000 01

force caused by gas leakage. The spacecraft remains attitude stabilized over the entire encounter period, so that the solar panels remain pointed at the Sun, and the radiation pressure effect is in fact radial. Telemetry information indicates that a large part of the gas leak perturbation is radial also, but there is a tangential component as well. Therefore, the above solution is not entirely satisfactory. However, the astronomical unit is almost completely uncoupled from the radiation pressure coefficient in the encounter phase of the flight (see Fig. E-2). The correlation between A_E and ϵ is only -0.26. Therefore, the astronomical unit as determined from the encounter data is probably fairly reliable. However, the mass of Venus is correlated with ϵ by about one-half, and its value could easily shift outside of the limits of its probable error if the gas leakage effect were properly accounted for.

The astronomical unit as determined from the Mariner 2 encounter tracking data is

$$A_E = 149,599,244 \pm 278 \text{ km}$$

This is in excellent agreement with recent radar determinations from the tracking of Venus. Four such independent reductions give

Muhleman, et al. (Ref. 48) $A_E = 149,598,845 \pm 250$ km
(Goldstone)

Pettingill, et al. (Ref. 49) $A_E = 149,597,850 \pm 400$ km
(Millstone)

Thomson, et al. (Ref. 50) $A_E = 149,599,800 \pm 5000$ km
(Jodrell Bank)

Kotelnikov (Ref. 51) $A_E = 149,599,500 \pm 800$ km

The mass ratio of the Sun to Venus from the above encounter solution is

$$M_S/M_V = 408,539.5 \pm 12.0$$

The probable error that results from the solution is arbitrarily multiplied by a factor of three to allow for the neglected gas leakage effect. Again this value of the mass ratio is consistent with recent determinations by Clemence (Ref. 52) and Rabe (Ref. 53).

Clemence	$M_S/M_V = 409,300 \pm 1400$
Rabe	$M_S/M_V = 408,645 \pm 208$

REFERENCES

1. Plummer, H. C., "An Introductory Treatise on Dynamical Astronomy", Dover Publications, New York, pp. 236-253.

2. Moulton, F. R., "An Introduction to Celestial Mechanics", 2nd Ed., The Macmillan Co., 1914.

3. Kordylewski, K., Circ. No. 1760 Intern. Astro. Union, May 23, 1961.

4. "The Natural Satellites of the Earth", (news note), Sky and Telescope, Vol. 22, No. 1, July, 1961, p. 16.

5. "More About the Earth's Cloud Satellites", Sky and Telescope, Vol. 22, No. 2, August, 1961, p. 63.

6. Marshall, J. H., "The Motion of a Small Particle Near the Earth-Moon Libration Point L_4", Special Report ASE 396, The University of Texas, May, 1962.

7. Michael, W. H., Jr., "Considerations of the Motion of a Small Body in the Vicinity of the Stable Libration Points of the Earth-Moon System", NASA TR, R-160, 1963.

8. Rabe, E., and A. Schanzle, "Periodic Orbits About the Triangular Solutions of the Restricted Earth-Moon Problem and Their Orbital Stabilities", The Astronomical Journal, Vol. 67, No. 10, December, 1962, pp. 732-739.

9. Columbo, B. G., D. Lautman and C. Munford, "On the Libration Orbits of a Particle Near the Triangular Point in the Semi-Restricted Three-Body Problem", Smithsonian Astrophysics Observatory, Special Report No. 108, November 20, 1962.

10. Schnal, L., "The Stability of the Libration Points L_4 and L_5 in the System Earth-Moon", Astronomical Institute of Czechoslovakian Academy of Science, BAC (11), 1960, pp. 130-131.

11. Schechter, H. B., and J. V. McGann, "Acceleration Contours Around the Earth-Moon Libration Points", RAND Corp., Memo RM-3150-PR, September, 1962.

12. Lewallen, J. M., "Satellite Motion in the Vicinity of the Stable Earth-Moon Libration Points", M.S. Thesis, The University of Texas, May, 1963.

13. Steg, L., and E. Schoemaker, "Libration Point Satellites", Sec. C-2 of A Review of Space Research, National Academy of Sciences - National Research Council, Publication 1079, 1962.

14. Lorell, J., "Characteristics of Lunar Satellite Orbits", Jet Propulsion Laboratory Technical Memorandum No. 312-164, February 20, 1962.

15. Gates, C. R., ed., "The Behavior of Lunar Satellites and the Determination of Their Orbits: A Preliminary Investigation", Jet Propulsion Laboratory Technical Memorandum 33-107, September 18, 1962.

16. Sauer, C., "Guidance Requirements for the Establishment of Lunar Orbits, Jet Propulsion Laboratory Technical Memorandum No. 312-177, March 22, 1962.

17. Kliore, A., "Injection and Station Keeping Near the Translunar Libration Point", Jet Propulsion Laboratory Technical Memorandum No. 312-257, December 17, 1962.

18. Kirhofer, W., "Conic Approximations Used in Circumlunar Trajectories", Jet Propulsion Laboratory Research Summary No. 36-11, November 1, 1961, pp. 8-12.

19. Arenstorf, R. F., "The Existence of Periodic Solutions Passing Near Both Masses of the Restricted Three-Body Problem", Paper No. 2604-62, ARS 17th Annual Meeting, Los Angeles, Calif., November, 1962.

20. Benedikt, E. T., "Exact Determination of the Lunar Mass by Means of Selenoid Satellites", Nature (letter to the editor), Vol. 192, No. 4801, November 4, 1961, pp. 442-443.

21. Klemperer, W. B., and E. T. Benedikt, "Selenoid Satellites", Astronautica Acta., Vol. 4, 1958, pp. 25-30.

22. Anderson, J. D., G. W. Null, and C. Thornton, "The Evaluation of Certain Physical Constants From the Radio Tracking of Mariner 2", presented at AIAA Astrodynamics Conference, New Haven, Conn., August, 1963 (see Appendix E).

23. Clarke, V. C., "Constants and Related Data Used in Trajectory Calculations at JPL", Jet Propulsion Laboratory Technical Report No. 32-273, May 1, 1962.

24. Barber, T. A., "Extension and Revision of J. Reichert's Lunar Satellite Orbit Accuracy Determination Program, Jet Propulsion Laboratory Technical Memorandum No. 312-255, December 13, 1962.

25. Barber, T. A., "Lunar Satellite Orbit Determination Study", Jet Propulsion Laboratory Technical Memorandum No. 312-289, March 21, 1963.

26. Benedikt, E. T., "Exact Determination of the Lunar Mass by Means of Selenoid Satellites", Nature (letter to the editor), Vol. 189, No. 4759, June 14, 1961, pp. 127-128.

27. Anon., "New Natural Satellites of the Earth", Sky and Telescope (news note), Vol. XXII, No. 1, August, 1961, p. 16.

28. Anon., "More About the Earth's Cloud Satellites", Sky and Telescope, Vol. XXII, No. 2, August, 1961, p. 63.

29. Raney, J. L., "Solution of N Simultaneous Differential Equations by Adams-Moulton Method Using a Runge-Kutta Starter and Partial Double Precision Arithmetic", UTD2-02-003 (D2 UTEX RKAMPDP), The University of Texas Computation Center, Austin, Texas, August 8, 1961.

30. The American Ephemeris and Nautical Almanac, 1961.

31. Lanzano, P., "A Study of the Jacobi-Integral for the Earth-Moon System", Space Technology Laboratories, Report No. GM-TN-0165-00165, July 29, 1958.

32. Moulton, F. R., "An Introduction to Celestial Mechanics", The Macmillan Co., New York, 1958.

33. Deutsch, A. J., "Orbits for Planetary Satellites from Doppler Data Alone", A.R.S. Journal, June, 1960, Vol. 30, No. 6, pp. 536-42.

34. Smart, W. M., Spherical Astronomy, Cambridge Univ. Press, 1956.

35. Makemson, M. W., R. M. L. Baker, Jr., and C. B. Westrom, "Analysis and Standardization of Astrodynamic Constants", U. C. L. A. Astrodynamical Report No. 12, February, 1961 (Journal of the Astronautical Sciences, VIII, No. 1, Spring, 1961).

36. Smart, W. M., Celestial Mechanics, Longmans, Green and Co., New York, 1953.

37. Blanco, V. M., and S. W. McCuskey, Basic Physics of the Solar System, Addison-Wesley Reading, Massachusetts, 1961.

38. Munch, Guido, "Fundamental Astronomical Constants", Space Technology Laboratories, Report No. GM-TM-0165-00234A, December, 1958.

39. Allen, C. W., Astrophysical Quantities, University of London, The Athlone Press, 1955.

40. Brower, D., and G. M. Clemence, Methods of Celestial Mechanics, Academy Press, New York, 1961.

41. Alexandrov, I., "The Lunar Gravitational Potential, Advances in the Astronautical Sciences", Vol. 5, pp. 320-24, The Plenum Press, New York, 1960.

42. Kozai, Y., "The Motion of a Close Earth Satellite", Astronomical Journal, Vol. 64, No. 9, November, 1959, pp. 367-77.

43. Lass, H. and C. B. Solloway, "Motion of a Satellite on the Moon", A.R.S. Journal, February, 1961, pp. 220-22.

44. Kozai, Y., Smithsonian Institution Astrophysical Observatory Special Report No. 22, Cambridge, Massachusetts, March 20, 1959.

45. Siefert, H., et al., "Space Technology", J. Wiley and Sons, New York, 1959, Chap. 7.

46. Brouwer, D. and G. M. Clemence, Methods of Celestial Mechanics, Academic Press, 1961, Ch. VIII.

47. Holdridge, D. B., "Space Trajectories Program for the IBM 7090 Computer", Jet Propulsion Laboratory Technical Report No. 32-223, March 2, 1962, pp. 4-6 and 80-85.

48. Muhleman, D. O., D. B. Holdridge, and N. Block, "The Astronomical Unit Determined by Radar Reflections from Venus", Astronomical Journal, Vol. 67, May, 1962, pp. 191-203.

49. Pettingill, G. H., et al., "A Radar Investigation of Venus", Astronomical Journal, Vol. 67, May, 1962, pp. 181-190.

50. Thomson, J. H., G. N. Taylor, J. E. B. Ponsonby, and R. S. Roger, "A New Determination of the Solar Parallax by Means of Radar Echoes from Venus", Nature, Vol. 190, 1961, p. 519.

51. Kotelnikov, U. A., "Radar Contact with Venus", A paper presented at the 12th International Astronautical Congress, Washington, D. C., October, 1961.

52. Clemence, G. M., "The Motion of Mercury, 1765-1937", Astron. Papers Am. Emhm., Vol. II, Part 1, 1943.

53. Rabe, E., "Derivation of Fundamental Astronomical Constants from the Observations of Eros During 1926-1945", Astronomical Journal, Vol. 55, 1950, pp. 112-125, and "Additional Note on the Solar Parallax from Eros", Astronomical Journal, Vol. 59, 1954, pp. 409-411.